Design and Synthesis of Colorimetric Halide Sensors Based on Dimeric Dye Chromophores

Research Thesis

Presented in Partial Fulfillment of the Requirements for Graduation "with Research Distinction in Chemistry" in the Undergraduate Colleges of The Ohio State University

by

Cassandra J. Henderson

The Ohio State University

August 2013

Project Advisors: Noel M. Paul and J. Clay Harris, Department of Chemistry and Biochemistry

Table of Contents

List of Figures

List of Tables

List of Schemes

Abstract

Investigation of current ion sensing technology has revealed both the great need for new anion sensors in medicine and environmental science, as well as a number of trends in structural development that can aid in the design of new colorimetric halide indicators for use in aqueous media. Previously, a survey of commercial dyes led the way to a new bromide-sensing design based on the structure of Sudan Black B. Building off of this success, a new approach was taken for the synthesis of iodide detectors from Victoria Blue BO units in a dimeric fashion, incorporating a three-dimensional ion binding site and chromogenic signaling unit in one molecule. Syntheses were attempted for a methylene chain linked dimer through substitution reactions, and a *para*-phenylene linked dimer through Pd-catalyzed Buchwald-Hartwig coupling. Through promising TLC and prep TLC results were obtained by using methods from Marshall and Lewis, NMR and HPLC-TOF mass spectroscopy revealed that almost no product was formed. Rather, partially due to the heat of the reaction conditions, VB appears to have degraded into three major unknown compounds. Future experiments should strive for more mild reaction conditions when working with VB, as well as better purification methods so that modes of analysis can be properly used.

Chapter 1: Motivation and Background Information

The Necessity of a Quantitative Anion-Selective Indicator

A devastating genetic disorder, cystic fibrosis is caused by mutations in the cystic fibrosis transmembrane conductance regulator (CFTR) gene. The encoded CFTR protein is a cAMP-mediated cell chloride channel, allowing chloride to flow in and out of cells according to the electrochemical gradient. But when mutated, these chloride channels can no longer be stimulated by cAMP, leading to imbalance in the chloride and sodium ion gradients. Clinically, this manifests as persistent sinopulminary infections, gastrointestinal complications, and occasionally clubbing of the digits or congenital absence of the vas deferens.[1,2]

The first-line test for cystic fibrosis is the "sweat test," which has been used since 1959. It involves inducing the patient to sweat, then testing the sweat sample for chloride concentration. A typical CF patient will have chloride levels elevated to 60 mmol/L or beyond, due to the malfunctioning chloride channels which do not allow reabsorption of chloride into the epithelial cells after it has been secreted in the sweat.[2] Chloride concentration is determined using an electronic chloridometer, which costs in the range of five to ten thousand dollars.[3]

Though chloride cell channels are called such, they are not necessarily selective to chloride anions alone. Other anions such as iodide may pass through the channels even more readily; however, chloride is the most commonly observed as it is present in cells in the greatest abundance.[4] This has implications for the observation of channel activity, since anions used in cell assays are not limited to chloride. For example, halide sensors have been produced which detect the passage of iodide through chloride cell channels by the introduction of an iodide-

quenched fluorescent protein.[5] Unfortunately, these cost several hundreds of dollars and are not yet available for clinical use.[6]

The great expense involved in cystic fibrosis diagnostic testing and analysis of chloride channel function severely limits testing in underfinanced areas or developing countries. The development of a quantitative anion-selective indicator (QUASI) for chloride detection would allow cheap and immediate determination of chloride concentration gradients, and would be beneficial to both diagnostic and research efforts. Thus far, however, such a selective colorimetric indicator has not been produced.

In other industries, chloride and other halide concentrations are currently determined by ion-selective electrodes, ion chromatography, and other alternative methods. Ion-selective electrodes (ISEs) have the major benefit of portability. Typical ISEs cost about $200 to $300 apiece, and a different one is required for each ion being tested. Their use typically requires making standard solutions and calibration curves, as well as adding agents to samples that help reduce interference from competing ions and matrix effects. Not only are they suspect to interference from other ions present in aqueous samples, but their sensitivity is limited by interference from ions embedded in the electrode membrane itself. ISE technology has vastly improved in recent times with the lowering of detection limits and reduction of interference, but is not yet perfected.[7]

Ion chromatography is the most sophisticated ion detection method. It can provide extremely sensitive detection limits and capillary technology has increased its efficiency and waste economy. The latest Thermo Scientific Dionex models boast a mass detection limit of 70 fg and a 0.4 mm capillary column that requires a sample size of only 0.4 μL. The instrument can be operated continuously and it will always be ready to use without having to wait for startup

and calibration times. Even when operated continuously for an entire year, only 5.2 L water will be consumed.[8] However, these large instruments are not portable, and they are extremely expensive to the tune of many thousands of dollars. They also require a great amount of knowledge and experience to use.

Alternative methods for ion detection exist, all of them extremely specific to the ion of interest. These methods involve complex laboratory procedures, often creating metal or cyanide waste that is detrimental to green chemistry efforts. For example, a 6-step method identifies chloride by mercury(II) chloride titration with a diphenylcarbazone colorimetric indicator.[9,10] Another method for chloride detection adds mercury(II) thiocyanate which reacts with chloride, liberating thiocyanate ions. The thiocyanate ions then react with iron to form orange iron(III) thiocyanate.[11] Iodide can be detected by spectrophotometry following addition of nitric acid, NaCl, $NH_4Fe(SO_4)_2$, and KSCN.[12] All of these methods require skilled analysis from trained technicians as well as laboratory access.

All of the currently used analytical methods for halide detection involve some skill and chemistry knowledge, as well as access to a laboratory for part of or the entire procedure. Thus, these methods are not useful for field-testing in remote areas such as the testing done by NGOs and nonprofit organizations in developing countries. These methods cannot provide citizens of developing countries the agency to test their own water supplies without external training or assistance. However, a simple color change upon addition of a quantitative anion-selective indicator to a water sample would be easily understood by most people. The development of a QUASI would bring to the table a fast and simple way for untrained laypeople to test a water supply or any other aqueous solution for a given anion.

There are many other applications for specifically halide detection in drinking-water supplies. Bodies of water are often contaminated with chloride from road de-icing salt runoff, fertilizers, and other industrial sources. Thus, while alone it is considered nontoxic to humans, its presence in water in high concentration is an indicator of nearby pollution.[10] Its counter ion is typically sodium, which has been linked to hypertension and heart disease.[13] Communities with elevated sodium levels in their water supply have been shown to have higher blood pressure.[14] Chloride also complexes with metal cations to form water-soluble salts such as lead(II) chloride and mercury(II) chloride. The major cause of concern, however, is cadmium chloride. Highly soluble in water, it is introduced into water systems through mining, fertilizer waste, and pipe and pipe fitting erosion. From 1910 to 1945, a Japanese community exposed to high levels of cadmium chloride experienced an epidemic of *itai-itai* ("it hurts, it hurts") disease characterized by the severe osteomalacia, osteoporosis, and renal tubular disease resulting from cadmium poisoning.[15,16] Thus, a drinking-water supply shown to have a high concentration of chloride has the possibility of being contaminated with industrial wastes or heavy metals and may be unsuitable for human consumption.

It is also necessary to test for bromide concentration in drinking-water supplies. Bromide is introduced into water supplies by mining, 1,2-dibromoethane in fuel emissions, and fertilizers and pesticides. The recently banned fumigant methyl bromide is degraded in the soil, releasing bromide ions.[17] While bromide, like chloride, is not highly toxic in itself, its presence in drinking-water supplies carries risks. Water supplies are often treated with ozone or chlorine as disinfecting agents. However, when ozone is used as a water treatment, it will form the carcinogenic bromate ion if bromide is present.[18] Additionally, when chlorine is used as the treatment, bromide in the water will be oxidized to bromate or elemental bromine. Both of these

species will then form highly toxic tribromomethanes with other dissolved organic compounds.[17] Thus, it is important to test for bromide contamination before continuing water treatment processes.

Even though at low concentrations fluoride reduces tooth decay, at high levels it can cause crippling skeletal fluorosis. Since the 1940s, it has been known that fluoridating drinking water reduces the incidence of dental caries. A concentration of 0.1 mg/L is necessary to prevent dental decay, and the beneficial effects increase with increasing concentration up to 1 mg/L. After this, increased concentration is less beneficial. At a concentration of 10 mg/L, dental fluorosis in children with developing enamel will be observed. This is mainly a cosmetic effect characterized by yellow and brown mottling and pitting of the teeth, but when severe can cause enamel erosion. When fluoride intake reaches the level of 6 mg/day, there is risk of developing skeletal fluorosis. This risk becomes severe at about 14 mg/day dosages. Skeletal fluorosis is characterized by osteosclerosis, ligamentous and tendinous calcification, and extreme skeletal deformity. The World Health Organization reports that about 2.7 million people in China and India suffer from severe skeletal fluorosis, and these people would benefit from an easy colorimetric indicator to test their water supplies.[19]

Iodide concentration in the body has medical significance as it is essential to thyroid function and concentrates in the thyroid, especially in young children as the organ develops. The 2011 Fukushima nuclear disaster released 4.3 million curies of volatile radioactive iodine-131 into the air, which was later distributed via precipitation onto produce eaten by the Japanese people. Mothers who consumed contaminated spinach risked passing radioactive iodide to their nursing infants, who could develop high rates of thyroid cancer later on. Though iodine-131 is detected with expensive gamma-ray detectors, those mothers would be given the agency to test

their own breast milk for abnormally high iodide levels if an appropriate iodide-selective indicator existed.[20,21]

Besides the many applications for halide indicators, halide salts are also easy to procure and work with and are thus the obvious first choice in initial QUASI development. However, an existing halide-selective indicator would also elucidate potential mechanisms for additional anion detection. When based on an organic dye, this means that knowledge of chromophore properties and molecular interactions with the halide anion could be applied in the creation of structurally similar indicators tailored to the detection of different anions. Existing literature regarding anion detection is comparatively small, and thus creation of a basal indicator for anion detection may lead the way to many successful new syntheses.

For example, indicators tailored for the detection of arsenate and arsenite would be welcomed by the millions of people affected by arsenic poisoning. Arsenate, AsO_4^{3-}, is chemically similar to phosphate and replaces it in many biochemical pathways. Arsenolysis occurs when arsenate outcompetes phosphate in the pathways for the formation of ATP, forming arsenate analogues that simply hydrolyze and cannot be used for the body's metabolic needs. Arsenite, AsO_3^{3-}, binds with biochemically important molecules that contain thiol groups, preventing their natural action. It also inhibits pyruvate dehydrogenase, preventing the formation of acetyl-CoA which is necessary for the citric acid cycle.[22] Arsenic groundwater contamination has been problematic in many Asian countries, especially Bangladesh and the Indian state of West Bengal, where 72% of districts tested in 2001 had arsenic levels above World Health Organization maximums, affecting a population of 147.6 million. The same study identified 12,195 people with clinical manifestations of arsenic toxicity, including skin lesions and melanosis, asthmatic bronchitis, and arteriosclerosis obliterans or cancer requiring amputation.[23]

Colorimetric Sensor Structural Design Overview

The field of host-guest chemistry provides a particular intriguing avenue for QUASI structural development. Host-guest relationship refers to more than one molecule interacting at transient noncovalent sites to form a supramolecular complex. Typically the larger molecule or a larger combination of molecules is designated the "host," and engulfs the "guest" molecule within a structural cavity containing functional group active sites. In this way, host-guest chemistry can be thought of as the synthetic application of enzyme-substrate complexes. The simplest hosts are comprised of a single bowl-shaped molecule, termed a cavitand. More complex hosts can be a combination of multiple molecular units that self-assemble with the guest molecule in solution.

In the context of molecular indicators, host-guest complexes have the ability to provide a high degree of specificity as both the size of the cavity and the active sites within can be finely tailored to attract an anion of choosing.[24] For example, a silicon surface decorated with tetraphosphonate cavitands was shown to selectively bind sarcosine to create a chip for prostate cancer screening (Figure 1). In this case, sarcosine complexed with the cavitands via hydrogen bonding on one end of the molecule, as well as hydrophobic interaction on the other end.[25] A halide ion, however, is unimolecular and does not have the discriminating benefit of multiple interaction sites. In the area of cation detection, indicators based on calixarene and resorcinarene cavitands have been reported (Figure 2). Li^+ is selectively bound to calixarenes with hydroxyl groups, Na^+ is bound to those with carboxymethoxy groups, and K^+ is detected by calixarenes bearing crown ether additions.[26] Resorcinarenes functionalized with thioamide groups have been shown to bind Pb^{2+} cations in competitive media. In this instance, when the thioamide group was positioned further away from the cavitand rim with the addition of a methylene bridge, a

smaller cavity was produced for a tighter fit around the ion.[27] All of the above examples utilize electron-donating groups to complex with cations. Conversely, an anion detector should contain electron acceptors in order to accommodate the negative charge of the guest ion.

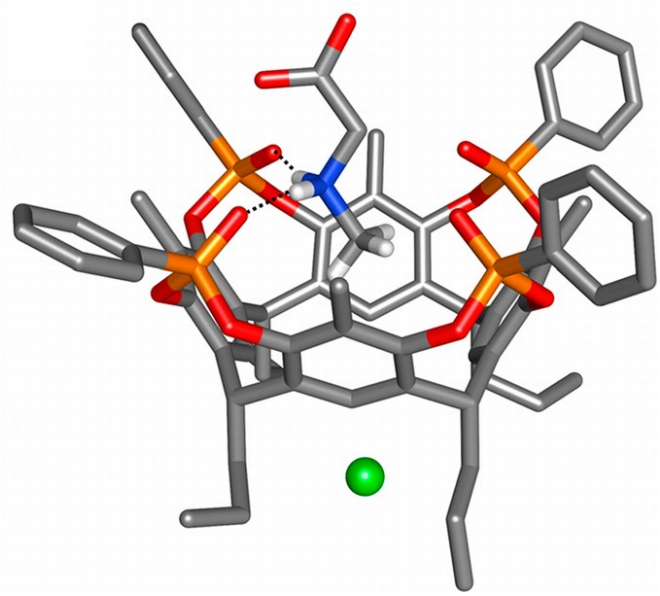

Figure 1: Sarcosine bound within a tetraphosphonate cavitand.[25]

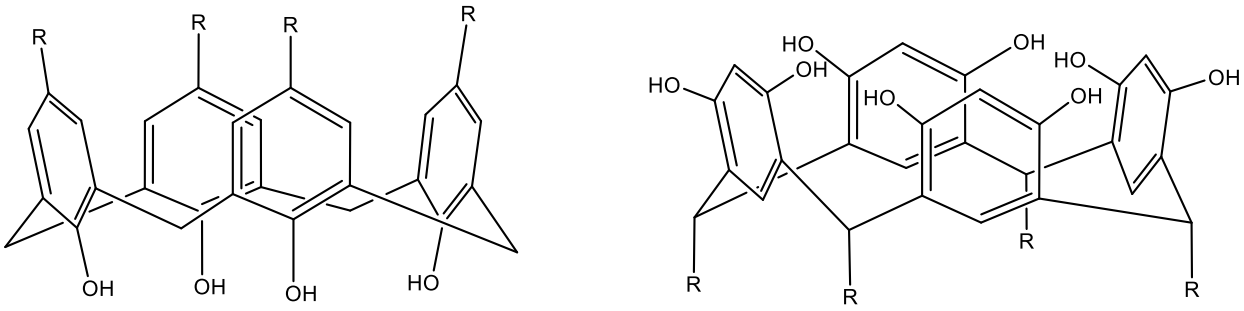

Calix[4]arene Resorcinarene

Figure 2: Calixarene and resorcinarene cavitands.

Cavitands provide an elegant and highly tailored option for the development of ion sensors, but they are not in themselves capable of a colorimetric response. In order to enact a visible effect, the molecule must be outfitted with an additional piece containing some

chromophore or fluorophore. Some success has been found in addition of these units to calix[4]arenes for both cation and anion detection.[28,29,30,31] Fundamentally, a simple scheme is typically employed in the development of new ion sensors. An ion binding site is covalently connected to a spacer structure, which is then connected to a signaling unit containing the chromophore or fluorophore (Figure 3A). Ion binding at the active site produces a shift in electron density along the length of the molecule, generating a change in the absorption and/or emission spectrum of the signaling unit. The binding site can be a cavitand that utilizes the cavity's size to enhance selectivity for an ion of a particular radius, a foldamer that wraps around the ion in solution to shield it from competitive species, a heterocyclic ring that encircles the ion, or it can be a structure of less defined three-dimensional shape as well. It can be anything that selectively binds to the ion of choice in competitive media, and it typically contains two or more sites that attract or complex with the ion. For example, structures that bind anions can incorporate amine-based hydrogen bond donor groups such as pyrroles, amides, and ureas or thioureas. Another option is positively charged receptors such as guanidinium for charge-charge interaction.[30, 32,33]

Figure 3: Ion sensor fundamental design.

The spacer structure is important in the building of fluorescent PET indicators, where it is typically an aliphatic chain purposed to minimize ground-state interactions. These indicators only produce changes in the emission, not absorption, spectrum upon binding with the ion. If a shift in the absorption spectrum is desired, the spacer must be a conjugation-extending piece, which directly shifts π-system density along the molecule. Sometimes, sensors will follow a dual structural scheme with spacers separating two signaling units from the binding site in a bis format. The spacer can be left out of the design of colorimetric (or sometimes dually colorimetric and fluorescent) indicators, and the binding site and signaling unit instead incorporated into one entity (Figure 3b). In this case, the chromophore is typically an organic dye such as azobenzene, nitrobenzene, indoaniline, or anthraquinone.[30,32] The example below was used by Nishizawa, et al. to produce a colorimetric response selectively in the presence of acetate (Figure 4). The thiourea binding site complexes with acetate through two hydrogen bonding interactions, and the connected nitrobenzene signaling unit produces the visible color change.[34] In this way, the sensor acts as a molecular translator to turn information about the chemical make-up of the solution into visual information that can be more easily understood by the chemist.

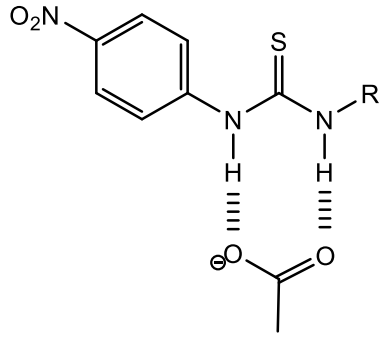

Figure 4: Acetate sensor using a thiourea binding site and nitrobenzene signaling unit.

Previous Efforts and Advancements

Initial Design and Azo Dye Approach

The idea of an ion sensor based on an organic dye that incorporates binding site and signaling unit into one entity was the starting point for this study. It was speculated that some of the larger, more complex dyes might already have the ability to selectively bind certain anions, or contain advantageous structural features that could be further explored. In order to investigate this, a range of commercially available dyes was screened for any preexisting colorimetric properties. The benefit of this approach is that the issue of designing a molecule that absorbs light in the visible range is already accounted for by virtue of the dyes' intrinsic chromophores. Thus, the variable of the signaling unit is already partially eliminated, allowing a unidirectional approach by investigating the binding unit. Alternatively, we could have started with a structure known to selectively bind an anion, and then attached a chromophore to that.

The screening of commercial dyes yielded three potential hits that responded selectively to either chloride, bromide, or halide. Because of fluoride's basicity and often different behavior from the other halides, it was not tested in these initial studies. The first two dyes found to exhibit colorimetric effects were Janus Green B and Sudan Black B, both in the azo dye class (Figure 5). The third was Victoria Blue BO, of the triarylmethane dye class, and will be discussed in later sections. Azo dyes are a large structural class of synthetic dyes characterized by at least one azo entity usually bridging multiple aryl groups. They are used for dying wool, silk, leather, and cotton, plastic, and food. Some, like methyl orange, are used as colorimetric pH indicators.[35] Azo-based structures have also been used as signaling units in ion indicators such as the one in Figure 6, which selectively detects nitrate.[36] The azo dye approach

summarized herein was spearheaded by researcher Heather Robison and subsequently described in her honors research thesis.

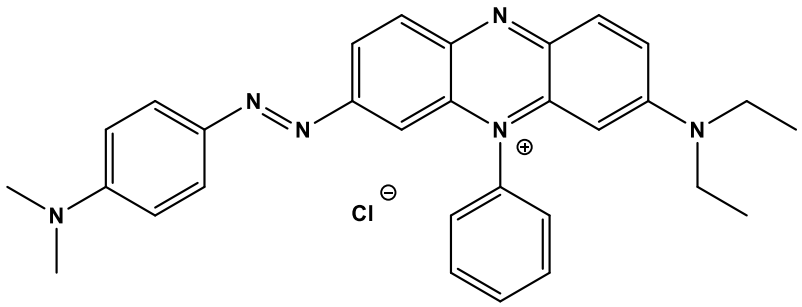

Janus Green B

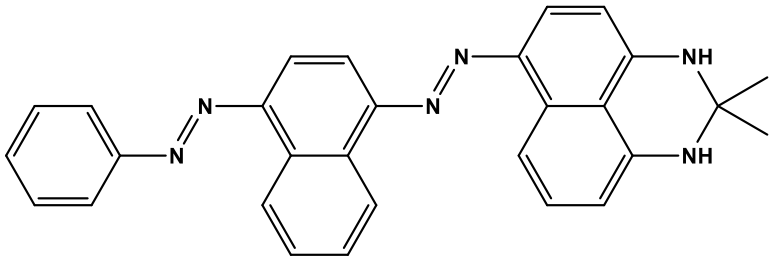

Sudan Black B

Figure 5: Azo dyes found to have colorimetric properties.

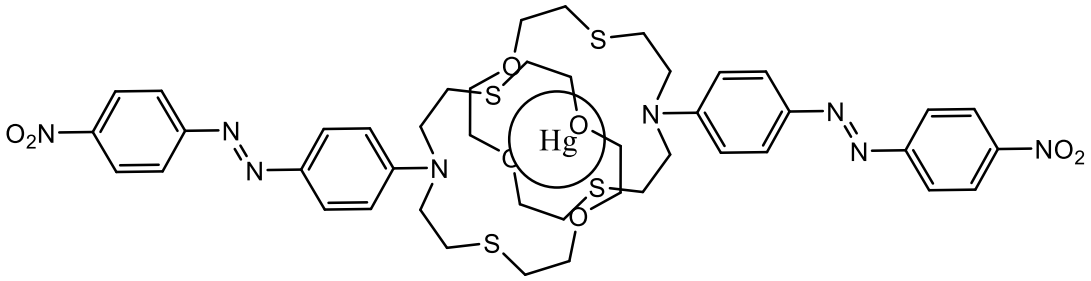

Figure 6: Colorimetric nitrate sensor featuring azo dye signaling units.

The UV-Visible spectrum of Janus Green B in water showed distinct responses to acidic pH and to the presence of potassium chloride (Figure 7). The same response was not seen for bromide or iodide salts. Addition of KCl produced a blue shift of about 40 nm in the absorbance

maximum, large enough to visibly detect a color change. However, the addition of acid had a profound effect, increasing the height of the original peak while also producing a smaller shoulder at 543 nm. Although this second shoulder seems to be close to the absorbance max caused by KCl addition, the same shape occurred whether the acid was HCl or methanesulfonic acid, indicating that it was indeed a pH effect distinct from the chloride response. When acid and KCl were added simultaneously, the pH effect obscured the chloride response considerably.[37]

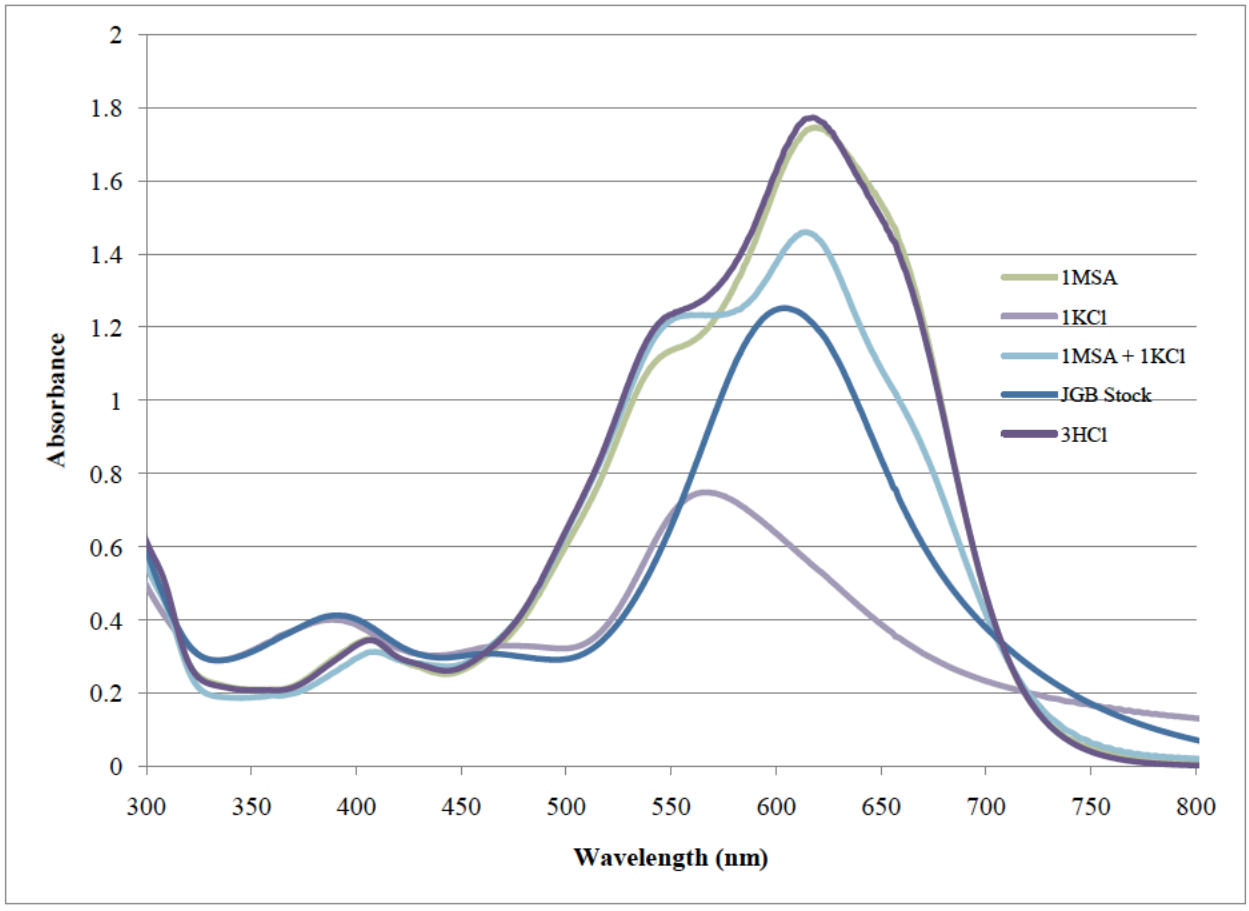

Figure 7: Janus Green B response to acid and potassium chloride in water.[37]

The UV-Visible spectrum of Sudan Black B showed responses quite different to those of Janus Green B, with a selective spectral shift in the presence of bromide rather than chloride

(Figure 8). Because Sudan Black B is insoluble in water, tests were instead run in dimethyl sulfoxide, which has a similar dielectric constant to water and has been used in the literature for comparison. However, this made it difficult to test the response to halide salts due to their low solubility in DMSO. Instead, acid halides were used, followed by addition of hydroxide equivalents to illustrate the pH effect. It was found that in DMSO, addition of hydrobromic acid caused a blue shift of 36 nm in the absorbance maximum which was unchanged upon addition of hydroxide. The addition of methanesulfonic acid also produced little change, indicating that the bromide shift is independent from pH effects. It should be mentioned that when the same tests were performed in dichloromethane rather than DMSO, the pH effect was much more pronounced. The results in DMSO indicate that a pH-independent response is possible; however, caution will be needed when transitioning to aqueous media as it is shown that solvent choice can greatly affect the UV-Vis spectrum.[37]

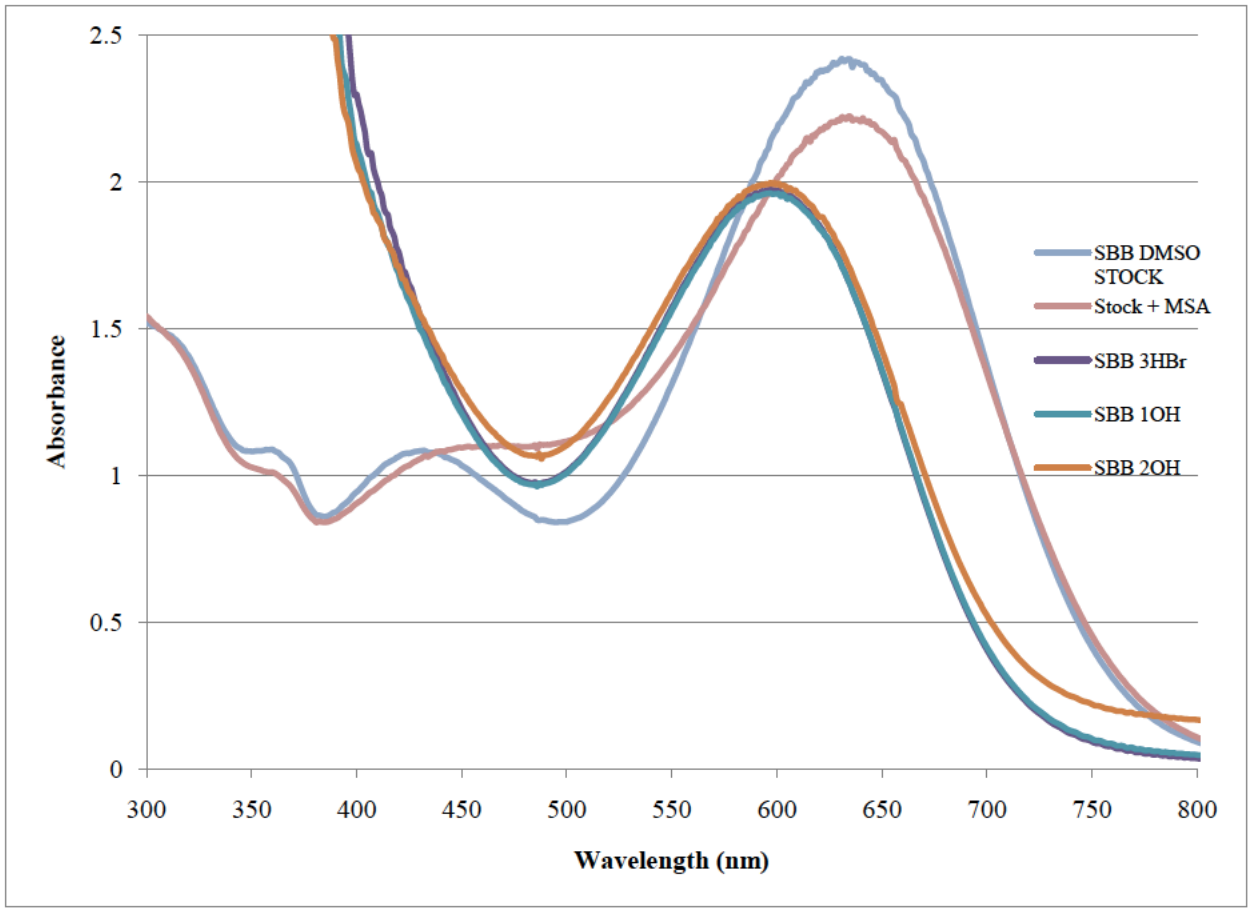

Figure 8: Sudan Black B response to acid, bromide, and base in DMSO.[37]

The bromide response exhibited by Sudan Black B was further characterized by the incremental addition of hydrobromic acid, followed by graphing the response curve (Figure 9). The abrupt cessation of the increasing spectral shift at 36 nm is speculated to be due to saturation of the binding site. When only the early data points are graphed, the response is linear (Figure 10).[37] If saturation is occurring, it is likely because Sudan Black B, like most commercial dyes, is not a pure substance. In addition to side products and analogs formed during the synthetic process, commercial dyes can also contain small amounts of other dyes for shading purposes.[38] Sudan Black B specifically was shown to have two major components and at least eight minor components in a TLC study by Marshall.[39] Thus, it is probable that only some or one of the

components is responsible for the linear colorimetric effect, and once it is saturated no more spectral shift can occur.

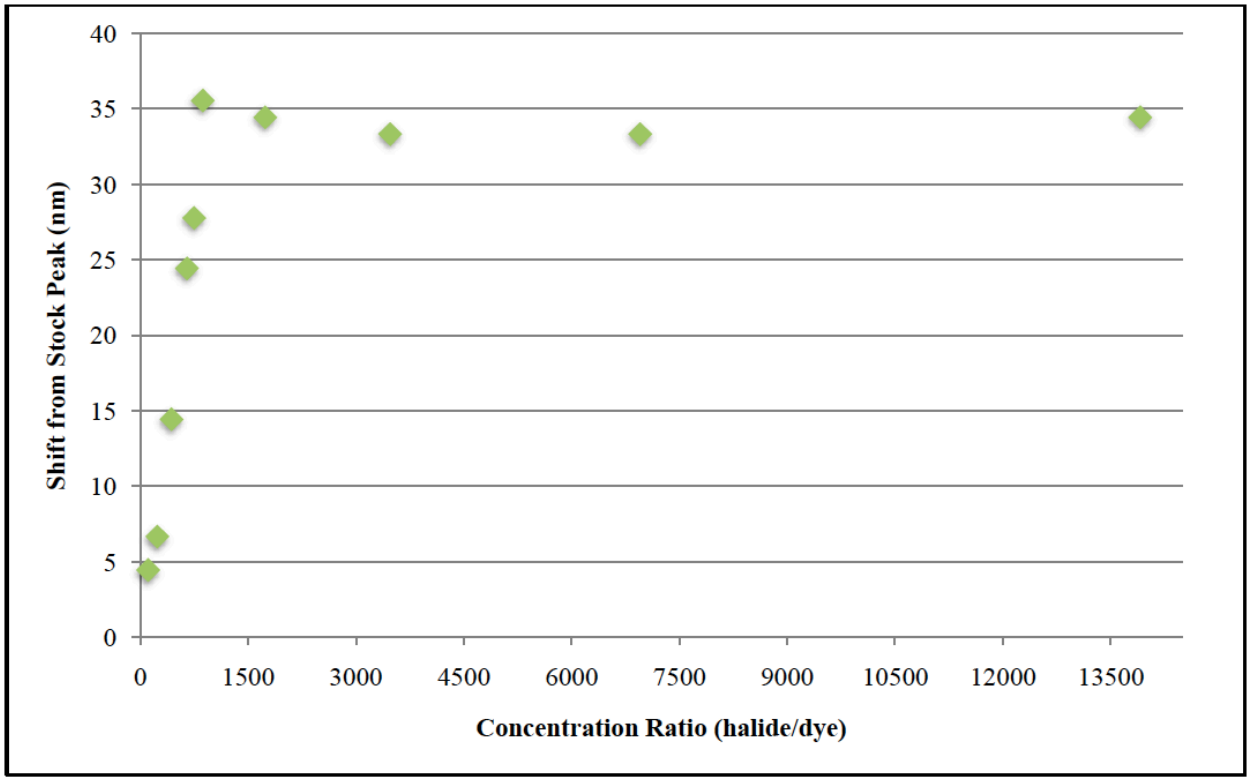

Figure 9: Sudan Black B response to incremental addition of bromide.[37]

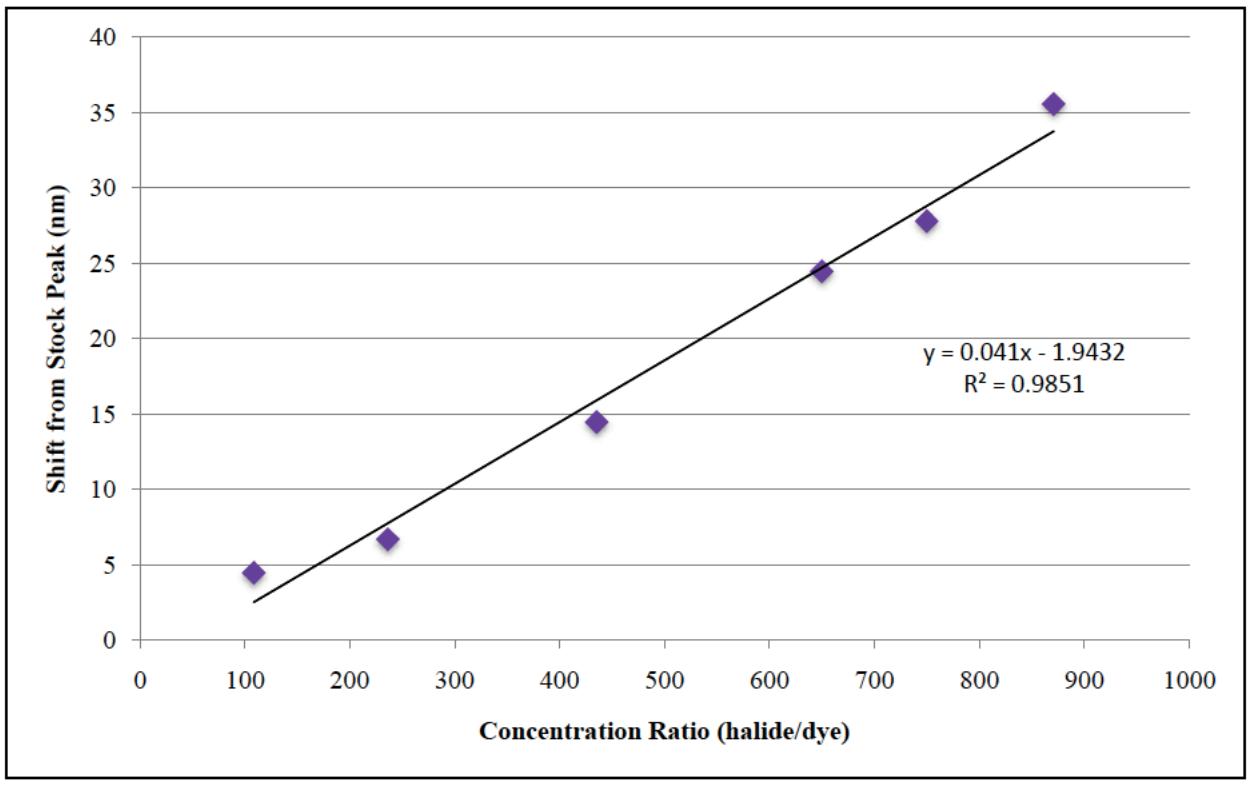

Figure 10: Sudan Black B response to incremental addition of bromide, prior to saturation.[37]

From the results described above, it was determined that Sudan Black B had the greater potential for a structural starting-point in the design of a new halide sensor. Though Janus Green B exhibited a characteristic response to chloride, it was occluded by the pH effect. Janus Green B is also more structurally complex and contains more functional groups, making it difficult to tell which components are responsible for the colorimetric properties. Sudan Black B's response to bromide was pH-independent in DMSO and the molecule is much simpler. Thus, it was decided that new structural designs based off of Sudan Black B's key features would be explored.[37]

Once Sudan Black B had been determined as the structural inspiration for the new sensor design, a survey of many different alterations needed to be tested. This survey required the gathering of a large amount of data. Thus, a project was designed in conjunction with the

Research Experiences to Enhance Learning (REEL) program, which provides organic chemistry students an opportunity to experience real research in the classroom. By pooling data from all of the participating classes, the survey could be completed much faster and the students themselves benefitted from participating in an actual ongoing research project. The structural starting-point was designed in an attempt to preserve the colorimetric effect while increasing aqueous solubility (Figure 11). The azophenyl group was removed for simplicity, and the acetone aminal group was replaced with the free diamine in order to increase solubility. Molecular modeling in unpublished work by Ryan Yoder of The Ohio State University revealed that the central naphthalene portion of the molecule is an area of low charge density that may participate in binding of the anion, and thus was designated as the variable portion. The survey was then conducted by diazotization of variably substituted anilines followed by coupling with naphthalene-1,8-diamine in a scheme modified from the well-known synthesis of methyl orange, a pH indicator azo dye.[37]

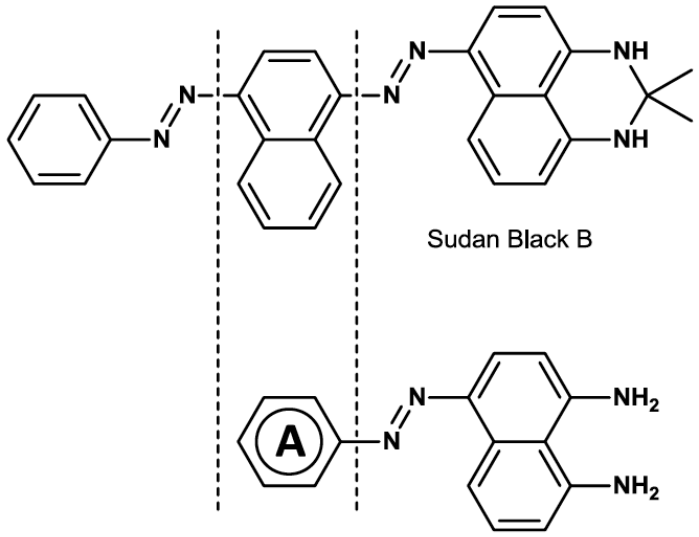

Figure 11: REEL project structural skeleton based on Sudan Black B, where A is a substituted aryl ring of low electron density.[37]

The REEL project synthetic modification survey yielded one structure, 3-ABA-ND (Figure 12), which exhibited solubility in acidic aqueous solution and a blue shift of the absorbance maximum with the addition of bromide, averaged to a difference of 33 nm over several student groups. This similarity to Sudan Black B's response was considered a success even though further characterization revealed that the change in absorbance maximum was not due to a straightforward shift of the spectrum, but instead was due to the flattening of the major spectral peak relative to the secondary one at 428 nm (Figure 13). As the major peak flattens, the secondary peak becomes the maximum value, which was the single value reported by REEL students.[37]

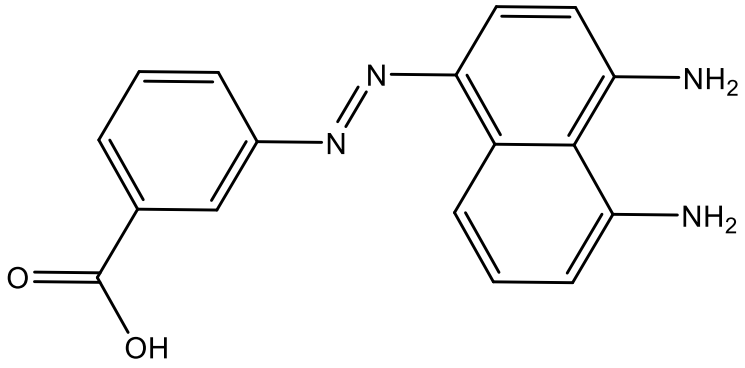

Figure 12: 3-ABA-ND.[37]

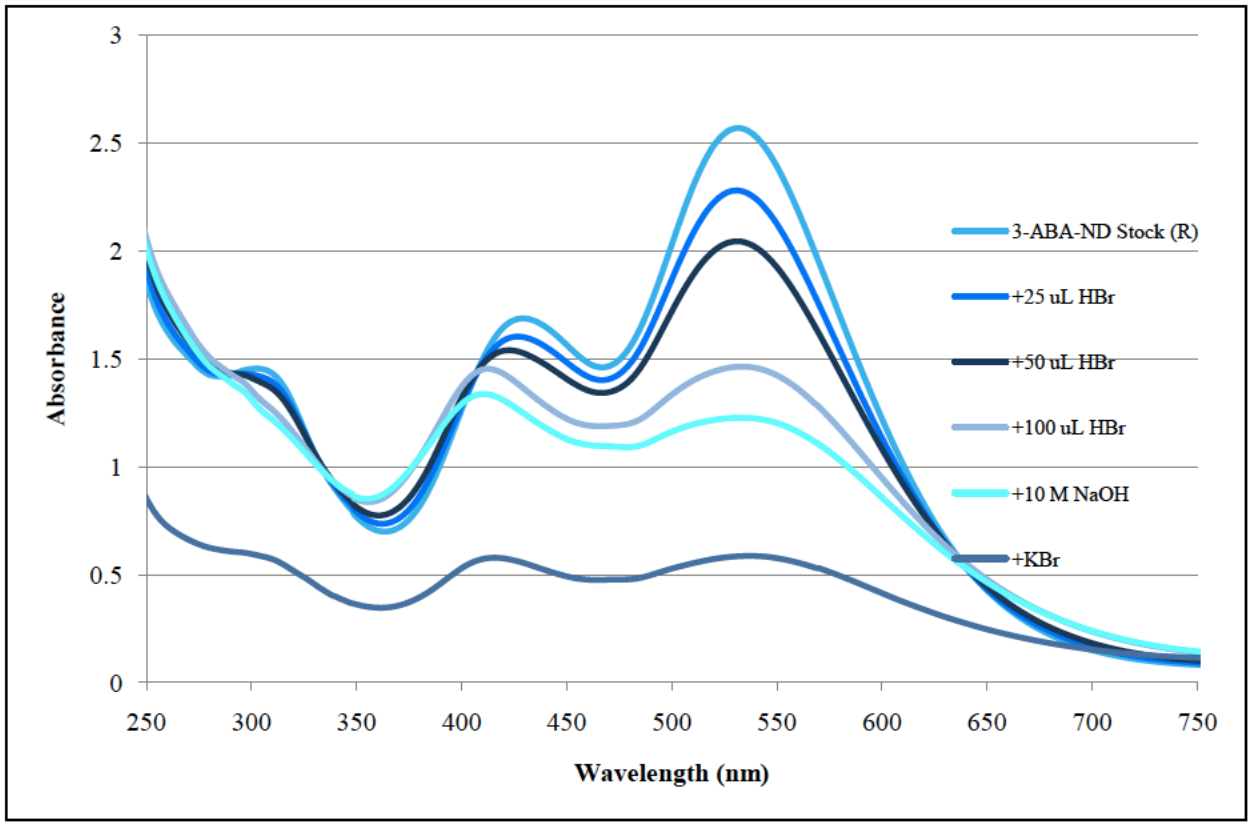

Figure 13: 3-ABA-ND response to bromide.[37]

As characterization and purification efforts continued, it was discovered via NMR spectroscopy and TLC analysis that there were several side products formed during the synthesis of 3-ABA-ND. Literature review revealed the possibility of a doubly substituted product, bis-3-ABA-ND (Figure 14), whose presence in the crude product was confirmed via HPLC-TOF mass spectroscopy. When the synthesis was altered to favor formation of the bis product, the bromide response seen previously in Figure 13 was even more pronounced, with the same flattening of the primary absorbance peak giving way to the new blue-shifted absorbance maximum (Figure 15). Additionally, when the mono-substituted product was purified by preparative HPLC, the bromide response was completely absent and only a pH effect was seen (Figure 16).[37]

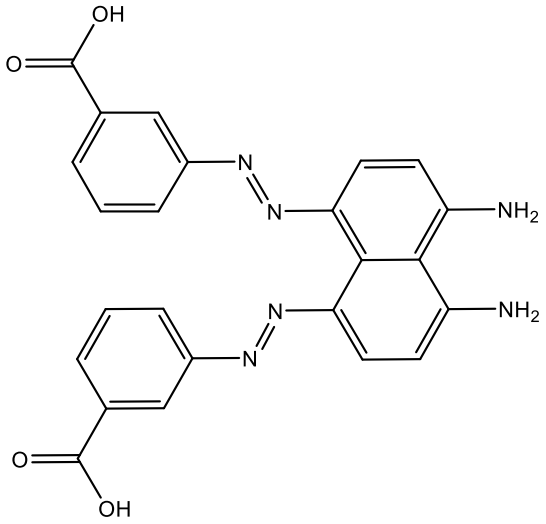

Figure 14: Bis-3-ABA-ND.[37]

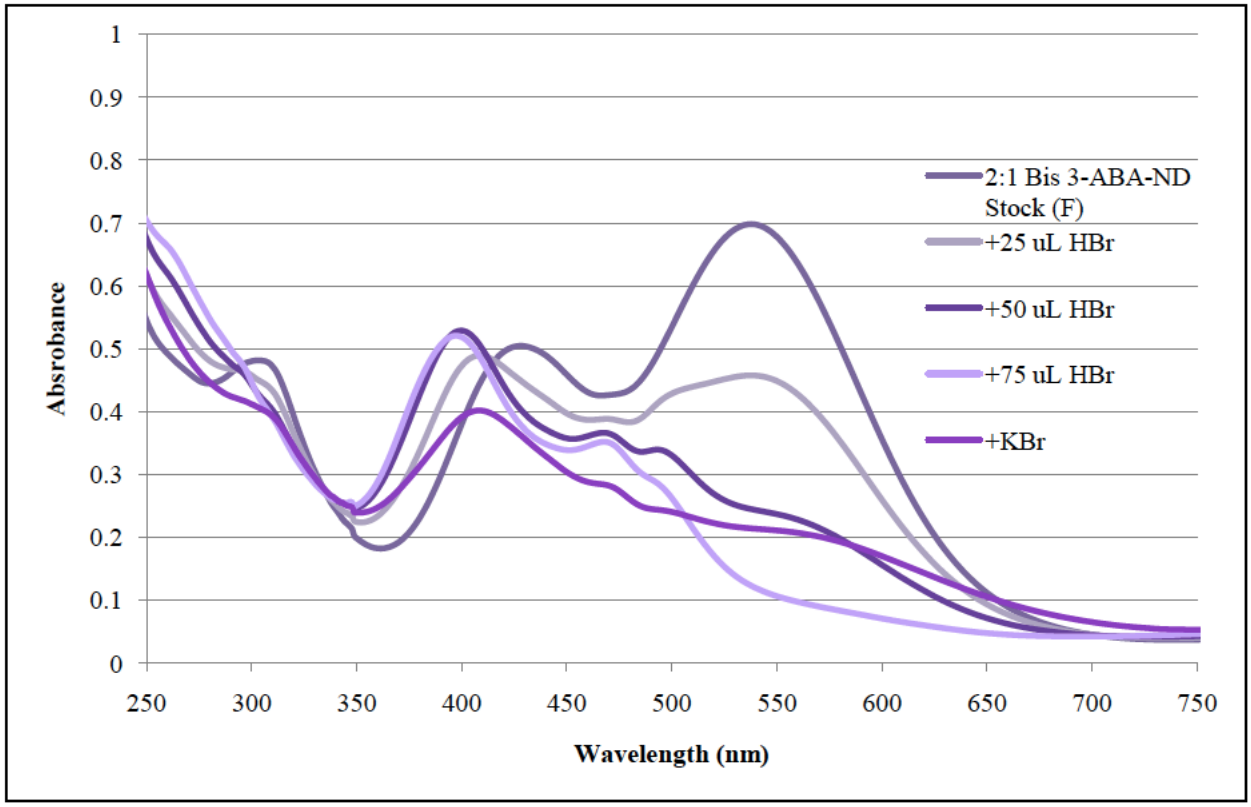

Figure 15: Response to bromide by bis-favored synthetic product.[37]

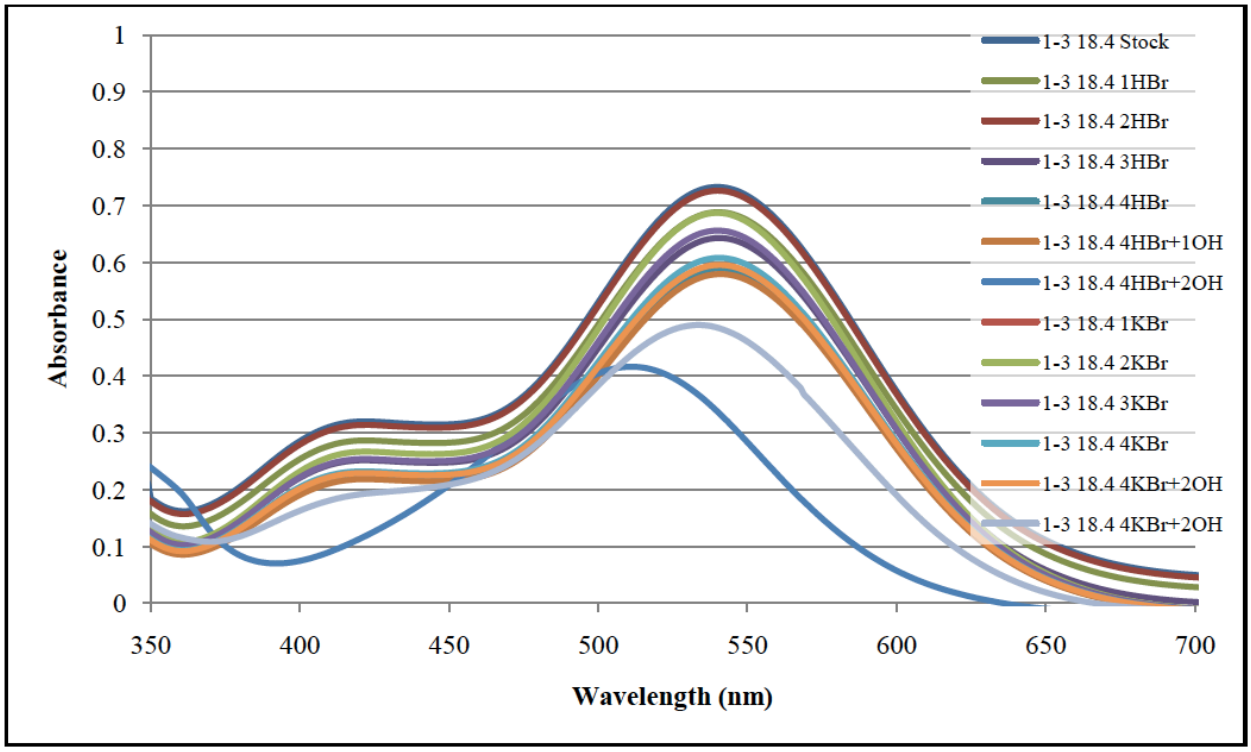

Figure 16: Response to bromide by purified mono-substituted product.[37]

These results support the conclusion that the doubly substituted product bis-3-ABA-ND is the species responsible for the colorimetric effect. This is consistent with the previous data showing a saturation effect in Sudan Black B's bromide response, and hints that a bis-substituted minor component of Sudan Black B may also be responsible for its colorimetric properties. Additionally, the idea that a bis structure may selectively bind bromide is consistent with trends in existing ion sensors described above. The structural features shown to selectively bind ions are cavitands, foldamers, heterocyclic rings, and other motifs having the ability to complex with the ion from multiple points in space. In the acidic solution tested, bis-3-ABA-ND contains a protonated azo group as well as two carboxylic acid groups. These three groups could conceivably hydrogen-bond with the anion from three separate directions, effectively binding bromide within a shallow bowl-shaped conformation.

Triarylmethane Dye Approach

During the initial survey of commercial dyes, three dyes had positive results and were subject to further analysis. Janus Green B responded selectively to chloride, and Sudan Black B responded to bromide. The third dye, Victoria Blue BO (Figure 17), showed a unique spectral shift in the presence of iodide. Unlike the other two, which are azo dyes, Victoria Blue BO belongs to the triarylmethane dye class. Di- and triarylmethane dyes can be considered branched polymethine dyes, in which the polymethine chain is incorporated into two aryl rings branching off of a central sp^2-hybridized carbon atom. The extended conjugation can be visualized by formally breaking the ring carbon bonds so that a polymethine chain subchromophore with two ethylene groups branching off is obtained (Figure 18). A third variable R group is bonded to the central carbon, and it must have π-electrons or lone pairs with which to interact with the rest of the molecule. When the R group is an aryl ring, the dye is called triarylmethane, and when it is not, the dye is called diarylmethane. Dyes containing electron-donating amino groups are very important, and are known as mono-, di-, and triaminotriarylmethane dyes. Victoria Blue BO, also called Victoria Pure Blue BO or Basic Blue 7, is one such triaminotriarylmethane dye and is obtained commercially as the cationic hydrochloride salt. It is used to dye paper and to color printing inks and ballpoint pen ink.[40] It is also used in biological staining, where it preferentially stains mitochondria due to the negative charge maintained within the mitochondrial membrane. Because tumor cells have increased mitochondrial membrane potential, Victoria Blue BO has been investigated as a chemotherapeutic agent where it selectively enters tumor cells and induces a phototoxic effect.[41]

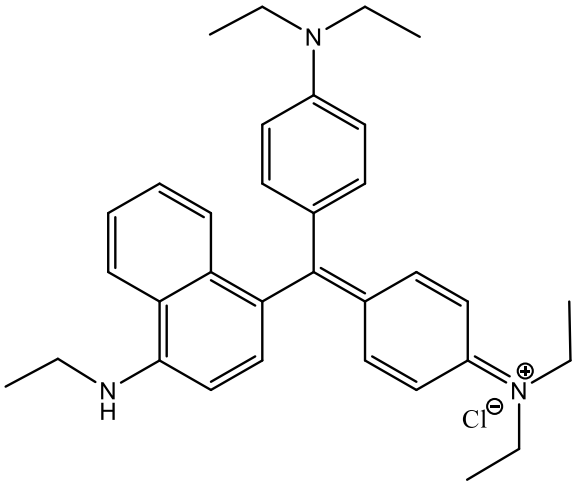

Figure 17: Victoria Blue BO.

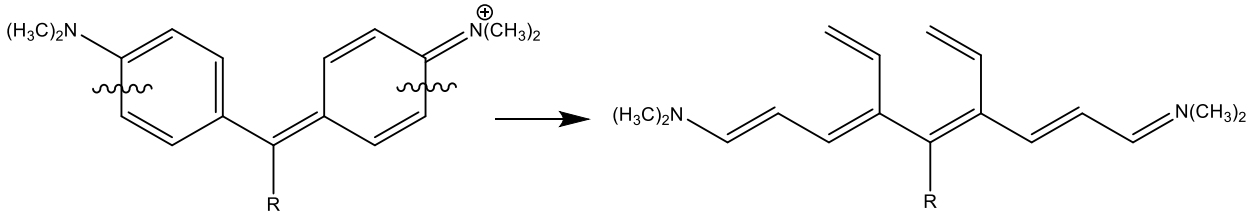

Figure 18: Visualization of the extended conjugation in a di- or triarylmethane dye chromophore.

Unpublished work by OSU researcher Bradford Britton showed the following response of Victoria Blue BO (hereafter VB) in the presence of several anions in aqueous solution (Figure 19). Initially, the UV-Visible spectrum of VB shows two peaks. These two peaks are seen in a variety of symmetrical triarylmethane dyes, and are theorized to be the result of a propeller isomer. The propeller isomer is visualized by twisting the three aryl rings out of the plane of the molecule, and as this form equilibrates with the planar form in solution, two absorbance maxima are observed.[42] Interestingly, when VB is allowed to crystallize slowly, it forms green crystals with a metallic appearance. The same metallic green is noted in solutions where VB is not well-solvated, and is hypothesized to be due to planar stacking of molecules into flat sheets which reflect the light. In the UV-Vis spectrum below, the more blue-shifted peak becomes dominant

upon addition of sodium iodide. If this peak is indeed present due to the existence of a propeller isomer, its dominance may indicate a stabilization of the propeller by complexation with iodide.

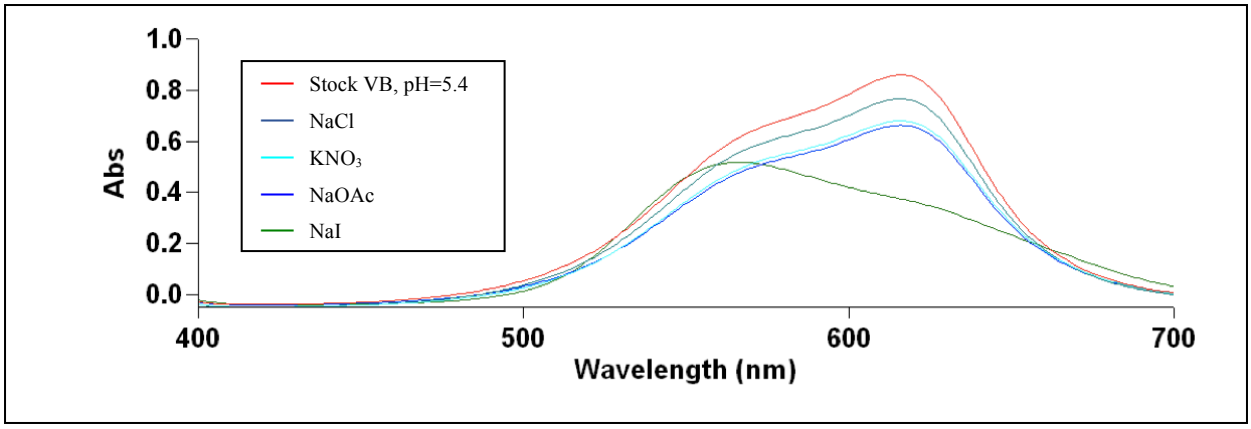

Figure 19: Victoria Blue BO response to iodide and other anions.

Designing a novel indicator based on VB has several benefits. Firstly, VB is water soluble and thus its chromogenic properties are more likely to translate to a structurally similar sensor in aqueous solution. Second, VB is a far more homogeneous dye than Sudan Black B. It was obtained as a 95% pure compound from MP Biomedicals and an equally pure compound from Tokyo Chemical Industry. Though TLC analysis showed some minor contaminants, NMR spectroscopy confirmed that it was pure enough to be confidently used in synthesis, and its colorimetric effect is undoubtedly caused by the nominal dye rather than a contaminating compound. And lastly, its single secondary amine group is likely the most reactive site for substitution, reducing the number of side-products formed. It may also be subject to nucleophilic attack at the central sp^2 carbon, but this can be easily evaluated because these adducts are colorless.[43] One point of caution should be noted regarding its dramatic response to basicity and therefore occasional use as a pH indicator. As seen in the spectrum below (Figure 20), at a pH of about 10.82 the range of absorbance becomes very broad. Visually, this corresponds to a dark

pinkish or brownish red color depending on the solvent, and is likely due to deprotonation of the naphthyl amine, which corresponds to a neutral structure brought about by the change in conjugation (Figure 21). When deprotonated, VB becomes soluble in nonpolar solvents such as diethyl ether due to its loss of the positive charge. Such profound pH effects warrant caution when investigating an ionochromic indicator based on its structural components.

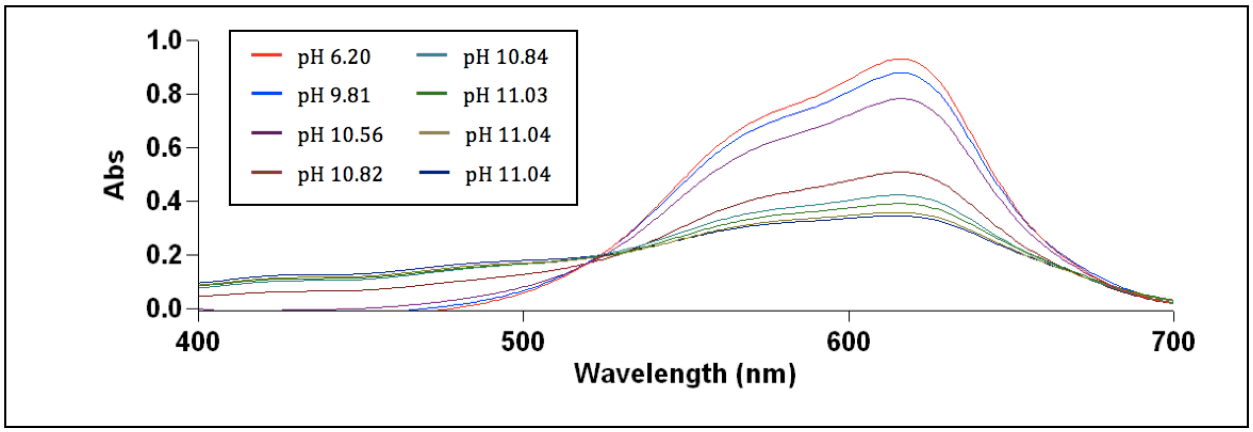

Figure 20: Victoria Blue BO response to incremental pH increases.

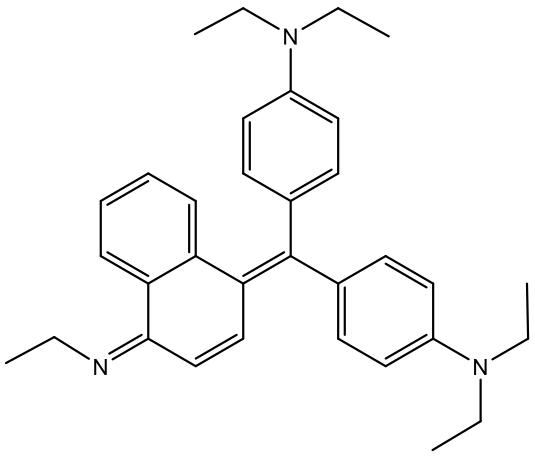

Figure 21: Deprotonated Victoria Blue BO.

In the design of a novel indicator structure based on VB, it was deemed beneficial to include the entirety of the triarylmethane structure due to the possibility of the propeller isomer.

If the colorimetric effects were indeed due to stabilization of the propeller upon complexation with iodide, then the preservation of this effect would require this whole basic unit rather than splitting it into further subunits like the design of the Sudan Black B-based indicator. Instead, the triarylmethane structure was doubled in a bis manner reminiscent of the bis-3-ABA-ND structure described in the sections above (Figure 14). By doubling the triarylmethane with some linking structural unit or chain at the naphthyl amine site, it was hypothesized that the selectivity and binding strength would increase. The linker structure could possibly allow the ion to complex with the triarylmethane structure from two different directions, sandwiched in between each half of the dimer. A number of potential linker structures were proposed, and these are outlined in appendix A.

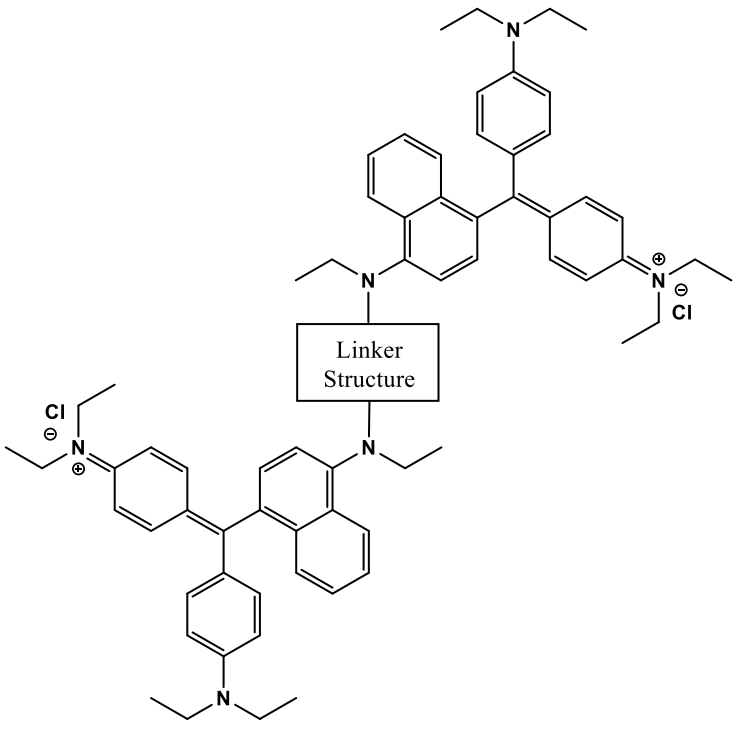

Figure 22: Generic structure of novel dimers based off of Victoria Blue BO.

Chapter 2: Synthesis and Isolation Efforts

Synthesis of Dimer 2

As a starting point and simple basis for the project, it was attempted to synthesize dimer 2 (Figure 23), with a simple aliphatic chain of variable length connecting the two halves. This approach provides the most fundamental basis as it simply doubles the essential triarylmethane unit without adding any additional conjugation or functional groups. It was attempted to synthesize dimer 2, hereafter deemed $(VB)_2(CH_2)_n$, in both n=1 and n=2 forms.

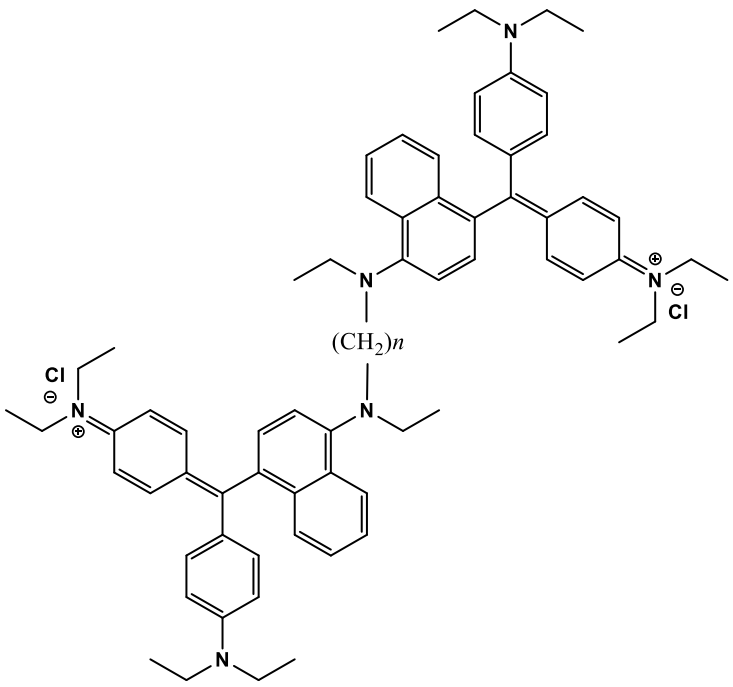

Figure 23: $(VB)_2(CH_2)_n$

Synthesis of $(VB)_2CH_2$

The procedure for synthesis of $(VB)_2CH_2$ was adopted from a 2005 paper by Beifuss, et al. in which condensation of N-methylaniline and formaldehyde in room temperature aqueous

solution produced the N,N-acetal in 69% yield.[44] However, the much larger amount of steric hindrance seen in the triarylmethane structure presented a much greater difficulty for this reaction. Though it is possible to imagine the conformation below (Figure 24) as a minimization of steric interference, ultimately there was no reaction, as confirmed by TLC analysis in acetonitrile. The structure looks promising if one is to imagine the formation of a shallow bowl in which to hold an ion, but the closeness of so many groups seemed unreasonable compared to the conformational freedom of a longer chain analog, so this reaction was not pursued further.

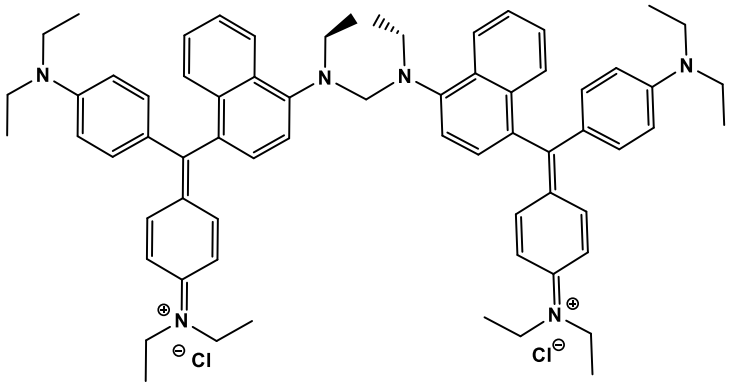

Figure 24: Possible conformation of $(VB)_2CH_2$.

Synthesis of $(VB)_2(CH_2)_2$

The procedure for the synthesis of $(VB)_2(CH_2)_2$ (Scheme 1) was adopted from a 1999 paper by Spencer, et al. in which N-methyldodecylamine was refluxed with 1,2-dibromoethane and potassium carbonate in ethanol to give the bis product in 58% yield.[45] It was hoped that utilizing a procedure that involved this larger amine would translate better to a reaction involving VB than most similar procedures found, which involved small anilines and short-chain substituted amines. However, VB is highly branched while the original N-methyldodecylamine

is not, so steric hindrance was still a factor of uncertainty. Additionally, although the mechanism appeared to be a bimolecular nucleophilic substitution, the original procedure called for ethanol as the solvent. It was thought that a polar aprotic solvent might favor this mechanism more efficiently, so the reaction was attempted both in ethanol and in acetonitrile. This reaction was attempted twice with ethanol as the solvent, and three times with acetonitrile, for a total of five runs (Table 1). Additionally, run 5 was split into two portions, with 5a being stopped at 48 h and 5b being stopped at 96 h.

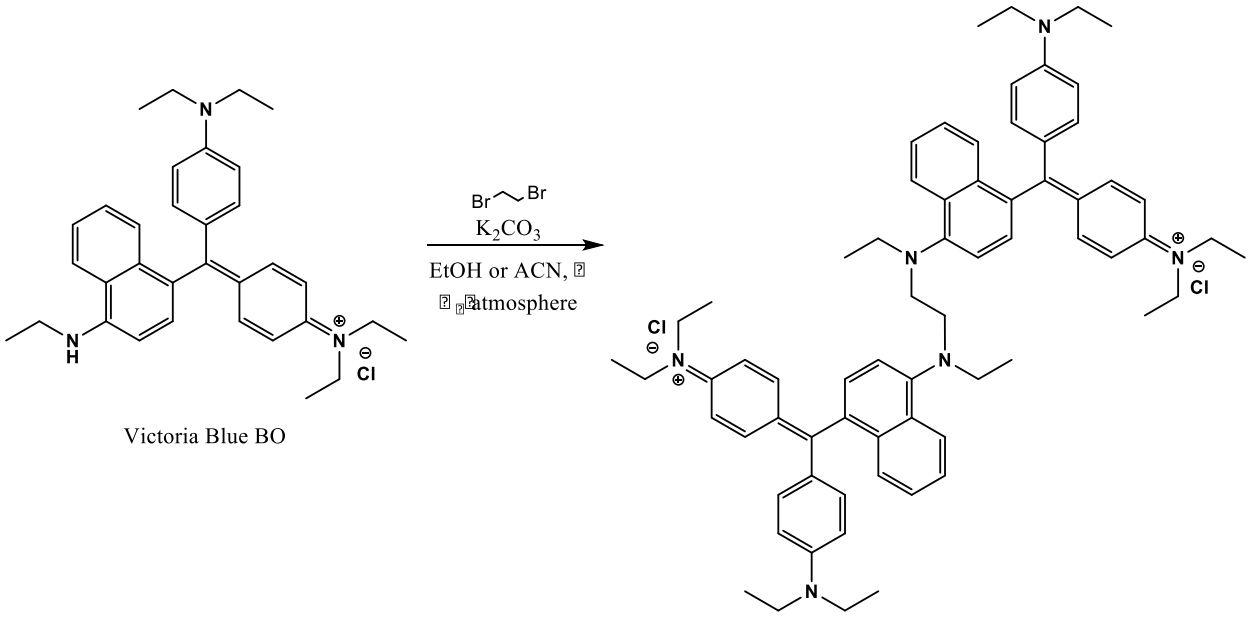

Scheme 1: Synthesis of $(VB)_2(CH_2)_2$.

Run	Solvent	Reaction Time (h)	Product Appearance	Prep TLC?
1	EtOH	96	Dense gritty solid, dark red	Yes
2	EtOH	96	Dense gritty solid, dark blue-black	Yes
3	ACN	96	Flaky solid, red with green metallic sheen	Yes
4	ACN	26	Flaky solid, red with green metallic sheen	Yes
5a	ACN	48	Flaky solid, red with green metallic sheen	No
5b	ACN	96	Flaky solid, red with green metallic sheen	No

Table 1: $(VB)_2(CH_2)_2$ synthetic runs.

For each of these products, a suitable method of isolation was necessary. Due to the high molar absorptivity of these highly conjugated compounds, solutions nearing saturation are extremely deep in color. This made it difficult to tell when a solution was at or near saturation, and thus recrystallization attempts failed. Extraction was also impossible due to the unknown properties of the desired product and the possibility of losing unknown side-products of interest. Thus, a chromatographic approach was necessary because it allows separation of mixtures without much prior knowledge about the components. Once separated, the components are subject to spectroscopic analysis and further characterization.

TLC was always the first effort for characterization of the crude products, as it allows instant feedback about all components and their relative polarities. It also only requires a small sample, and thus many TLC methods can be tried without running out of product. Once an appropriate TLC method is found, the method can then be utilized at the preparative scale. A great deal of time was thus spent investigating TLC methods and fluid phase solvent systems. It was found that fair separation could be achieved on silica TLC plates by spotting samples dissolved in methanol or chloroform, and using a 15% methanol/chloroform fluid phase. However, by varying the methanol proportion, some very polar and some very nonpolar compounds were revealed in the products from the ethanol runs 1 and 2 (Figure 25). Additionally, the aqua umbrella-shaped spot on the plates below only became visible after exposure to UV light and did not disappear later, indicating some UV-prompted reaction on the plate. From these TLCs, it is clear that there are many more components than desired in the crude product, and it is unknown what these side-products could be. Additionally, due to the overlap of so many of the components, this TLC method was not suited for preparative analysis.

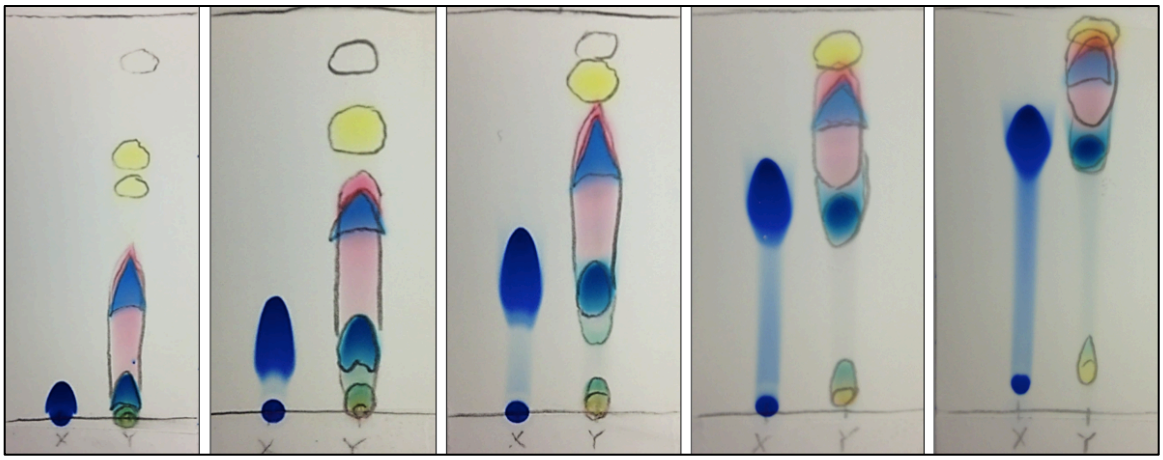

Figure 25: TLC analysis of $(VB)_2(CH_2)_2$ run 2 (EtOH). Left: VB, Right: $(VB)_2(CH_2)_2$ crude product. Fluid phase from left to right: 5%, 10%, 15%, 20%, and 25% MeOH in $CHCl_3$.

In order to find a TLC method that would be effective on the preparative level, a return to the literature was needed. A series of articles were found in which a new TLC method by Marshall and Lewis for analysis of dyes used in Romanowsky blood stains was successfully applied by Marshall for the separation of a number of commercial organic dyes, including sudan and triarylmethane dyes. Marshall separated a large number of components from each dye, including 23 components from samples of Victoria Blue B and 22 components from samples of Victoria Blue 4R. Our Victoria Blue BO starting material was reagent grade, so not as contaminated as these examples, but still did have some extraneous components. The method involves a quick Fischer esterification using 1-butanol, ammonium chloride, and formic acid; then extracting the butanol layer for use as a fluid phase. This solution (M&L eluent) can be used for both regular and preparative TLC.[46,47,39]

Using the M&L eluent, the following TLC was obtained for runs 1-3 (Figure 26). This looks much cleaner than the previous TLC attempts, although it is still not giving perfect

separation. This picture looks deceptively simple, with the two ethanol runs on the right showing a simpler composition than the acetonitrile run in lane number 2. Additionally, VB looks very pure. However, a different TLC run, Figure 27, shows that additional contaminants are present in the starting material. These contaminating spots in varying shades of blue trailing down under the main VB spot are also the same ones that appear in the acetonitrile run. Thus, the acetonitrile run actually looks to be the run with the least side products, since it is mostly VB. The yellow spot that is common to all three runs at the top of the plate was speculated to be product since it is the least polar compound present and since it is in all three crude products.

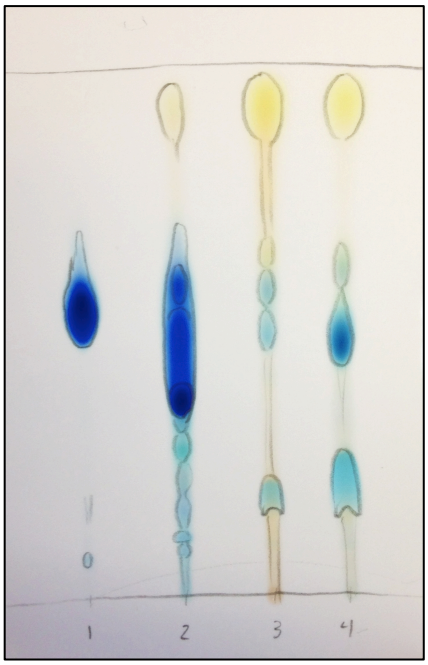

Figure 26: M&L TLC analysis of $(VB)_2(CH_2)_2$ runs 1-3. Left to right: VB, run 3 (ACN), run 1 (EtOH), run 2 (EtOH).

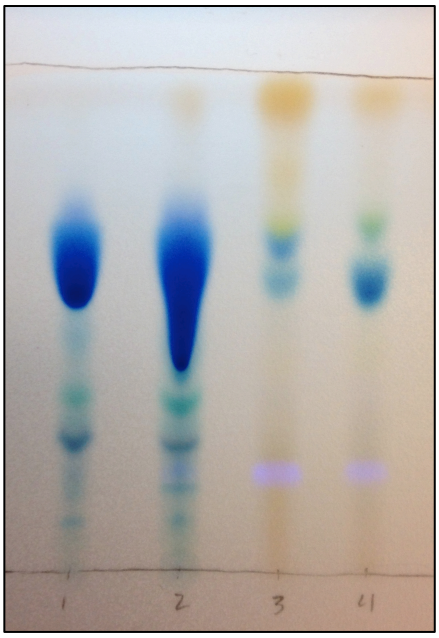

Figure 27: M&L TLC analysis of $(VB)_2(CH_2)_2$ runs 1-3, shown under UV light. Left to right: VB, run 3 (ACN), run 1 (EtOH), run 2 (EtOH).

At this point, it was decided that the transition to preparative TLC should be attempted, with the understanding that prep TLC bands do not always behave exactly the same as regular TLC spots. Using the Marshall and Lewis system, prep TLCs of runs 1-3 were obtained first (Figures 28-30). There was some difficulty determining a suitable solvent for use in rinsing the product out of the silica, especially in run 1 where low product solubility led to isolation of only a small amount of material from bands C and D, and none from band B. Ultimately the M&L eluent was used to great effect, even though the high boiling point of 1-butanol made it difficult to evaporate. Due to this difficulty as well as the complex pattern seen in run 2, only the yellow A bands from runs 1 and 2 (EtOH) were further analyzed. The three bands in the run 3 (ACN) prep TLC seemed fairly straightforward, corresponded well to the spots seen in TLCs above, and were easily removed from the silica, so all three were analyzed. The dullness in the yellow band

A appeared to be due to oxidation after the plate sat out in the air to dry, because aryl amines are known to be highly susceptible to developing brownish or black oxidation from air exposure.[48] For all of the prep TLCs, it was speculated that the yellow A bands corresponded to the desired product.

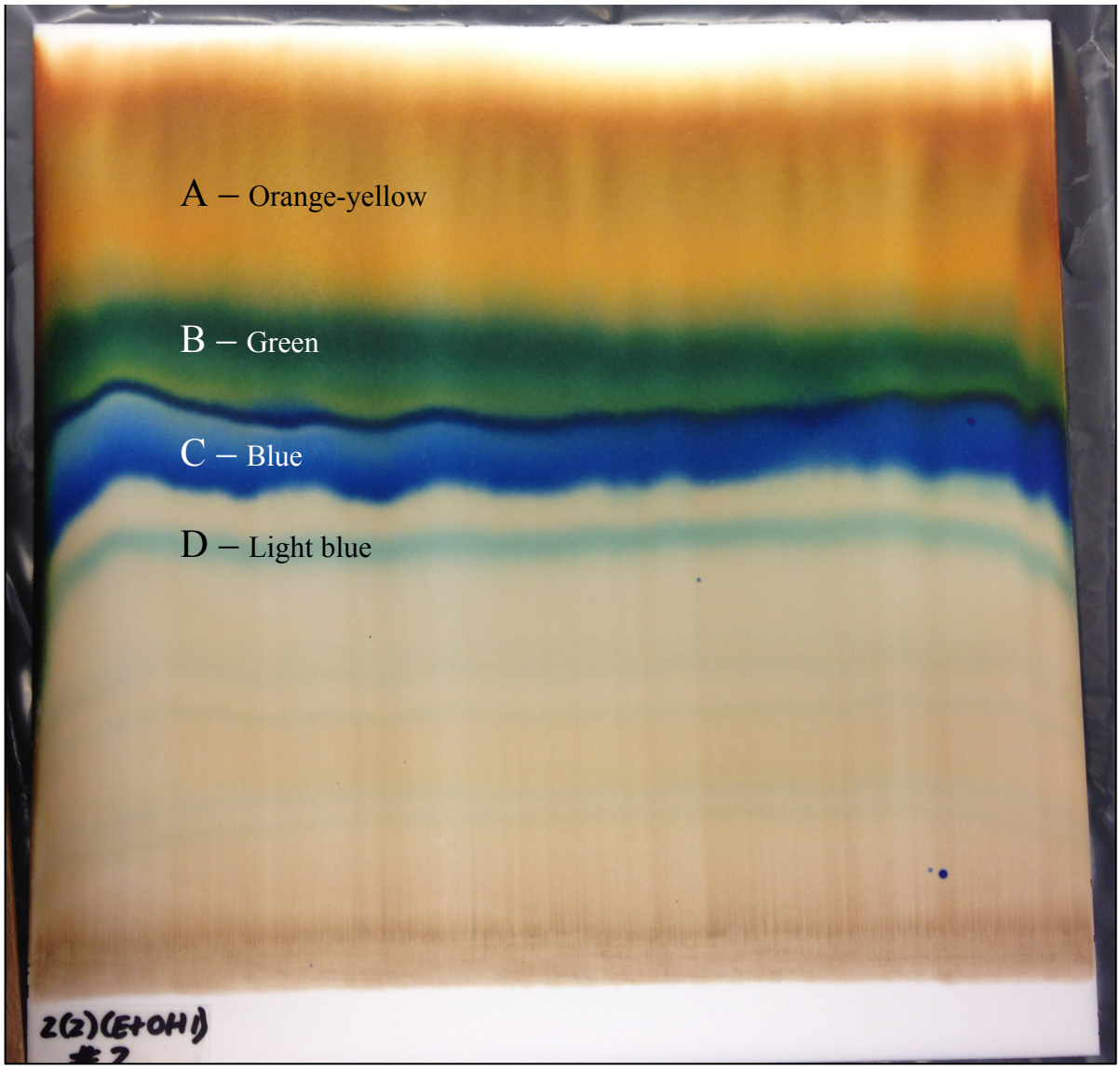

Figure 28: $(VB)_2(CH_2)_2$ run 1 (EtOH) M&L prep TLC.

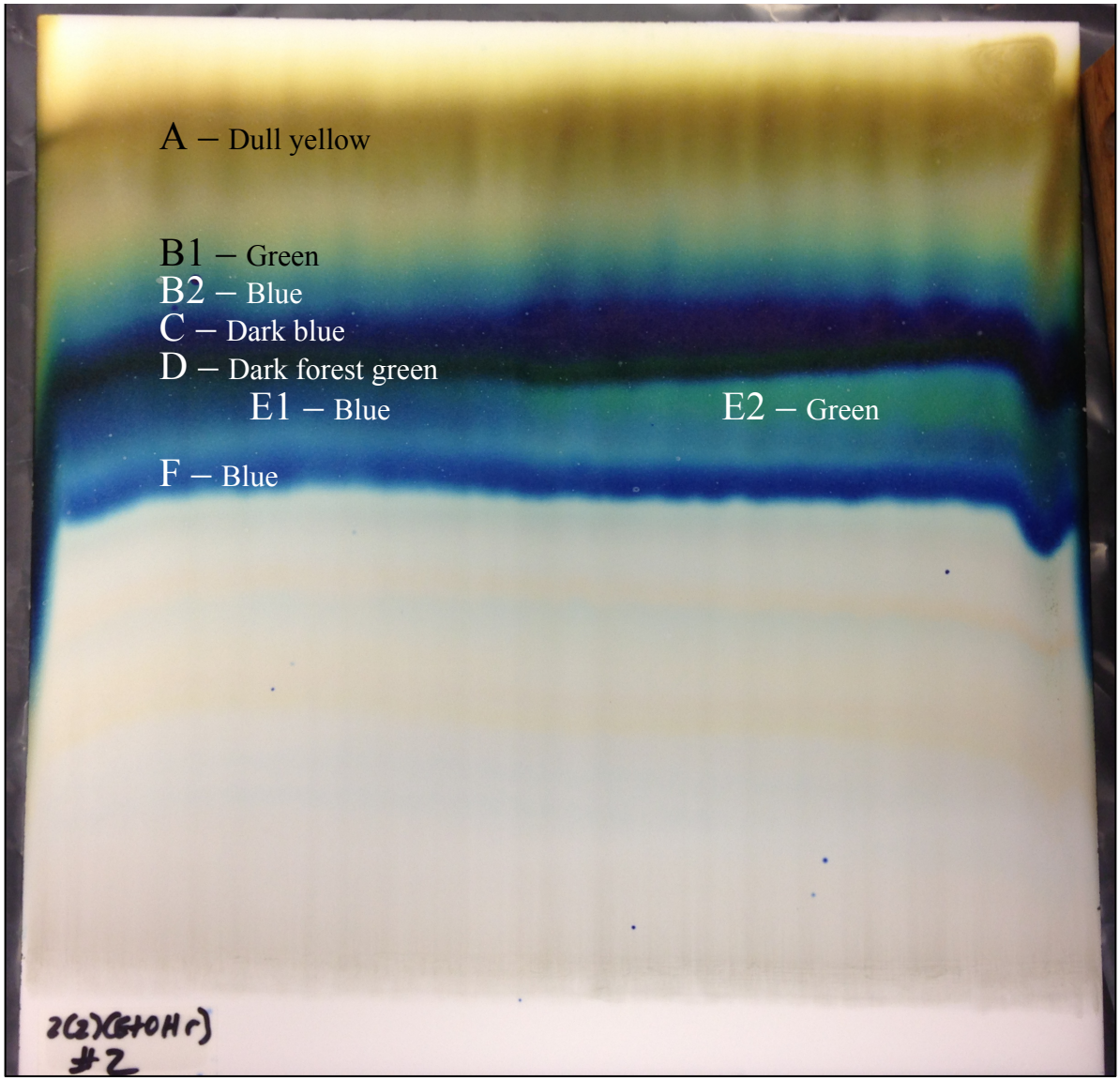

Figure 29: $(VB)_2(CH_2)_2$ run 2 (EtOH) M&L prep TLC.

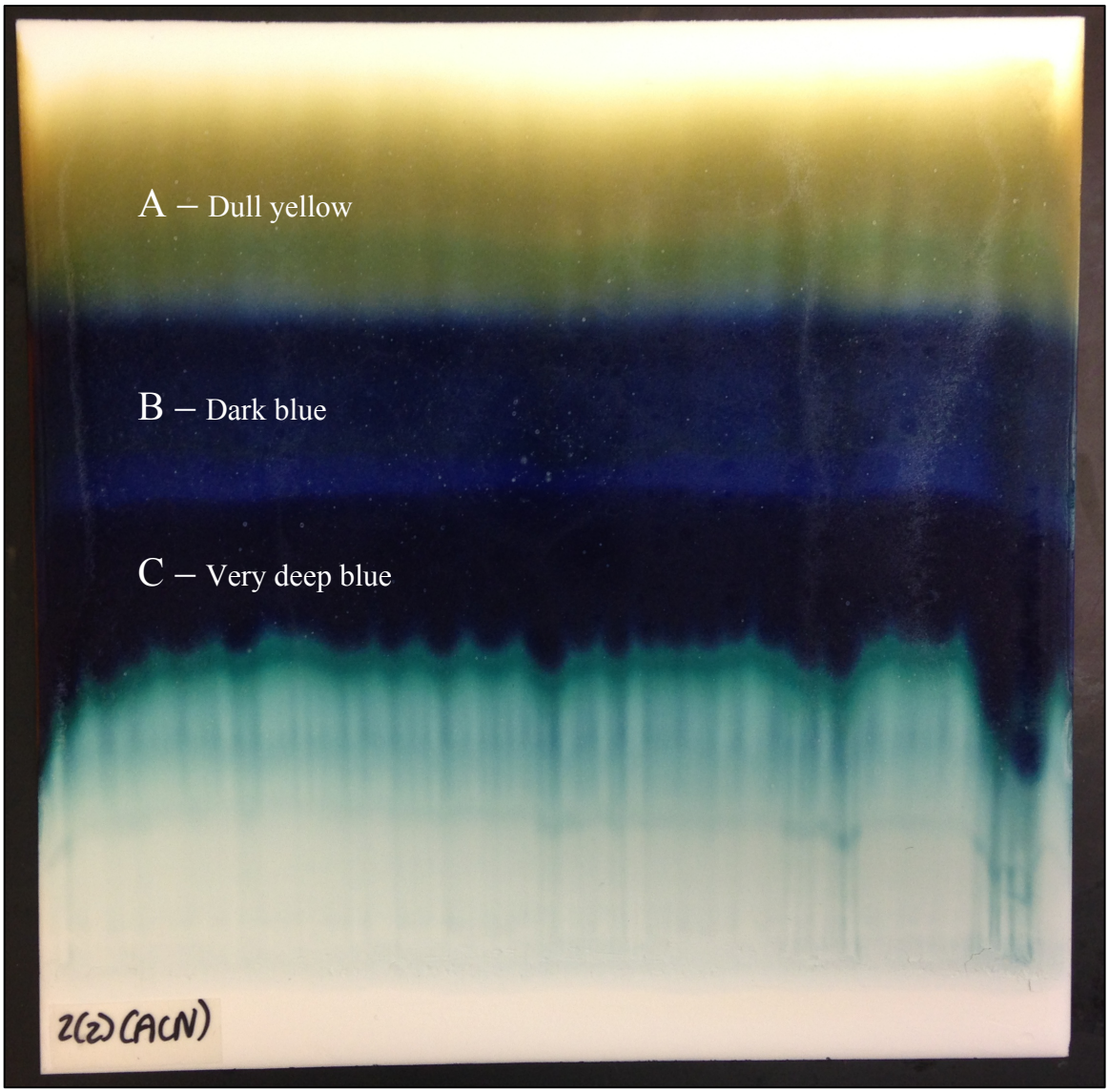

Figure 30: $(VB)_2(CH_2)_2$ run 3 (ACN) M&L prep TLC.

Run 4 of the $(VB)_2(CH_2)_2$ synthesis was done next in an attempt to minimize oxidation and obtain a purer product, and was run in acetonitrile since that seemed to provide the same yellow product while minimizing side-products as compared to the ethanol runs. More caution was taken in purging the reaction set-up and the crude product vial with nitrogen, the prep TLC plate was dried under a stream of nitrogen in a nitrogen-filled drying chamber, and the bands were immediately scraped off the plate and stored in nitrogen-purged vials until analysis could

be completed. VB was also spotted on the side of the plate next to the baseline in an effort to see which blue band (B or C) corresponded to starting material (Figure 31). The result was a very clean prep TLC plate with bands that corresponded to those in Figure 30 above, but were much clearer in color indicating less oxidation (Figure 32). This culmination of all of the TLC efforts provided the purest sample possible of yellow product A, giving 12.9 mg of solid once isolated from the silica. The VB spot corresponded to band B, leaving band C as the band with least knowledge of its components.

Figure 31: $(VB)_2(CH_2)_2$ run 4 (ACN) M&L prep TLC before developing, showing VB spotted on right side.

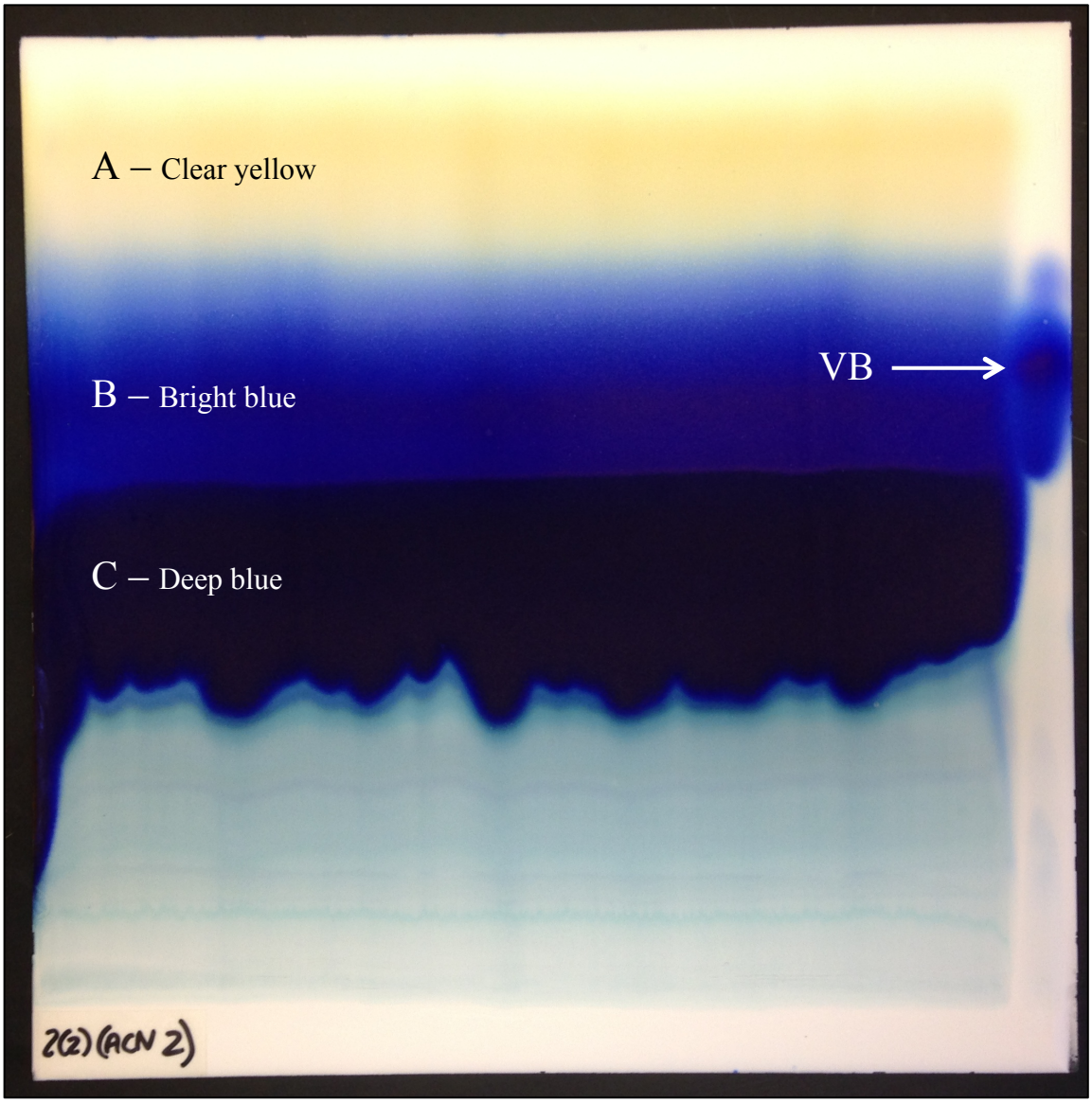

Figure 32: $(VB)_2(CH_2)_2$ run 4 (ACN) M&L prep TLC showing VB spot on right.

Lastly, a final run 5 of the $(VB)_2(CH_2)_2$ synthesis was done in acetonitrile. The purpose of this run was to determine the extent of the reaction after 48 hours and after 96 hours. For this run, half of the reaction mixture was removed at 48 h and designated run 5a, while the other half was allowed to run for 96 h and designated 5b. Prep TLCs were not done for either of these because HPLC-TOF allowed the determination of components in the crude products without the need for purification. HPLC-TOF data showed that these products were nearly identical.

However, it is possible that one sample was mistakenly submitted as both 5a and 5b. Thus, these results are not conclusive.

Synthesis of Dimer 3

Dimer 2 had an aliphatic chain linker, providing the simplest starting-point for these synthetic efforts. However, dimer 3 provides a more complex design and may allow for some electronic communication between the two halves of the molecule. Its synthesis requires aryl amination, which was known to be extremely difficult until the advent of palladium catalysis. Palladium-catalyzed coupling allows the formation of new C-C and C-heteroatom bonds that would normally be very difficult to create. Specific reaction schemes are typically named after their discoverers, such as the Suzuki-Miyaura and Stille coupling reactions for aryl-aryl bond formation and the Heck coupling reaction for alkene substitution. Aryl amination is performed with the Buchwald-Hartwig reaction discovered in 1995 (Scheme 2).[49,50]

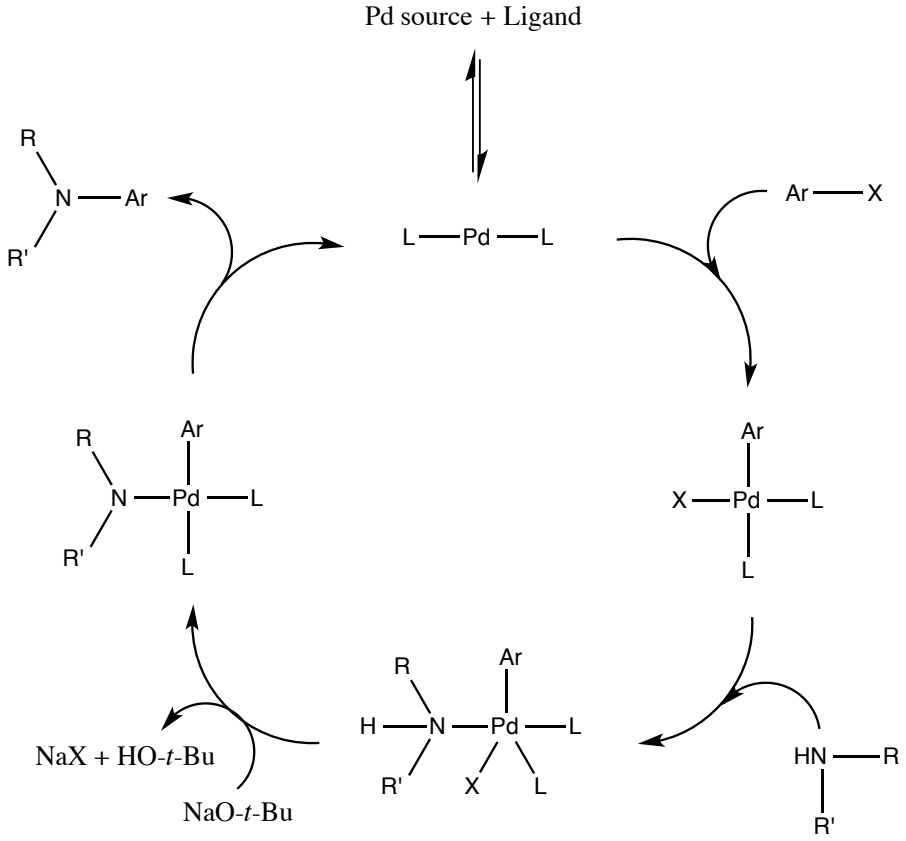

Scheme 2: Buchwald-Hartwig coupling reaction.

The palladium catalytic cycle for aryl amination has four steps. The catalyst itself is often formed *in situ* by adding a palladium source such as $Pd(OAc)_2$ or $Pd_2(dba)_3$ along with the desired ligand. For bidentate ("bi" = two, "dentate" = teeth) ligands such as DPPF (Figure 33), one ligand molecule has the ability to complex with Pd at two sites. Thus both L substituents on the catalyst above are part of the same bulky molecule. After the catalytic species is formed, an aryl halide adds oxidatively to palladium to form a quaternary structure. Next, the amine adds as well. Base deprotonates the amine and a halide salt is removed, which leads the way to reductive elimination of the aryl amine product and regeneration of the catalyst.[50]

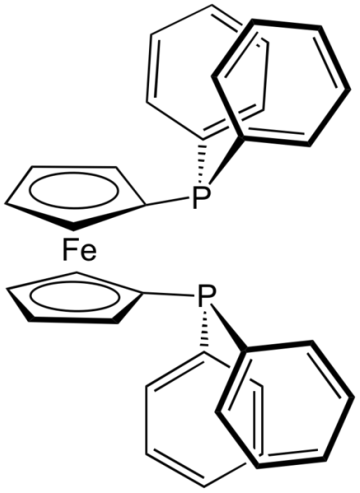

Figure 33: 1,1'-Bis(diphenylphosphino)ferrocene (DPPF).[51]

Synthesis of $(VB)_2C_6H_4$

The procedure for the synthesis of $(VB)_2C_6H_4$ (Scheme 3) was adopted from a 2010 paper by Ito, et al. in which a bulky secondary amine with two triarylamine substituents was refluxed with 1,4-dibromobenzene, palladium acetate, DPPF, and NaO-*t*-Bu in anhydrous toluene for 4 days to give the dendritic or "starburst" oligoarylamine product in 76.2% yield.[52]

This reaction was particularly relevant as the amine reactant is very similar in structure to VB, except that it is a triarylamine having nitrogen as its central atom rather than a triarylmethane having carbon. The dark red solid product was analyzed via HPLC-TOF; no TLC analysis was performed.

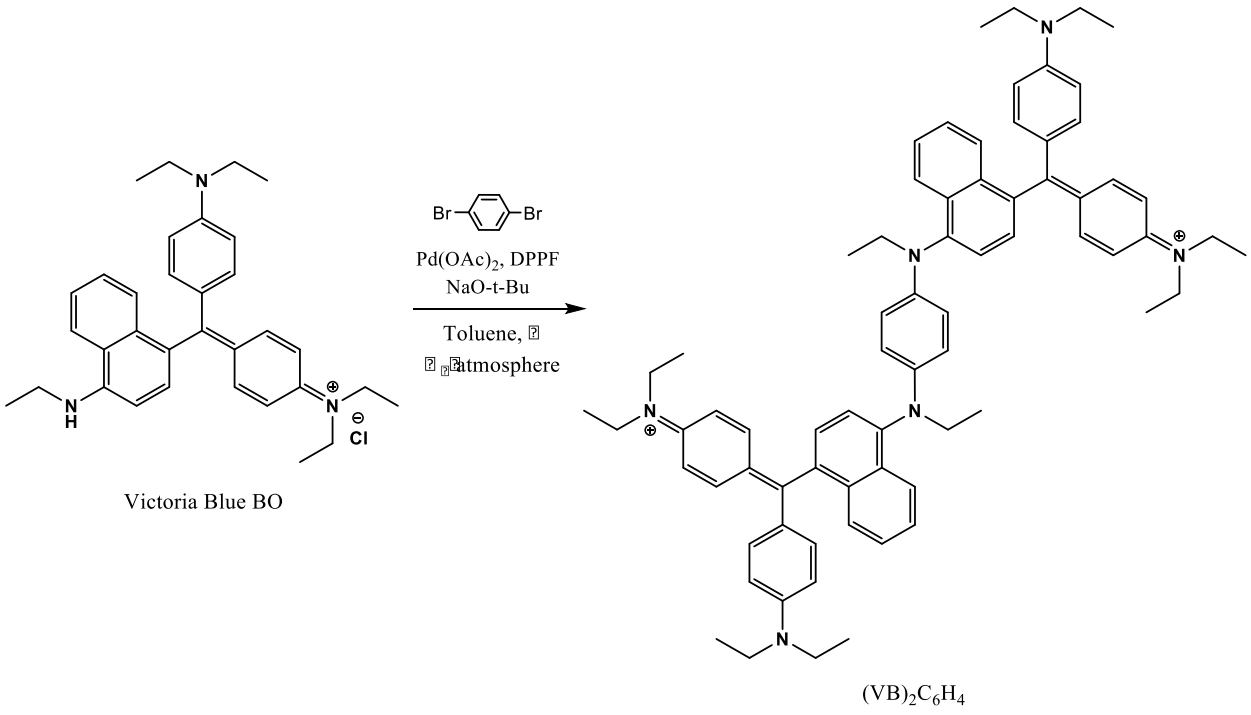

Scheme 3: Synthesis of $(VB)_2C_6H_4$.

Methodology

Synthesis of $(VB)_2CH_2$

A mixture of Victoria Blue BO (5.1414 g, 10.000 mmol), formalin (372 µL, 5.00 mmol), and water (25 mL) was added to a 50-mL Erlenmeyer flask and stirred for 24 h. It was determined via TLC that no reaction occurred.

Synthesis of $(VB)_2(CH_2)_2$

Run 1 (EtOH): A mixture of Victoria Blue BO (2.1210 g, 4.1253 mmol), ethylene dibromide (151 µL, 1.75 mmol), potassium carbonate (0.4839 g, 3.501 mmol), and ethanol (200 proof, 25 mL) was added to a 250-mL round-bottom flask with a magnetic stir-bar and refluxed for 4 days. The product was evaporated and collected with 70 mL chloroform, then washed with 2M sodium hydroxide (4 x 50 mL), dried with sodium sulfate, and evaporated at low pressure to yield a dark red crude product (1.3993 g). The product was isolated via preparative TLC, giving band A as a yellowish brown product (67.4 mg), band C as a tan product (0.3 mg), and band D as a green product (4.6 mg). Band B was unable to be isolated due to insolubility issues and small yield.

Run 2 (EtOH): A mixture of Victoria Blue BO (1.0615 g, 2.0645 mmol), ethylene dibromide (75 µL, 0.88 mmol), potassium carbonate (0.2442 g, 1.767 mmol), and ethanol (200 proof, 10 mL) was added to a 50-mL round-bottom flask with a magnetic stir-bar and refluxed under a nitrogen atmosphere for 4 days. The product was evaporated and collected with 40 mL chloroform, then washed with 2M sodium hydroxide (3 x 35 mL), dried with sodium sulfate, and evaporated at low pressure to yield a dark blue crude product (0.4105 g). The product was

isolated via preparative TLC, giving band A as a dark teal product (51.9 mg), band B1 as a green product (7.1 mg), band B2 as a dark blue product (6.0 mg), band C as a blue product (9.4 mg), band D as a green-purple product (5.2 mg), band E1 as a blue-purple product (6.7 mg), band E2 as a green product (2.6 mg), and band F as a blue product (8.4 mg).

Run 3 (ACN): A mixture of Victoria Blue BO (2.1211 g, 4.1255 mmol), ethylene dibromide (151 μL, 1.75 mmol), potassium carbonate (0.4857 g, 3.514 mmol), and acetonitrile (25 mL) was added to a 250-mL round-bottom flask with a magnetic stir-bar and refluxed under a nitrogen atmosphere for 4 days. The product was evaporated and collected with 70 mL chloroform, then washed with 2M sodium hydroxide (3 x 50 mL), dried with sodium sulfate, and evaporated at low pressure to yield a metallic red and green crude product (1.6842 g). The product was isolated via preparative TLC, giving band A as a dark green product (19.0 mg), band B as a coppery blue product (22.5 mg), and band C as a copper product (105.3 mg).

Run 4 (ACN): A mixture of Victoria Blue BO (2.1208 g, 4.1249 mmol), ethylene dibromide (151 μL, 1.75 mmol), potassium carbonate (0.4837 g, 3.500 mmol), and acetonitrile (25 mL) was added to a 100-mL round-bottom flask with a magnetic stir-bar and refluxed under a nitrogen atmosphere for 26 h. The product was evaporated and collected with 70 mL chloroform, then washed with 2M sodium hydroxide (3 x 50 mL), dried with sodium sulfate, and evaporated at low pressure to yield a metallic red and green crude product (1.4684 g). The product was isolated via preparative TLC, giving band A as a yellow-green product (12.9 mg), band B as a blue product (20.7 mg), and band C as a blue product with red metallic sheen (88.7 mg).

Run 5a and 5b (ACN): A mixture of Victoria Blue BO (2.1209 g, 4.1251 mmol), ethylene dibromide (151 μL, 1.75 mmol), potassium carbonate (0.4836 g, 3.499 mmol), and acetonitrile (25 mL) was added to a 100-mL round-bottom flask with a magnetic stir-bar and refluxed under a nitrogen atmosphere. At t=48 h, 12.5 mL reaction soln was removed and designated product 5a (ACN). The remaining reaction soln, designated 5b (ACN) was returned to reflux and continued until t=96 h. The products were evaporated and collected with 70 mL chloroform, then washed with 2M sodium hydroxide (3 x 50 mL), dried with sodium sulfate, and evaporated at low pressure to yield metallic red and green crude products (0.7575 g 5a, 0.6065 g 5b, 1.364 g total).

Synthesis of $(VB)_2C_6H_4$

A mixture of Victoria Blue BO (0.5093 g, 0.9906 mmol), 1,4-dibromobenzene (0.0780 g, 0.3306 mmol), palladium acetate (0.0048 g, 0.021 mmol), 1,1'-Bis(diphenylphosphino)ferrocene (DPPF) (0.0021 g, 0.0038 mmol), sodium tert-butoxide (0.1100 g, 1.145 mmol), and anhydrous toluene (20 mL, dried 24 h over powdered molecular sieves type 4a) was added to a 100-mL round-bottom flask (dried 24 h at 110˚C) with a magnetic stir-bar and refluxed under a nitrogen atmosphere for 4 days. The product was diluted with toluene, washed with dilute aqueous sodium bicarbonate soln (3 x 300 mL), dried with sodium sulfate, filtered through Celite, and evaporated at low pressure to give a dark red product (0.3109 g).

Preparation of Marshall & Lewis TLC Eluent

A mixture of 1-butanol, aqueous ammonium chloride soln (1% w/v), and aqueous formic acid soln (2% v/v) were mixed in a 12:5:2 ratio in a separatory funnel of appropriate size. After vigorous shaking, the organic layer was extracted and dried with sodium sulfate.

Preparative TLC

Samples were prepared by dissolving 100-200 mg crude product in 2-4 mL solvent to create a saturated soln, and applied to 20 x 20 cm Analtech Uniplate GF silica gel 1000-micron thick preparative TLC plates in one-inch horizontal bands about one inch from the bottom of the plate. Plates were placed vertically in a glass developing tank saturated with eluent vapors, and allowed to run 6-7 h until solvent front reached the top of the plate. Plates were dried under a stream of nitrogen in a nitrogen-filled drying chamber for 1.5 h, then significant bands were immediately marked in the silica, scraped off the plate, and sealed in vials purged with nitrogen. Bands were isolated from the silica by filtering through Celite in a sintered glass filter funnel then evaporating at low pressure to give solid products.

LC-TOF Instrumentation

Samples were prepared in 100% water, 10% methanol (aq), and 50% methanol (aq) solns at the 1 ng/μL level of concentration, then filtered through Agilent Captiva Premium Syringe Filters (PES, pore size 0.2 μm). Data was collected with an Agilent 1200 Series HPLC with an

Agilent ZORBAX 2.1 x 12.5 mm 5-micron C18 column and an Agilent 6224 TOF LC/MS with ESI, and analyzed with Agilent MassHunter Qualitative Analysis software.

NMR Instrumentation

Samples were prepared as saturated solns in chloroform-D. Data was collected using a Bruker Avance III 400 NMR with a 5 mm BBFO probe with Z gradient and auto-tune, and analyzed with ACD/Labs ACD/NMR Processor Academic Edition software.

Chapter 3: Analysis and Conclusions

The objective of this project was to design and synthesize a new colorimetric indicator for the sensing of halide anions in aqueous solution. By reviewing structural trends in literature designs for ion sensors, it was hoped that key components of commercially available dyes exhibiting colorimetric properties could be identified and incorporated into a novel design. A trend was noted in ion-binding structures that encircle, engulf, fold over, or otherwise hold an ion within a three-dimensional construct. Consistent with this observation, it was found that bis-3-ABA-ND, a novel molecule based off of the azo dye Sudan Black B's structural skeleton, exhibited a colorimetric effect in the presence of bromide. This molecule is hypothesized to form an indented shape with three hydrogen-bonding sites that could hold the bromide ion inside.

Building off of this success, a new approach was taken based on the triarylmethane dye Victoria Blue BO, which had been shown to exhibit a colorimetric response to iodide. It was thought that iodide could sit in the center of a propeller isomer formed by the three aryl rings rotating out of the plane of the molecule. Syntheses were proposed for novel dimers based off of the VB subunit joined with a variable linking structure at the naphthylamine nitrogen. This was hypothesized to increase binding ability by allowing the ion to be sandwiched between the two halves of the molecule.

The first synthetic attempt was a dimer created by a simple methylene chain linking structure. When only one methylene group was included, the $(VB)_2CH_2$ dimer could not be formed, likely due to steric hindrance. Thus, a different procedure was attempted which included a second methylene group to make the $(VB)_2(CH_2)_2$ dimer. Multiple attempts were made, with runs 1 and 2 using methanol as the solvent, and runs 3, 4, and 5 using acetonitrile.

All products contained a yellow component as seen in TLC analysis, which was speculated to be the product. However, better chromatographic separation was needed.

When the TLC method by Marshall and Lewis was employed, separation was greatly improved. However, the method was not powerful enough to clearly separate all of the components on the preparative scale. While experimenting with this method, a sample of the M&L eluent was analyzed by NMR spectroscopy. The spectrum, shown in appendix B, indicated that the eluent was almost purely 1-butanol. A tiny amount of the expected butyl formate was present, but only on about a 1:160 scale. Such a small amount is unlikely to make a difference in TLC resolving power, and calls into question the validity of such a method. Nevertheless, the M&L eluent was a significant improvement over other solvent systems, and should be noted for any future characterization of the organic dyes and products relevant to this project. Alternatively, TLCs using pure 1-butanol as the fluid phase may suffice.

Preparative TLC using the M&L method yielded the following isolated components (Table 2). Since band A was speculated to contain the product, it was imperative that it be analyzed. However, the EtOH runs 1 and 2 contained so many side-products and did not have as clear separation, so the rest of the bands were not further analyzed. Runs 5a and 5b were not subjected to prep TLC analysis.

Run	Solvent	Prep TLC Bands	Prep TLC Bands Isolated for Further Analysis
1	EtOH	A: Orange-yellow B: Green C: Blue D: Light blue	A
2	EtOH	A: Dull yellow B1: Green B2: Blue C: Dark blue D: Dark forest green E1: Blue E2: Green F: Blue	A
3	ACN	A: Dull yellow B: Dark blue C: Very deep blue	A, B, C
4	ACN	A: Clear yellow B: Bright blue C: Deep blue	A, B, C
5a	ACN	N/A	N/A
5b	ACN	N/A	N/A

Table 2: M&L prep TLC results for synthesis of $(VB)_2(CH_2)_2$.

The isolated bands indicated above were analyzed by NMR and HPLC-TOF mass spectroscopy. Immediately a problem arose regarding solubility of the A bands. All NMR samples were prepared using chloroform-D as the solvent, which allowed comparison between various spectra. However, the low solubility of the A bands in chloroform-D made the NMR spectra difficult to read. Additionally, there were large peaks corresponding to 1-butanol that obscured important areas of the spectra. Even after drying in a vacuum dessicator for days, the 1-butanol would not evaporate. Ultimately, very little information could be gained from these NMRs.

For the B and C bands, solubility was improved, but still not enough in the case of B. The spectra looked very noisy and were difficult to integrate properly. Additionally, the NMR

spectra were far different from expected. The B bands were expected to look very similar to the NMR spectrum of VB, but it seemed to be missing several key groups. The C bands were very messy and contained many components. It is likely that all of the components with the lowest R_f values did not have enough time to separate out, and thus congregated together within band C. For all bands, 1-butanol contamination obscured much of the data.

The NMR analysis was extremely disappointing. Even though VB is a fairly complex molecule, its NMR was quite clear with the exception of some small residual solvent peaks, and all peaks were able to be assigned for the molecule (Appendix B). Due to the apparent success in the TLC and prep TLC efforts, it was hoped that these prep TLC bands would be relatively pure and some knowledge could be gained from them. However, they were so convoluted and noisy that almost no peaks could be confidently assigned. Future analytical efforts should strive for complete evaporation of the M&L solvent, which would clear up the spectra considerably. Additionally, other deuterated solvents besides chloroform-D should be used to prepare samples of proper concentration.

Eventually, it was called into question whether any product had been formed at all. In order to find out definitively, the samples were analyzed with HPLC-TOF mass spectroscopy. This type of spectroscopy has many benefits and also some disadvantages. The instrument separates the sample components through a high-pressure column, then sends them to the time-of-flight mass spectrometer. Thousands of mass spectra are taken, so that the composition of the sample at each retention time can be seen. Time-of-flight technology allows m/z measurements with precision to four decimal places, unlike quadrupole mass specs, which are much less precise. After the spectra are taken, Agilent Masshunter software can be used to search for any desired compound simply by typing in the exact mass. The greatest benefit of this spectroscopic method

is that if only verification of a compound's presence is required, a pure sample is not necessary because the software can simply search the thousands of data points for the right one. The other main benefit is that only a tiny amount of sample is needed for analysis. The instrument is so sensitive that it can detect the presence of just a few molecules. Thus, there is no danger of running out of sample. This also makes the issue of insolubility largely irrelevant. Samples are prepared in water or in dilute methanol, because the necessary concentration is so low that anything will dissolve in water or methanol enough for the instrument to detect.

However, this extreme sensitivity can also be a disadvantage. The instrument does not only detect the desired components, but also every contaminant that could possibly enter along with the sample. It will detect contaminants from the water used as solvent, from the flask used to make the sample, from dust in the air, and from oil on the chemist's fingertips. This makes it impossible to simply look at the data and analyze the spectra alone – one is dependent on the software to sift through the thousands of extraneous spectra. This makes it very hard to obtain information about a sample unless a specific mass is known. It is possible to find the components present in the greatest quantity in a sample, and then guess their structures based on the masses and computer-generated empirical formulae. This was attempted for the samples in this project, but did not work as well as was hoped.

Using the Masshunter software, two main types of data were analyzed from the HPLC-TOF results. The first is the extracted-ion chromatogram (EIC). This is the chromatogram that is obtained when the software is asked to search for instances of a specific mass. Thus, it shows the presence and retention time of a certain compound, and it was used here to find out whether any of these samples contained the desired product. The following mass to charge ratios were extracted (Table 3), and their EICs can be seen in appendix C. The three unknowns indicated

were subjected to EIC analysis because of their ubiquitous and dominating presence throughout the total ion chromatograms (TICs).

Compound	m/z
Victoria Blue BO	478.3217
$(VB)_2(CH_2)_2$	491.3295
$(VB)_2C_6H_4$	515.3295
Unknown 1	296.2577
Unknown 2	318.2415
Unknown 3	613.4923

Table 3: Mass to charge ratio of items scanned in HPLC-TOF EICs.

The results of the EICs shown below in table 4 indicated some surprising results. Starting material was present in all products as expected, since it was used in excess. However, formation of the expected products was not observed. A trace amount of product may have been found in each of the $(VB)_2(CH_2)_2$ synthetic runs with the exception of run 4, but the yield was so small that it could hardly be distinguished from noise. Instead, the three noted unknown compounds were found in all of the samples but one. In fact, the amount of the second unknown present in run 2 was so great that the instrument was saturated. The only run in which they were not strongly represented was run 4, which is notable because its reaction time was only 26 h. The amount of the unknown components present seems to increase with reaction time, with only a trace amount present in the 26 h reaction and much more present in all of the longer reactions. It would have been helpful to directly compare the amount formed at 48 h in run 5a and at 96 h in run 5b, but unfortunately one sample may have been submitted for TOF analysis as both 5a and 5b. Thus, their results can only be taken to be indicative of a run in ACN with a reaction time greater than or equal to 48 h.

Sample	EIC Results					
	Victoria Blue BO	$(VB)_2(CH_2)_2$	$(VB)_2C_6H_4$	Unknown 1	Unknown 2	Unknown 3
VB starting material	Major component	N/A	N/A	Likely present	Likely present	Present
$(VB)_2(CH_2)_2$ run 1 (EtOH)	Present	Likely not present	N/A	Present	Present	Present
$(VB)_2(CH_2)_2$ run 2 (EtOH)	Present	Some present	N/A	Present	Major component	Present
$(VB)_2(CH_2)_2$ run 3 (ACN)	Present	Likely not present	N/A	Present	Present	Present
$(VB)_2(CH_2)_2$ run 4 (ACN)	Major component	Not present	N/A	Likely not present	Not present	Not present
$(VB)_2(CH_2)_2$ run 5a (ACN)	Present	Likely not present	N/A	Present	Present	Present
$(VB)_2(CH_2)_2$ run 5b (ACN)	Present	Likely not present	N/A	Present	Present	Present
$(VB)_2C_6H_4$ Pd synthesis	Present	N/A	Not present	Present	Major component	Present

Table 4: Compiled EIC results.

The presence of the three unknowns in the starting material indicates that they are not solely due to the reaction conditions. They were not as prominent in the starting material, however, and so it seems that the reaction conditions intensify their formation. Additionally, their presence in the palladium reaction is significant because that procedure was completely different from the others. Even the solvent was different in that case. Thus, their formation is likely not due to any of the reagents or solvents involved. Due to the surprising results shown above, it was desired to find out what these components could possibly be. To this end, a second type of data was used, which was computer-generated guesses for empirical formulae of the major components. These unknown components are listed with their suggested formulae below and their scores out of 100%, which indicates software confidence level (Table 5). Only selected results with a 90% confidence level and above are reported. The suggested empirical formulae

did not match up with any expected side-products or fragments, and so their identities at the moment remain a mystery.

Unknown m/z	**Unknown 1**	**Unknown 2**	**Unknown 3**
	296.2577	**318.2415**	**613.4923**
Suggested Formulae (charge state +1)	99.97% – $C_{13}H_{34}N_3O_4$	99.97% – $C_{18}H_{29}N_4O$	99.91% – $C_{36}H_{62}N_5O_3$
	99.41% – $C_{14}H_{30}N_7$	99.47% – $C_{15}H_{32}ClN_5$	99.52% – $C_{37}H_{73}BrO$
		95.02% – $C_{20}H_{31}NO_2$	99.40% – $C_{31}H_{63}ClN_9O$
		93.69% – $C_{17}H_{33}O_5$	99.15% – $C_{33}H_{65}ClN_6O_2$
		93.64% – $C_{16}H_{27}N_7$	93.55% – $C_{35}H_{67}ClN_3O_3$
Suggested Formulae (charge state +2)	99.99% – $C_{34}H_{64}N_5O_3$	99.96% – $C_{37}H_{64}NO_7$	100% – $C_{70}H_{24}Br_2ClN_4O_7$
	99.48% – $C_{31}H_{67}ClN_6O_2$	99.95% – $C_{36}H_{58}N_8O_2$	100% – $C_{81}H_{25}Br_2Cl_2$
	97.36% – $C_{33}H_{68}NO_7$	99.85% – $C_{33}H_{61}ClN_9O$	100% – $C_{75}H_{28}Br_3N_2O_2$
	96.75% – $C_{36}H_{66}N_2O_4$	99.84% – $C_{34}H_{67}ClN_2O_6$	99.99% – $C_{76}H_{21}BrCl_3N_2O_5$
	94.28% – $C_{33}H_{69}ClN_3O_3$	98.41% – $C_{32}H_{65}ClN_5O_5$	99.94% – $C_{68}H_{38}Br_3Cl_2O_4$

Table 5: Calculated empirical formula guesses for unknown components.

In sum, the HPLC-TOF results showed that while some $(VB)_2(CH_2)_2$ product may have been formed, the yield was incredibly small. Additionally, three major unknown components were found in almost all samples including the palladium reaction, which used a completely different procedure than the others. These unknowns were present in a small amount in the starting material, and appeared to increase with reaction time. The solvents used in these reactions were ethanol, with a boiling point of 78 ºC; acetonitrile, with a boiling point of 82 ºC; and toluene, with a boiling point of 111 ºC. Since the reactions were run at reflux for one to four days, the reagents were being kept consistently at these high temperatures for an extended period of time. Thus, it is likely that these products are due to some natural degradation of the VB starting material, which is expedited by the heat in these circumstances. Future work could try to recreate the reaction conditions while only including VB in the flask, then analyzing to see which

components are present. Confirming an increase of these same components would prove their creation was due simply to degradation of VB instead of some unknown side-reaction.

As a final analysis, it is interesting to look at the EICs for the $(VB)_2(CH_2)_2$ run 3 (ACN) prep TLC bands. In this case, samples far too concentrated were submitted to the HPLC-TOF, overloading the detector. This is not appropriate for regular analysis, but in this case allows the effectiveness to be ascertained of the M&L prep TLC method in separating out the trace amount of product. The resulting EICs for bands A, B, and C are shown in appendix C. While VB starting material is present in the greatest quantity and in all three bands, the expected product only appears in band A. Thus, though the yield was extremely small, the M&L prep TLC method was able to successfully separate the product from some of the impurities. The three unknown components do not seem to be present in any of the bands. This suggests that they were positioned farther down the plate with a lower R_f value than band C, indicating high polarities consistent with oxidized compounds. The EICs also confirm that band A was the correct product-containing band as projected. Future research could examine the efficiency of the M&L method for regular-scale TLC using HPLC-TOF as well. This would be done by running a normal M&L TLC, scraping off the yellow spot that appears with the highest R_f value (such as those in figure 27, corresponding to band A on the preparative scale), rinsing the silica over a small filter made from Kimwipe, and subjecting the resulting sample to TOF analysis. This is possible due to the extreme sensitivity of the HPLC-TOF instrument, therefore requiring only a tiny sample for analysis.

Ultimately, HPLC-TOF showed that these reactions were mainly failures. Although the initial data looked promising, the TLCs were deceiving and EICs for product masses showed that very little product was formed. If degradation of VB was being accelerated due to the heat, it

would make sense that the reaction would not proceed as desired. Thus, if this avenue is to continue being explored, a new milder set of reaction conditions should be employed. However, the M&L TLC system was a success despite the fact that it was likely just 1-butanol. The method was able to successfully separate VB and the products, and translated to the preparative scale with some success. This method should be noted for future work on this or related projects, and could even be used to purify the commercial dyes used as starting materials prior to reacting them. Though the desired products described herein were not able to be tested for colorimetric effects, this avenue should continue to be explored by attempting syntheses of differently-linked structures, such as those containing a longer chain to minimize steric hindrance between the two halves of the dimer. Alternatively, a different dye could be used, such as pararosaniline, which is symmetrical and much simpler than Victoria Blue BO. Not only would this reduce steric hindrance, but it would also make NMR and TOF analysis simpler due to the symmetry. Many options lie ahead for this project, and it should not be abandoned simply because these specific synthetic routes did not work.

Appendix A: Victoria Blue BO Linked Structures

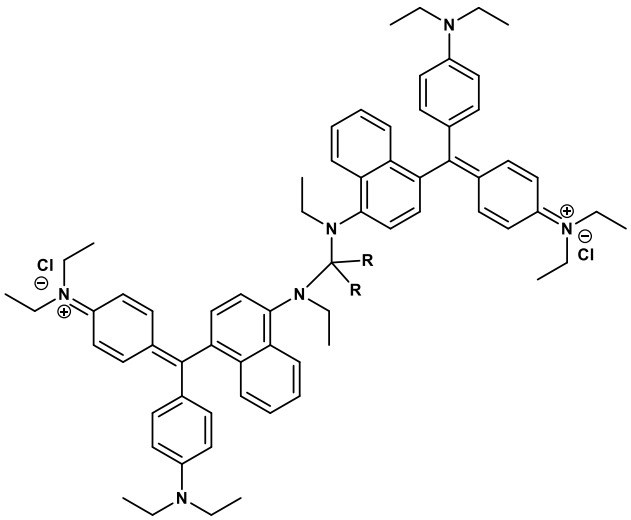

1.

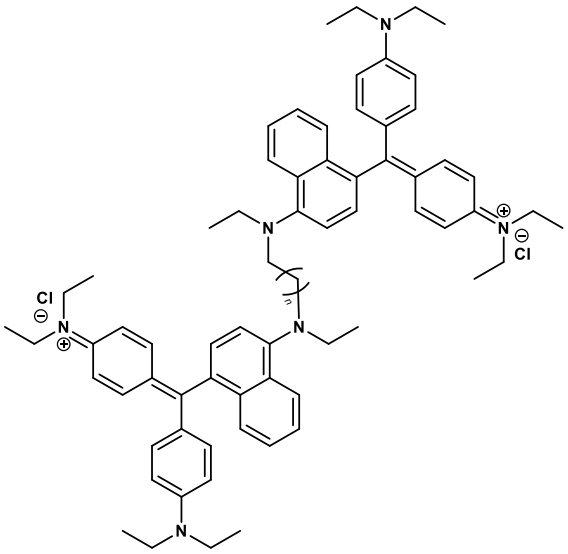

2.

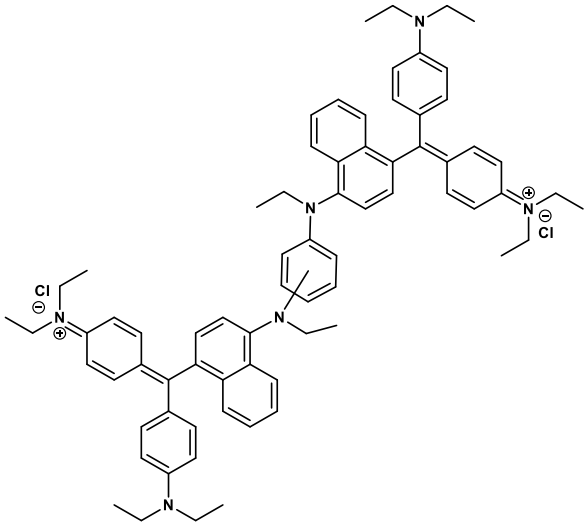

3.

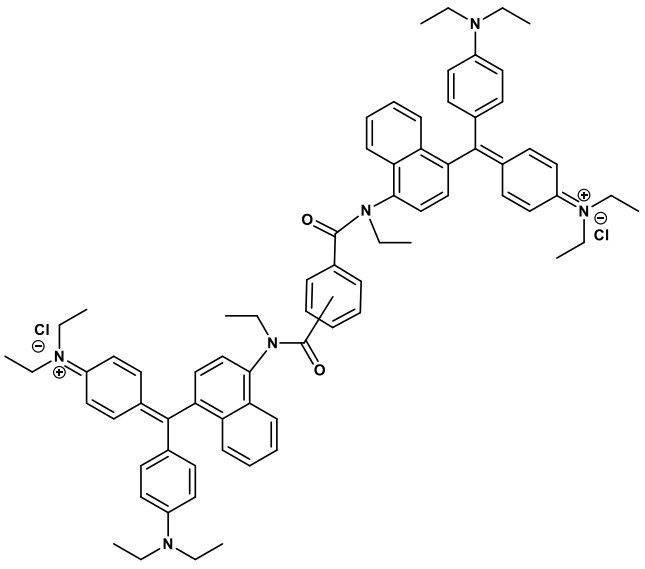

4.

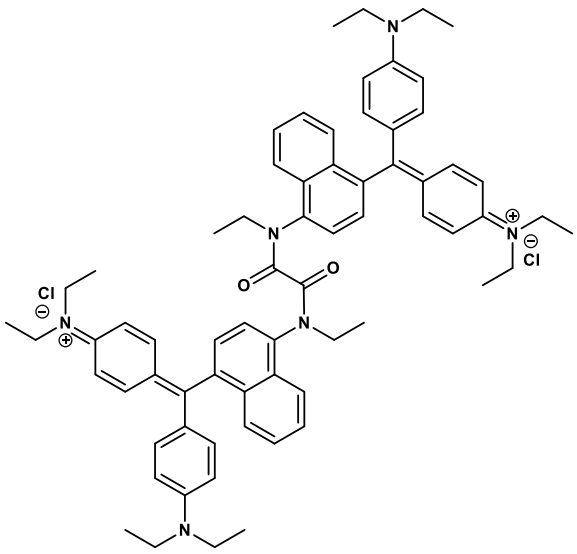

5.

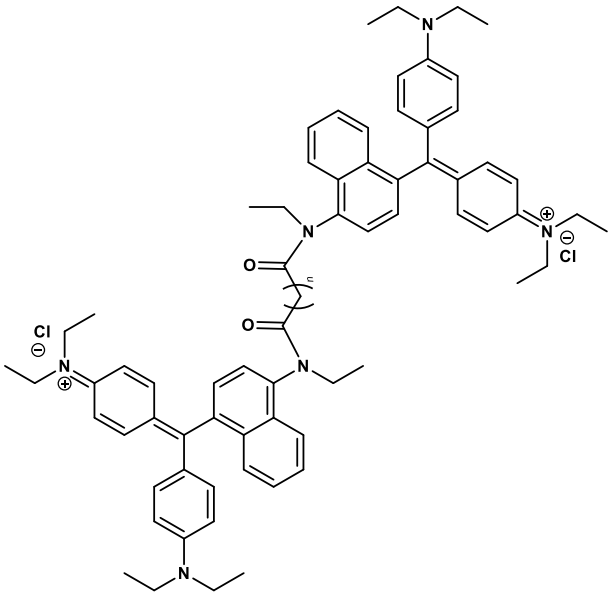

6.

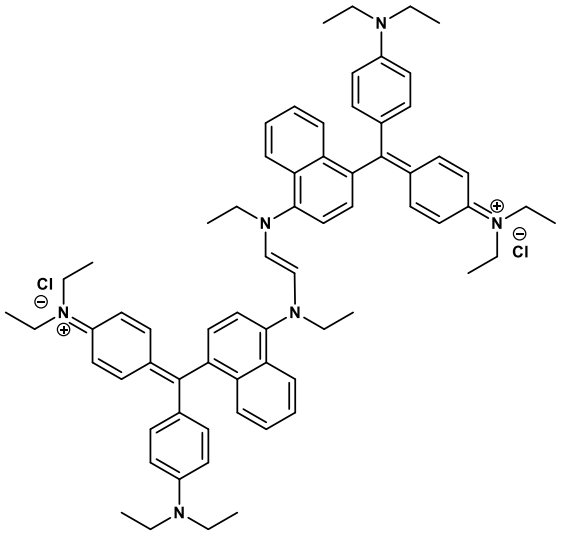

7.

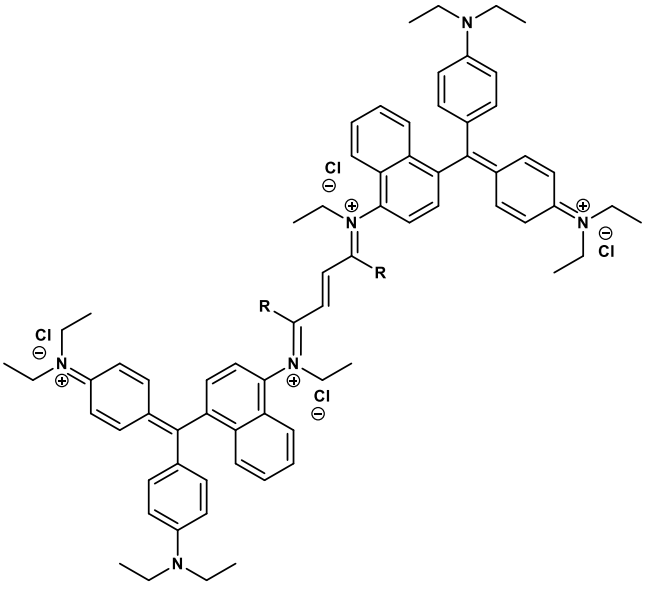

8.

Appendix B: NMR Spectra

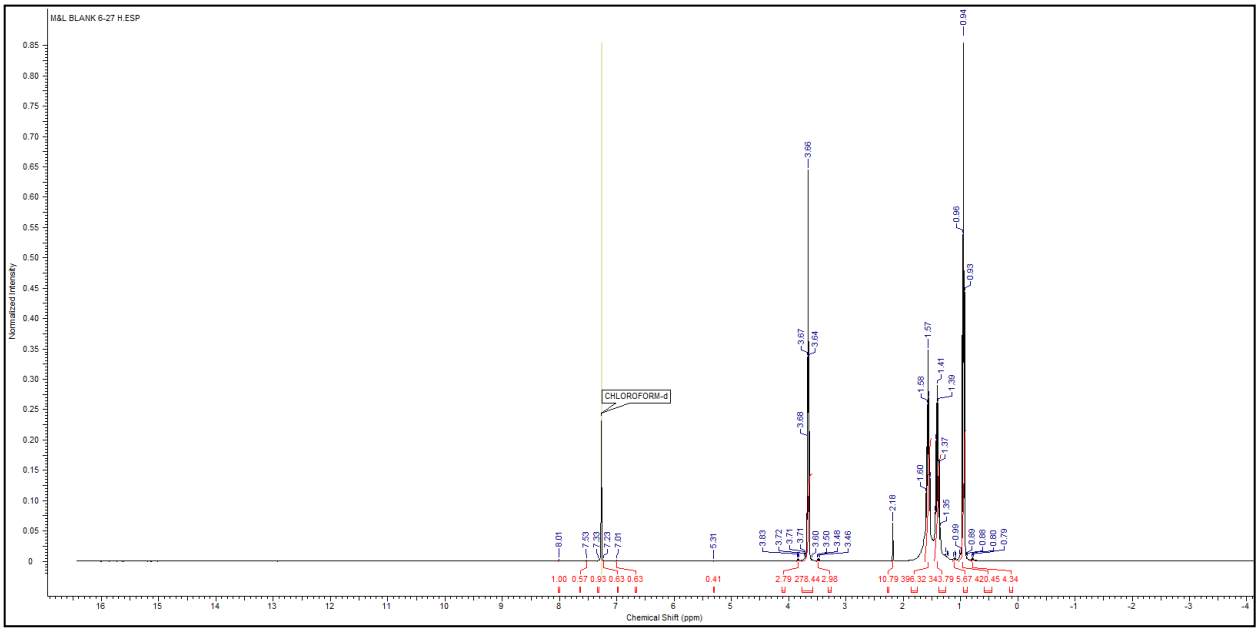

Marshall & Lewis eluent: ^{1}H NMR (400 MHz, $CDCl_3$) δ 8.01 (1H, s), 3.66 (278H, t), 1.57 (396H, tt), 1.41 (344H, tq), 0.94 (420 H, t)

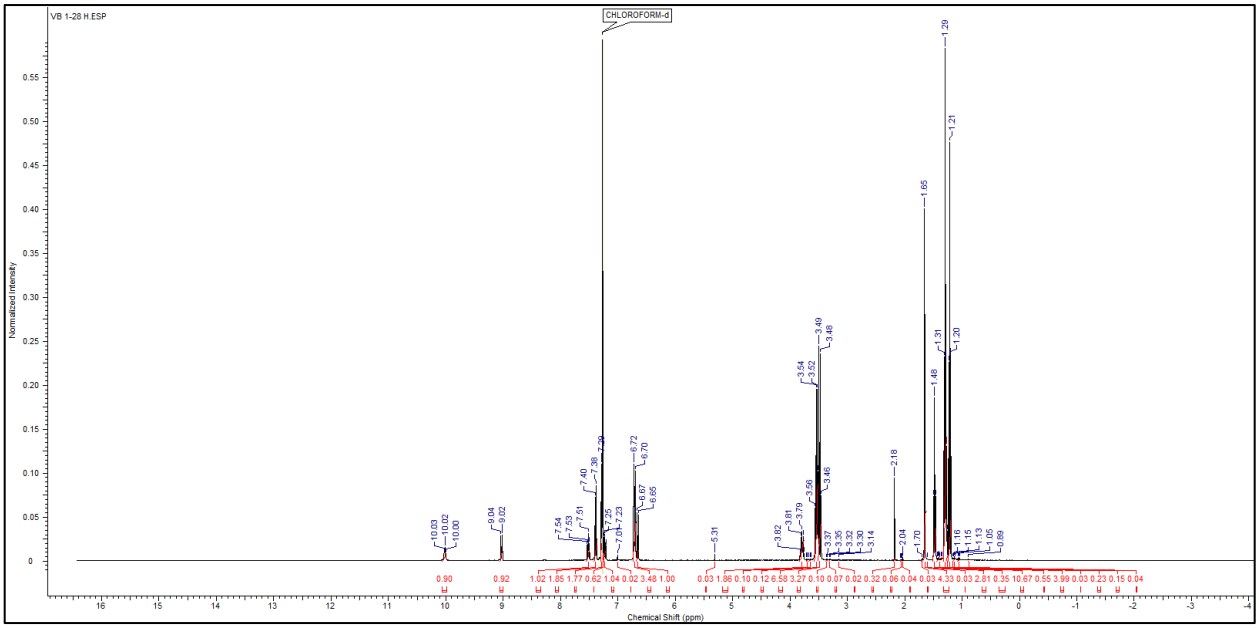

Victoria Blue BO: ^{1}H NMR (400 MHz, $CDCl_3$) δ 10.02 (1H, t), 9.03 (1H, d), 7.51 (1H, m), 7.39 (2H, d), 7.28 (4H, d), 7.23 (1H, m), 6.71 (4H, d), 6.66 (1H, d), 3.79 (2H, dq), 3.53 (8H, q), 1.48 (3H, t), 1.29 (12H, t)

The following spectra were too convoluted for peak assignment.

$(VB)_2(CH_2)_2$ runs 1 and 2 (EtOH)

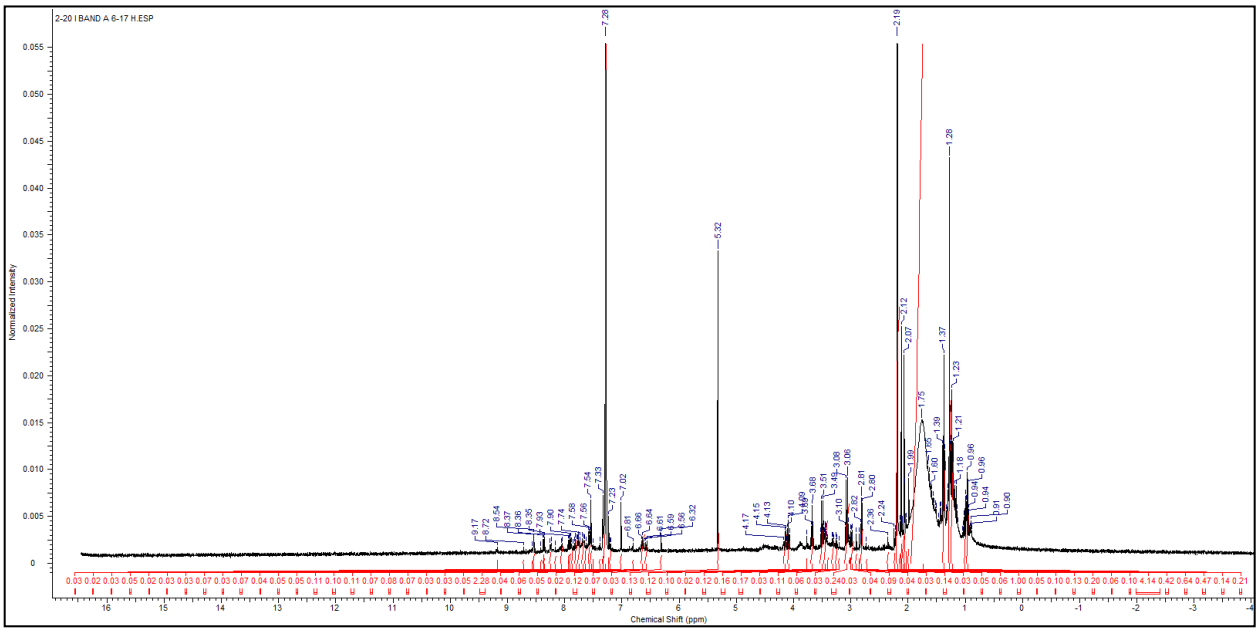

Run 1 (EtOH) M&L prep TLC band A

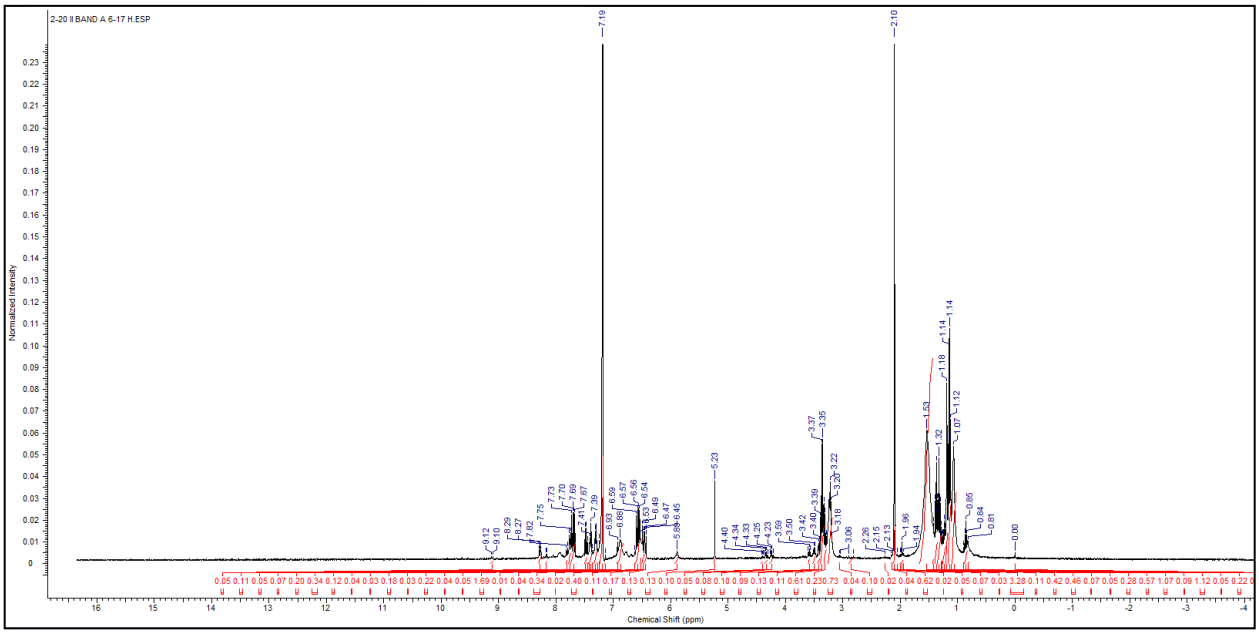

Run 2 (EtOH) M&L prep TLC band A

$(VB)_2(CH_2)_2$ run 3 (ACN)

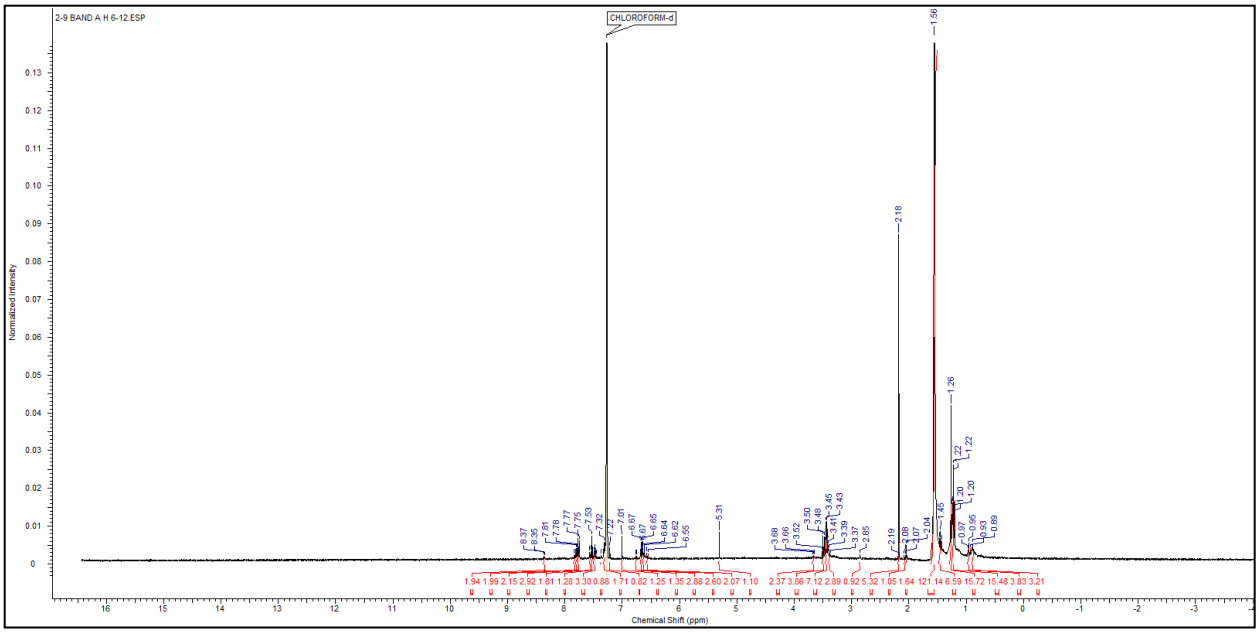

Run 3 (ACN) M&L prep TLC band A

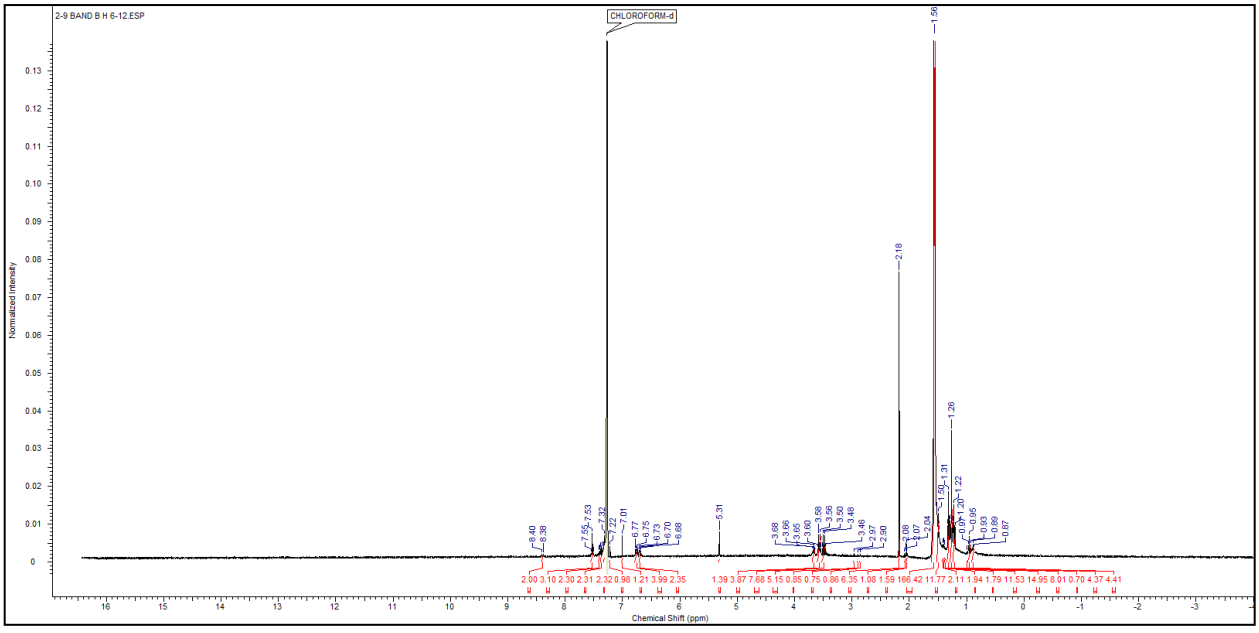

Run 3 (ACN) M&L prep TLC band B

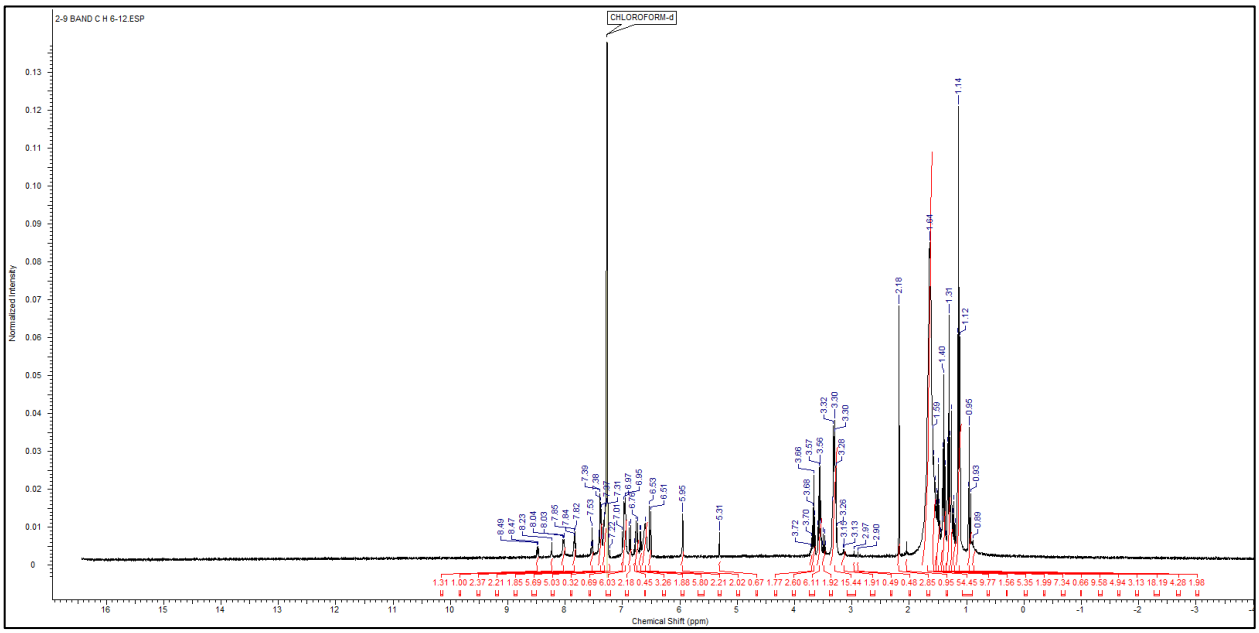

Run 3 (ACN) M&L prep TLC band C

$(VB)_2(CH_2)_2$ run 4 (ACN)

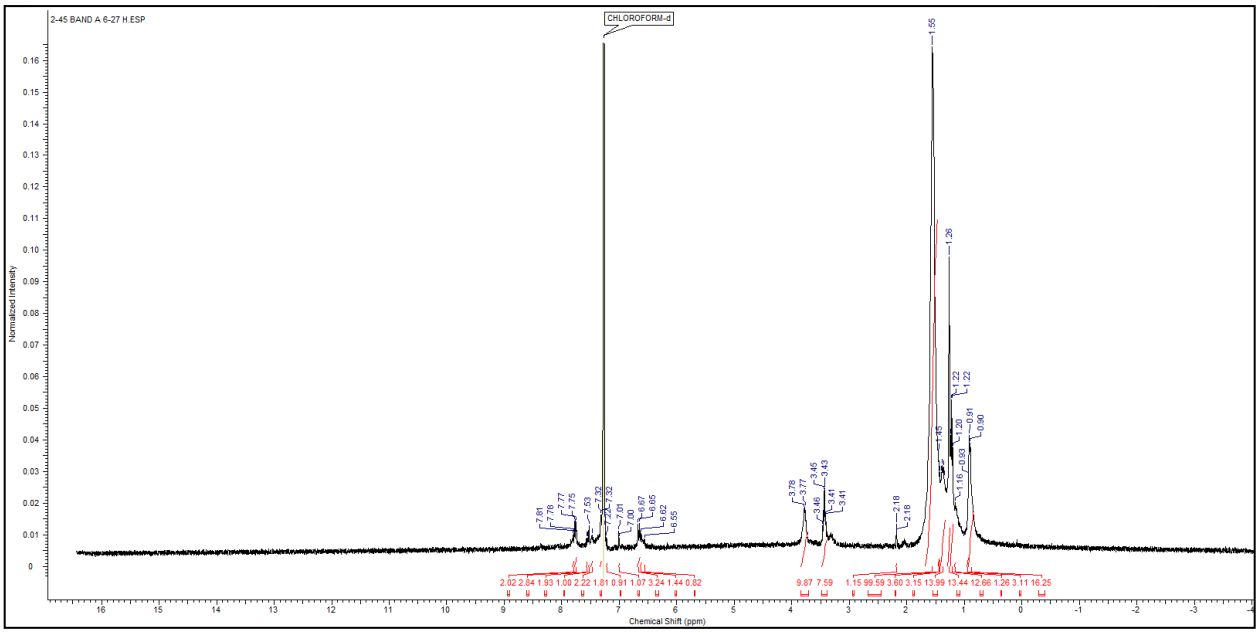

Run 4 (ACN) M&L prep TLC band A

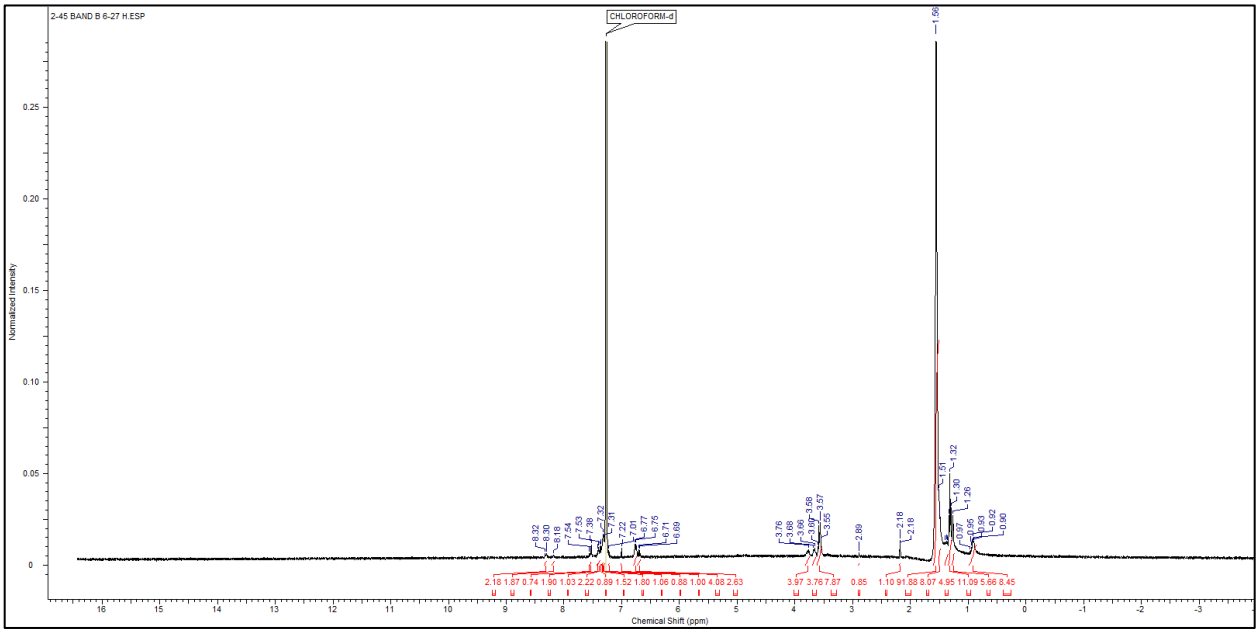

Run 4 (ACN) M&L prep TLC band B

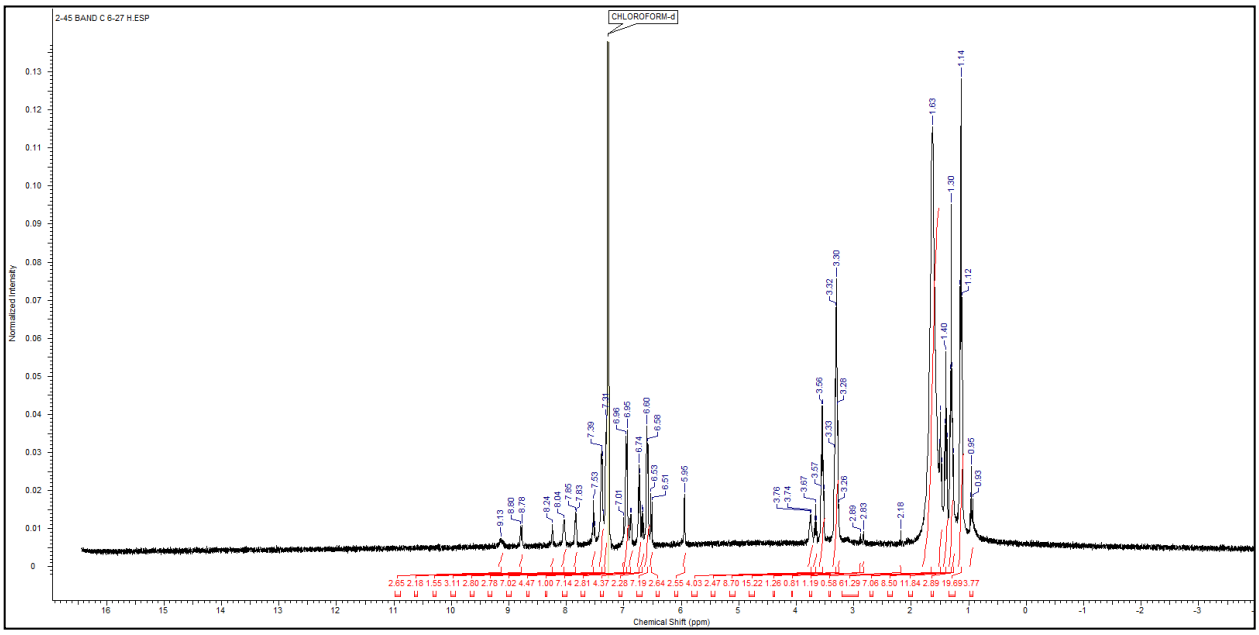

Run 4 (ACN) M&L prep TLC band C

Appendix C: HPLC-TOF Data

Victoria Blue BO

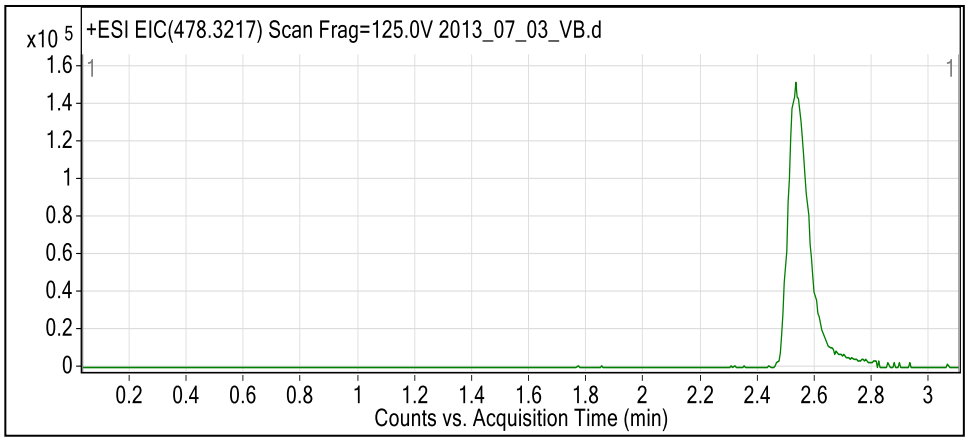

Major component = Victoria Blue BO.

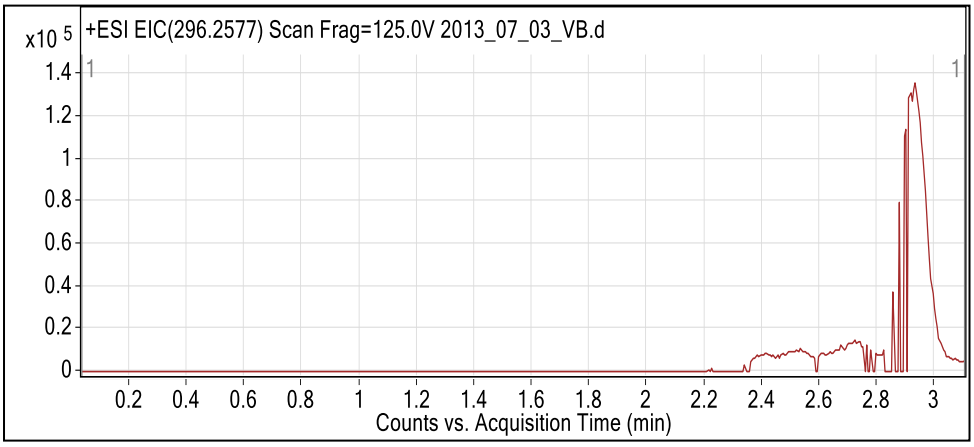

Unknown component 1.

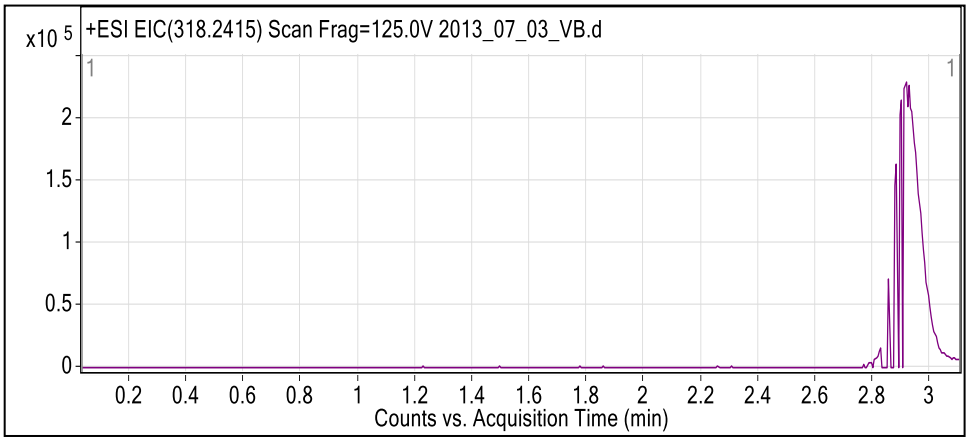

Unknown component 2.

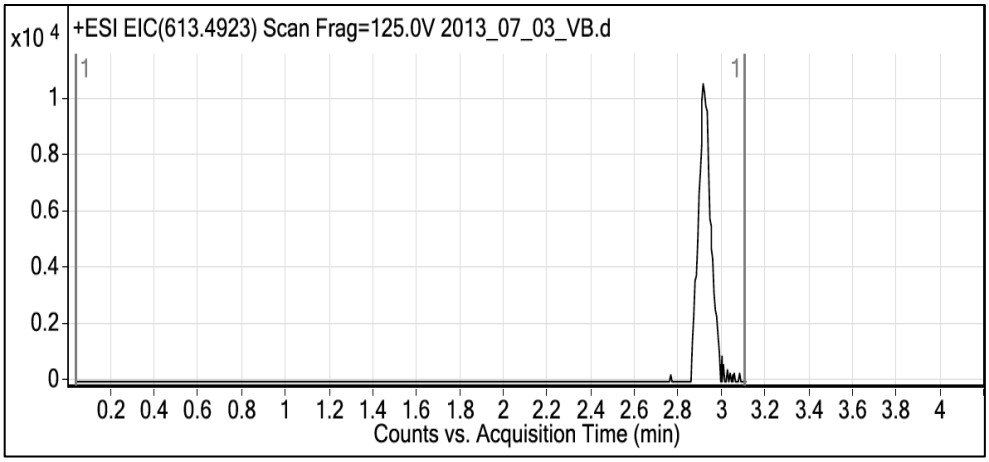

Unknown component 3.

$(VB)_2(CH_2)_2$ Synthesis run 1 (EtOH)

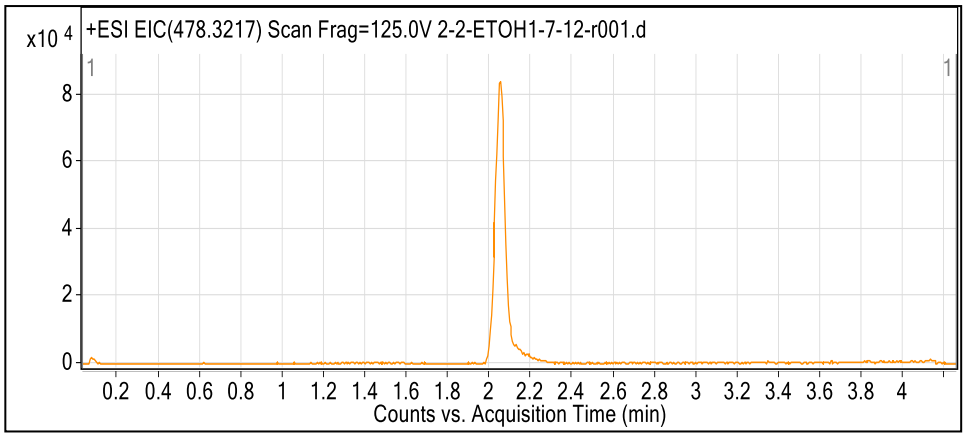

Starting material = Victoria Blue BO.

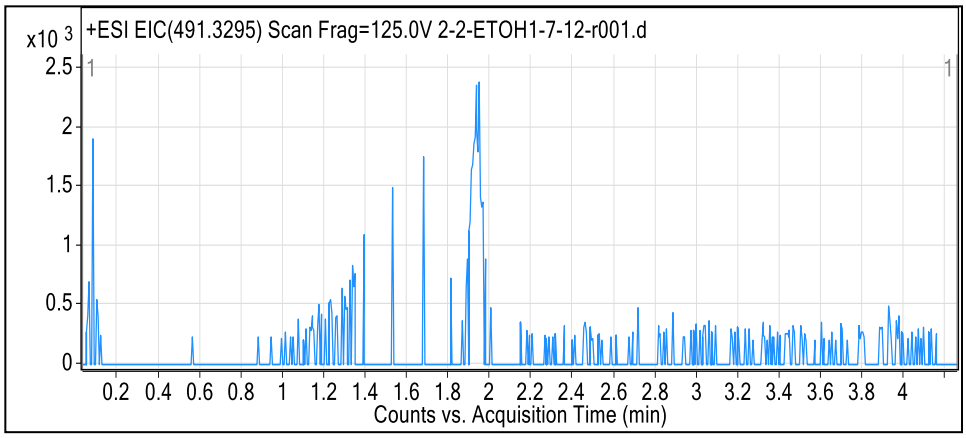

Expected product not found.

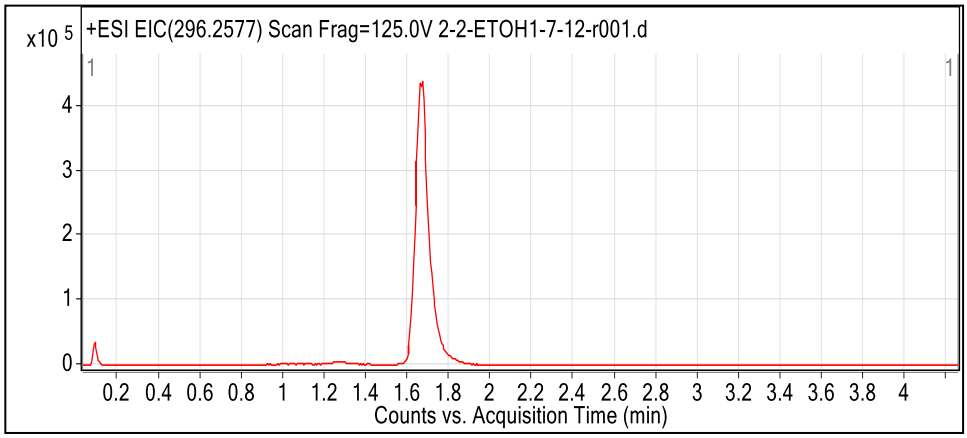

Unknown component 1.

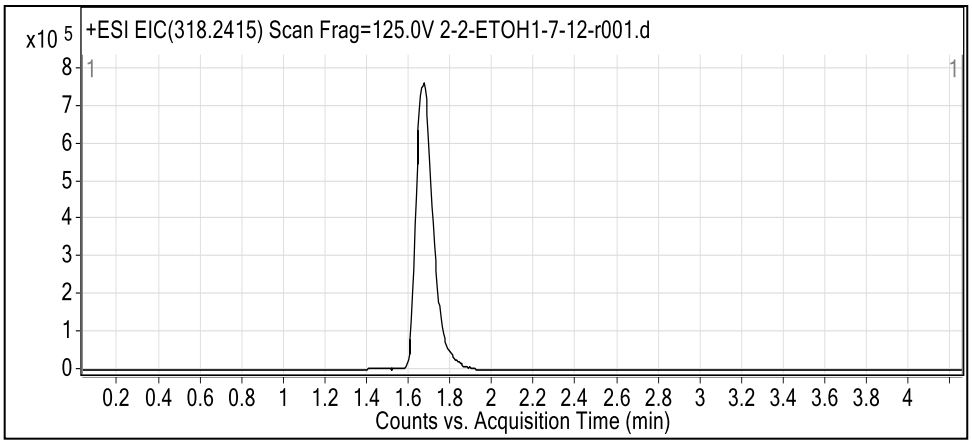

Unknown component 2.

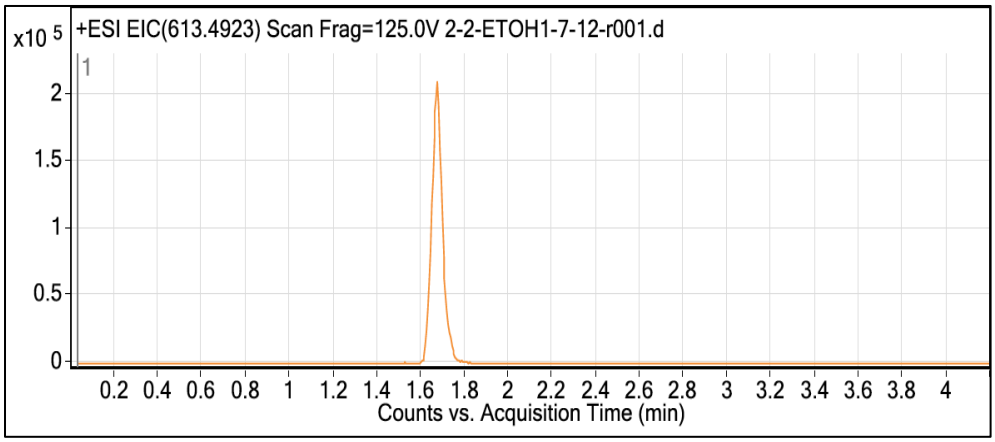

Unknown component 3.

$(VB)_2(CH_2)_2$ Synthesis run 2 (EtOH)

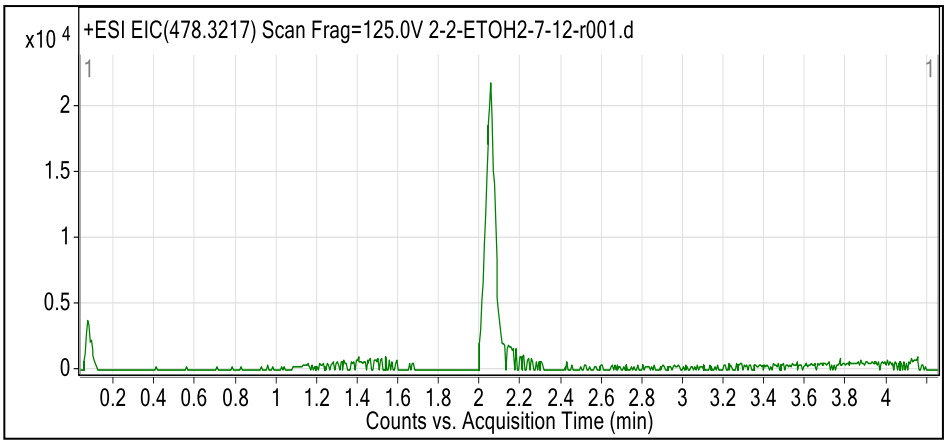

Starting material = Victoria Blue BO.

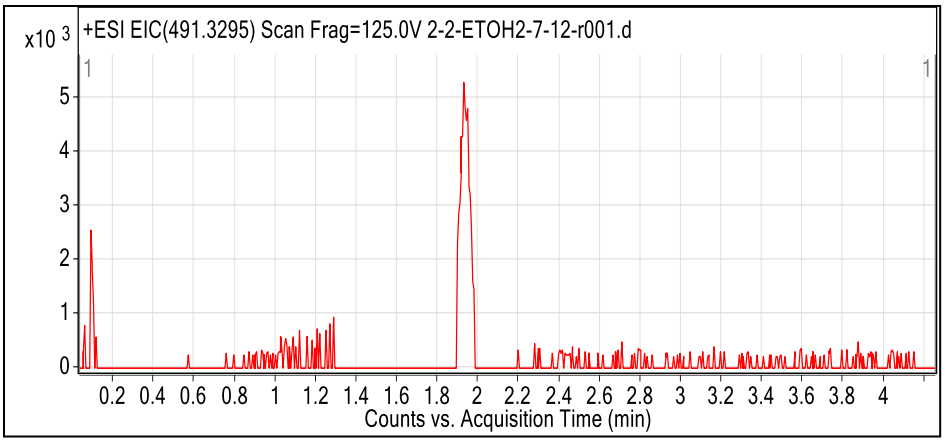

Some expected product found.

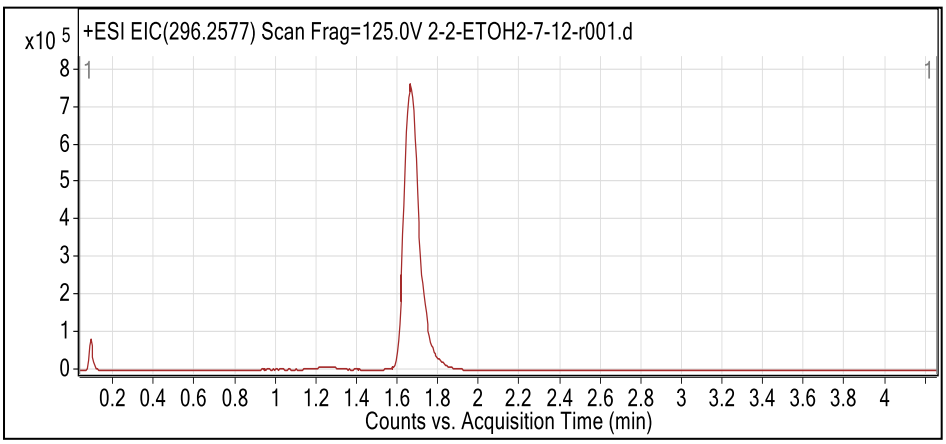

Unknown component 1.

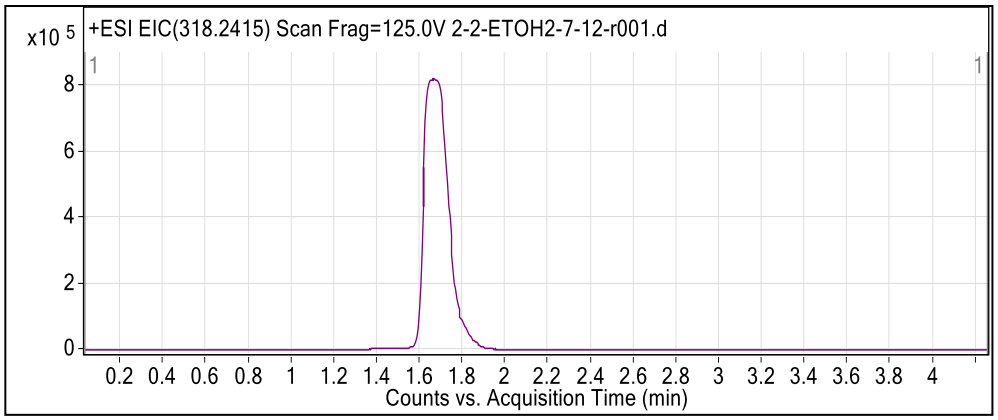

Unknown component 2. Rounded peak indicates detector saturation.

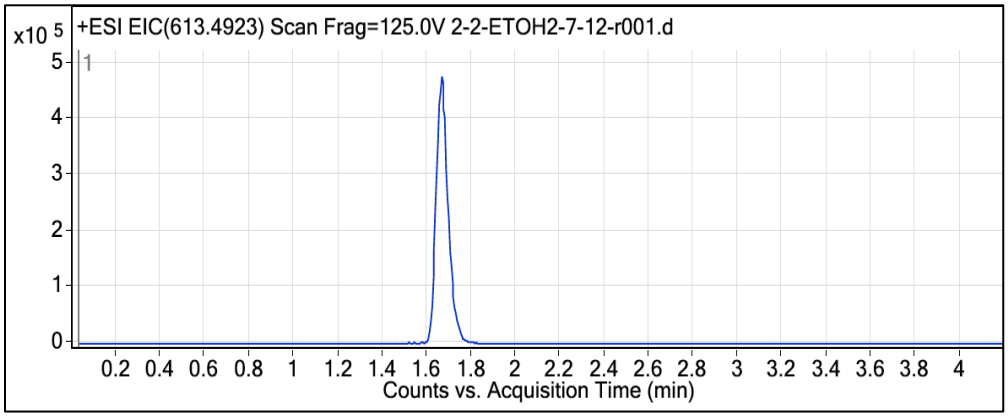

Unknown component 3.

$(VB)_2(CH_2)_2$ Synthesis run 3 (ACN)

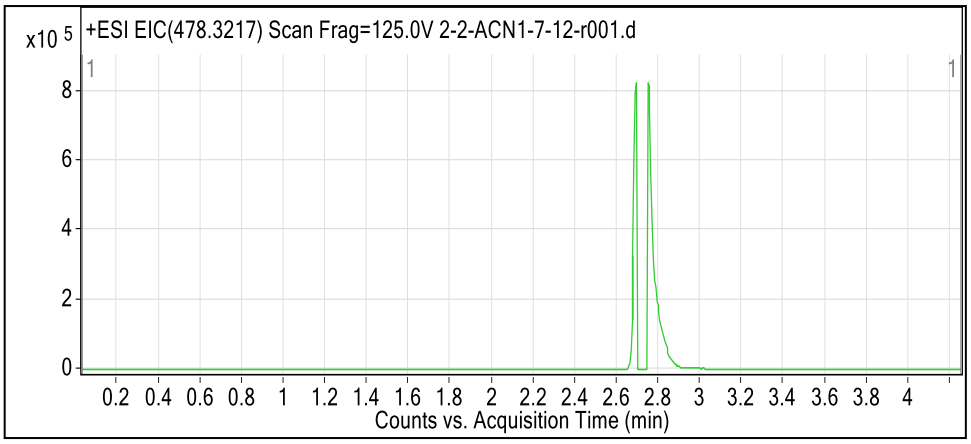

Starting material = Victoria Blue BO.

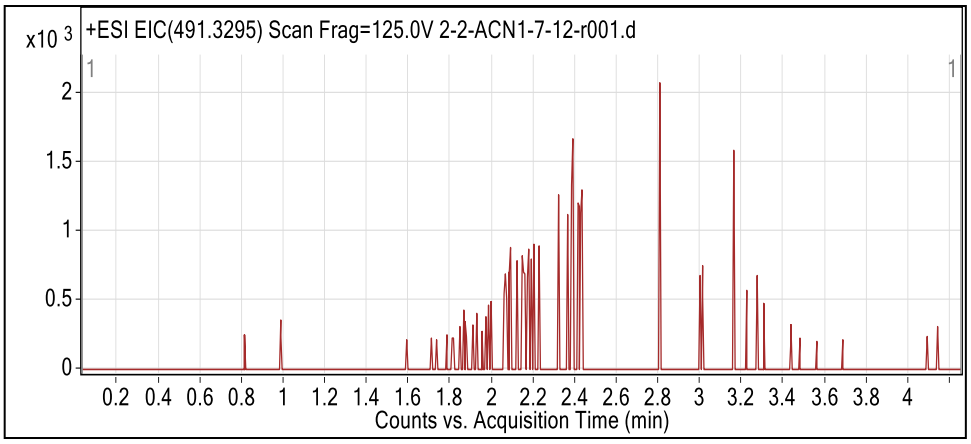

Expected product not found.

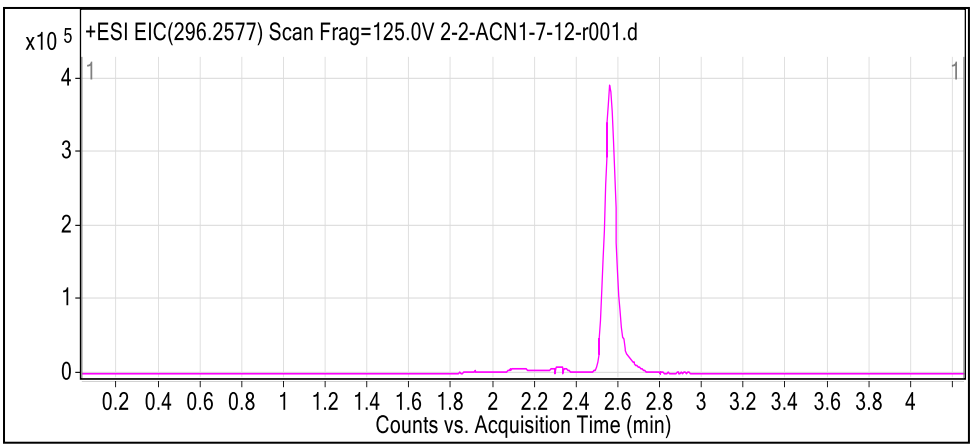

Unknown component 1.

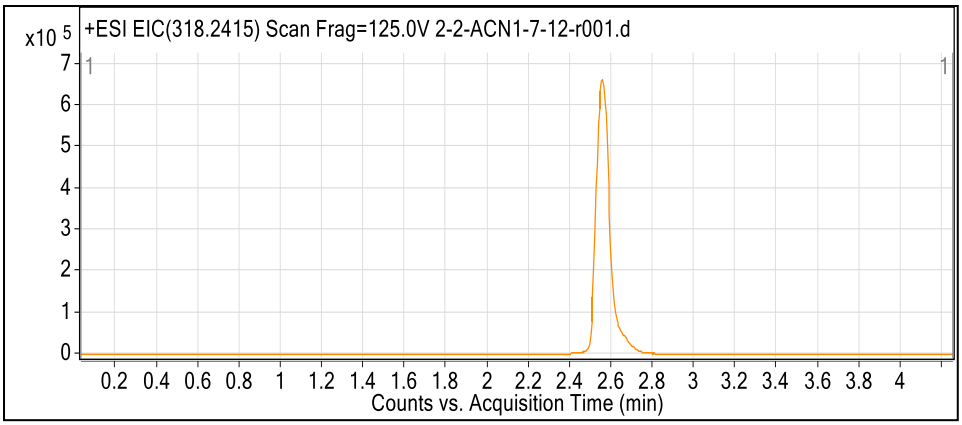

Unknown component 2.

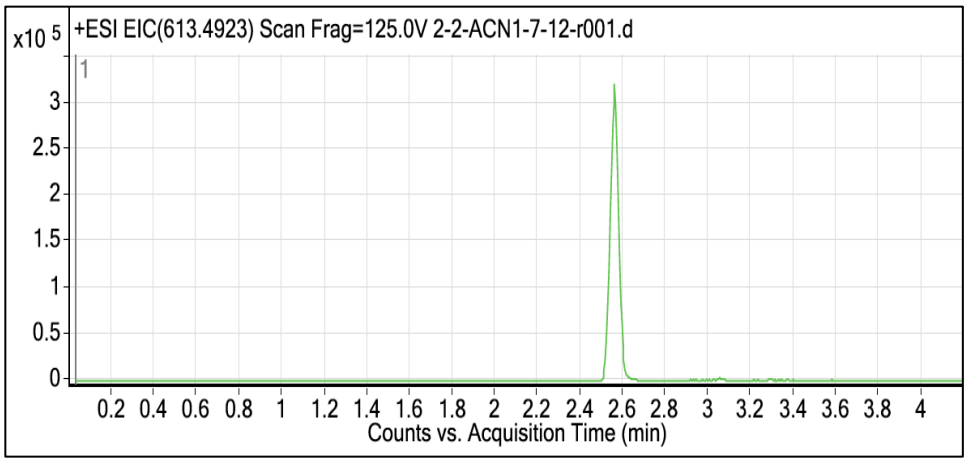

Unknown component 3.

$(VB)_2(CH_2)_2$ Synthesis run 4 (ACN)

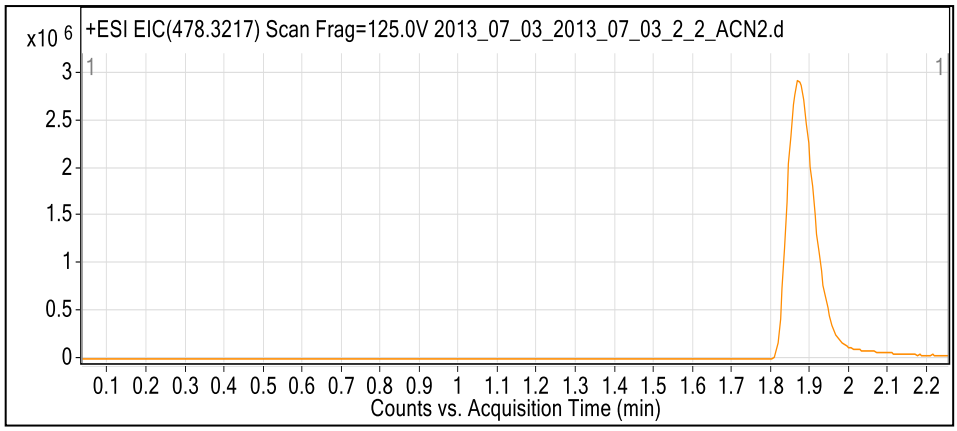

Starting material = Victoria Blue BO.

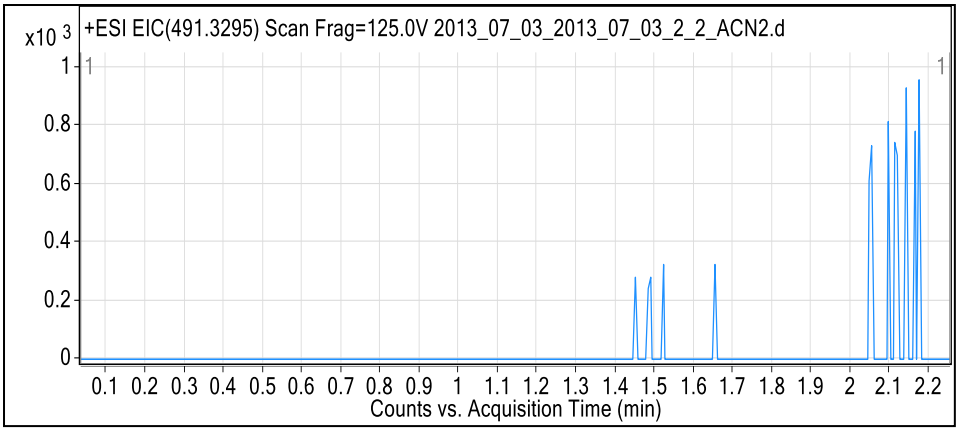

Expected product not found.

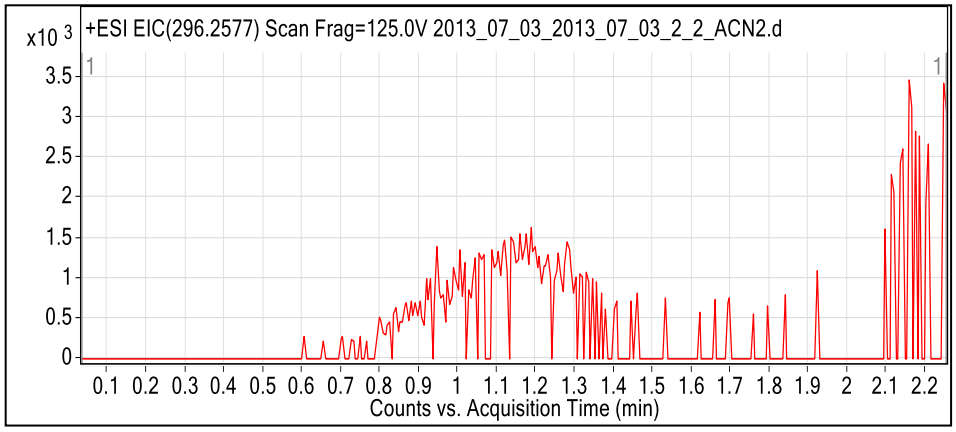

Unknown component 1 not present.

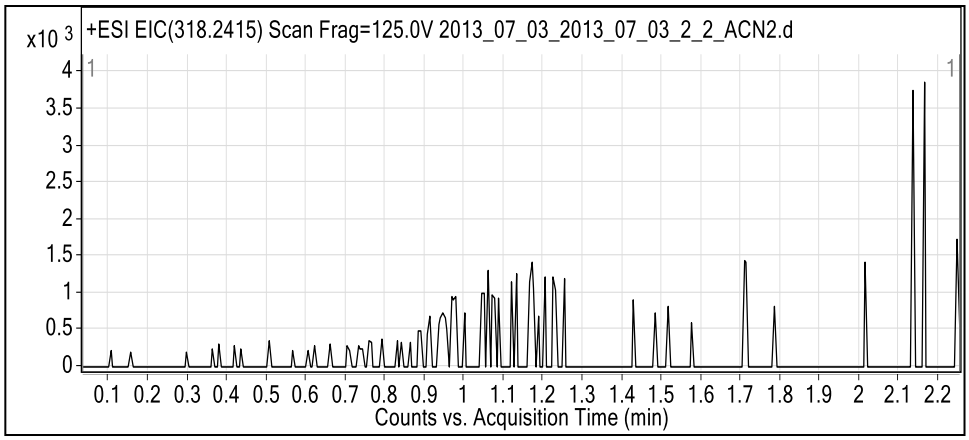

Unknown component 2 not present.

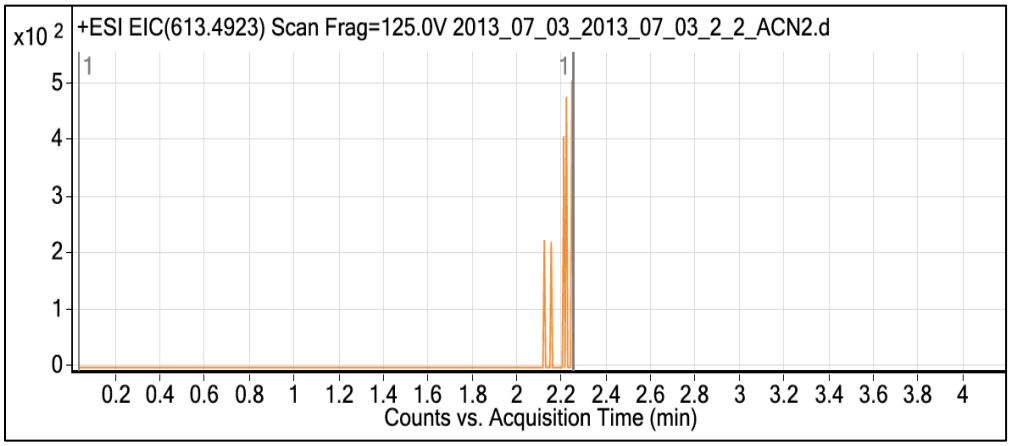

Unknown component 3 not present.

$(VB)_2(CH_2)_2$ Synthesis run 5a (ACN)

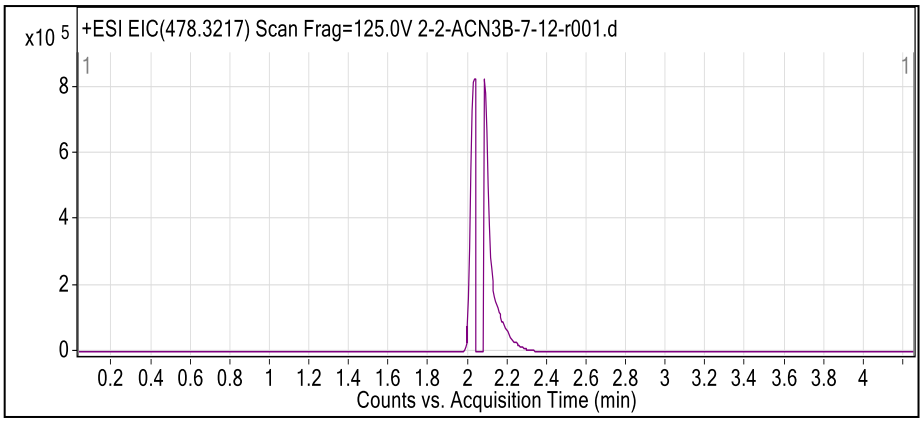

Starting material = Victoria Blue BO.

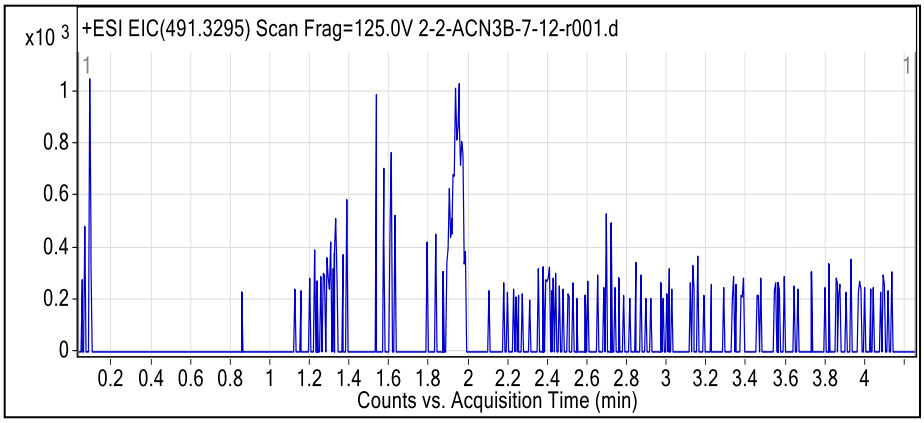

Expected product not found.

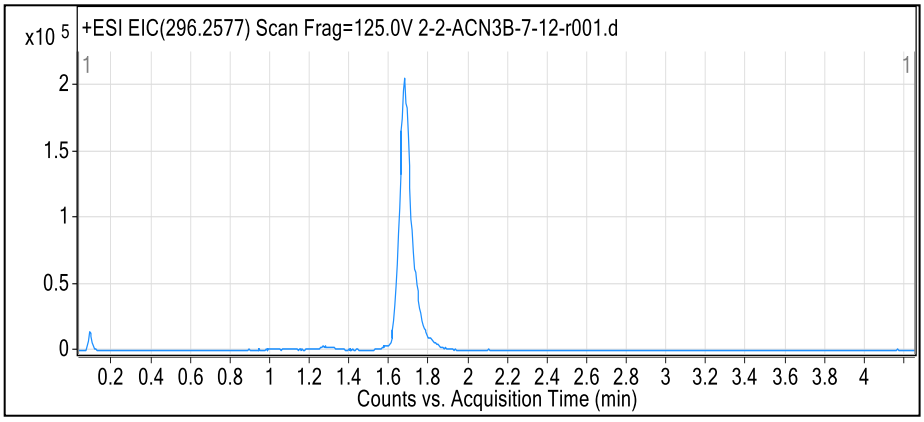

Unknown component 1.

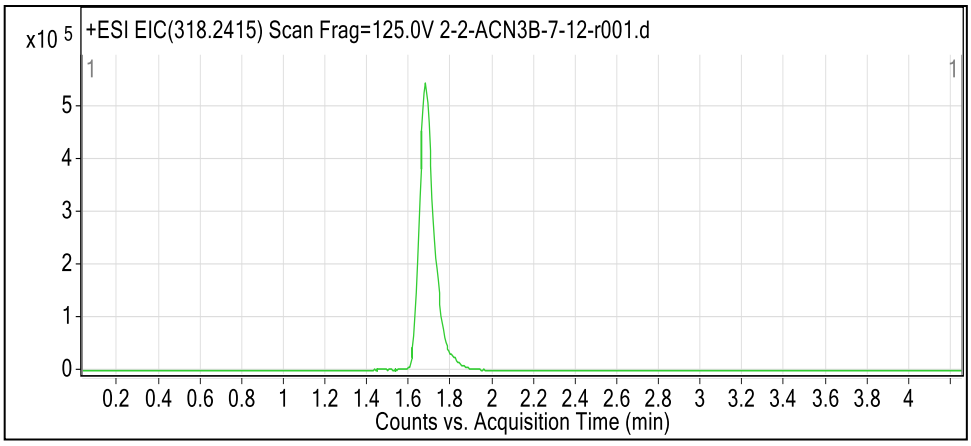

Unknown component 2.

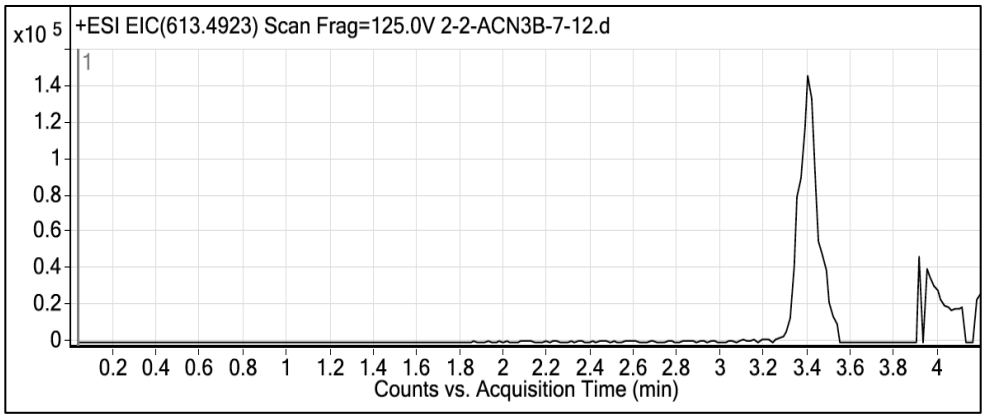

Unknown component 3.

$(VB)_2(CH_2)_2$ Synthesis run 5b (ACN)

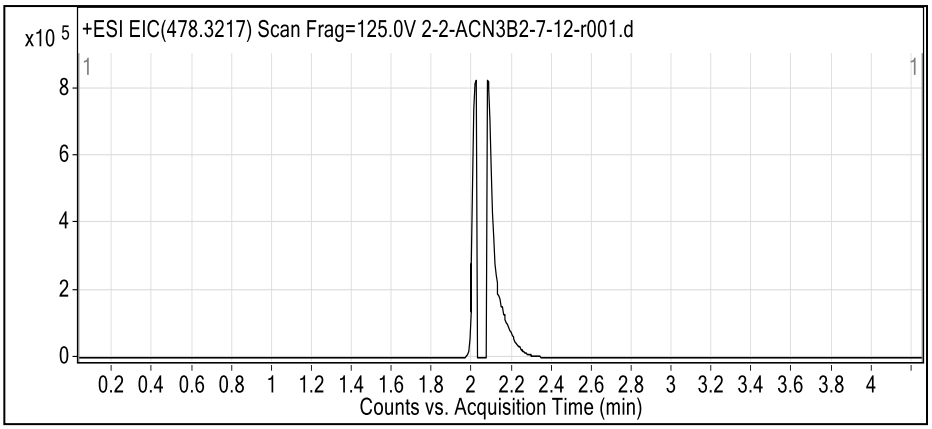

Starting material = Victoria Blue BO.

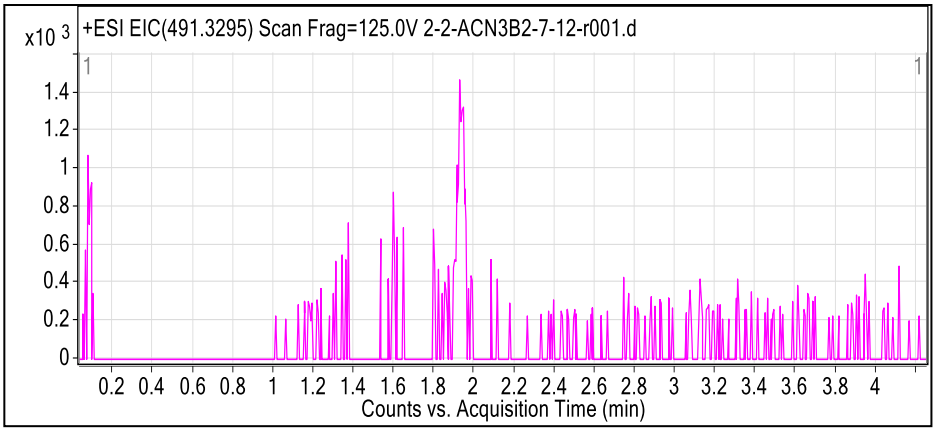

Expected product not found.

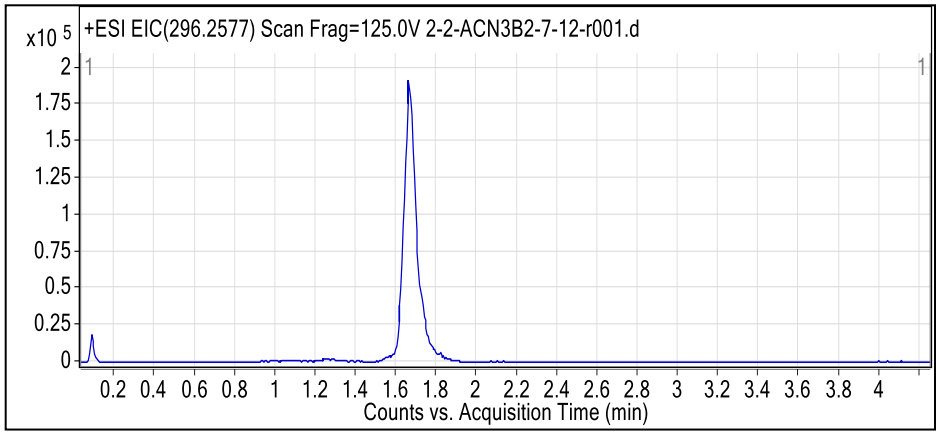

Unknown component 1.

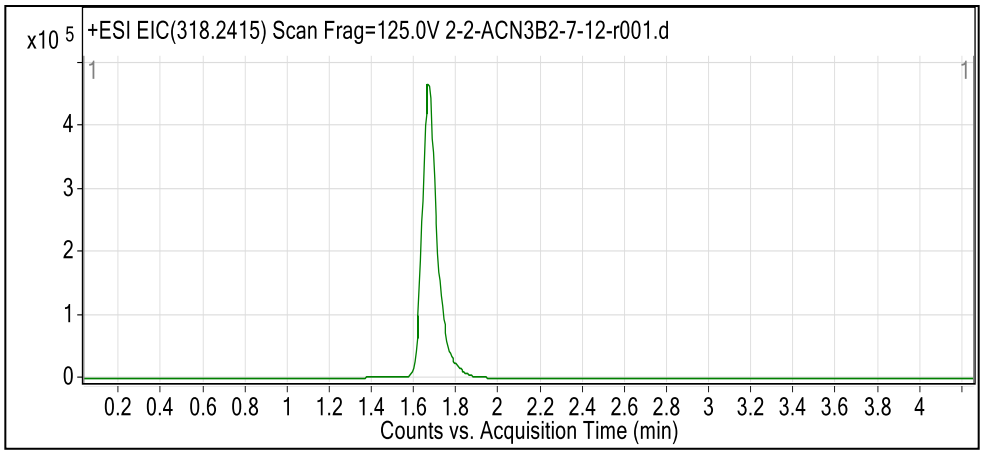

Unknown component 2.

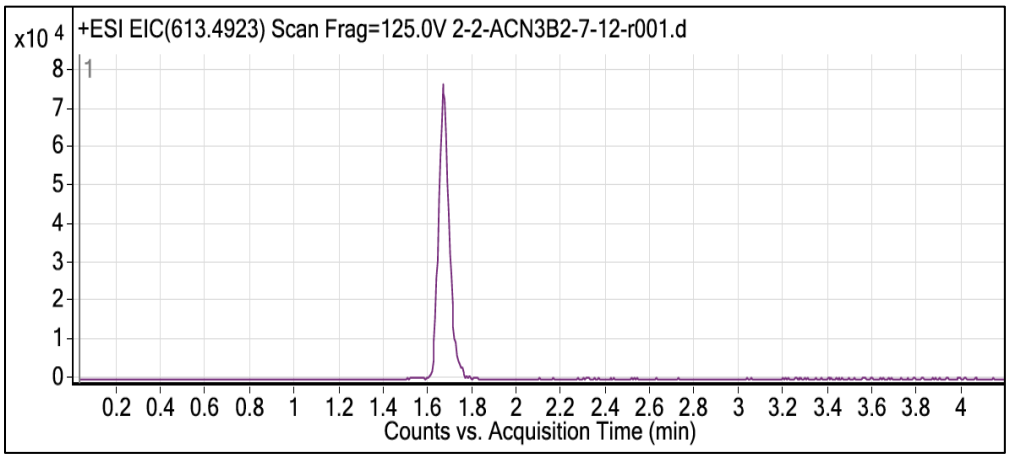

Unknown component 3.

(VB)C_6H_4 Pd Synthesis

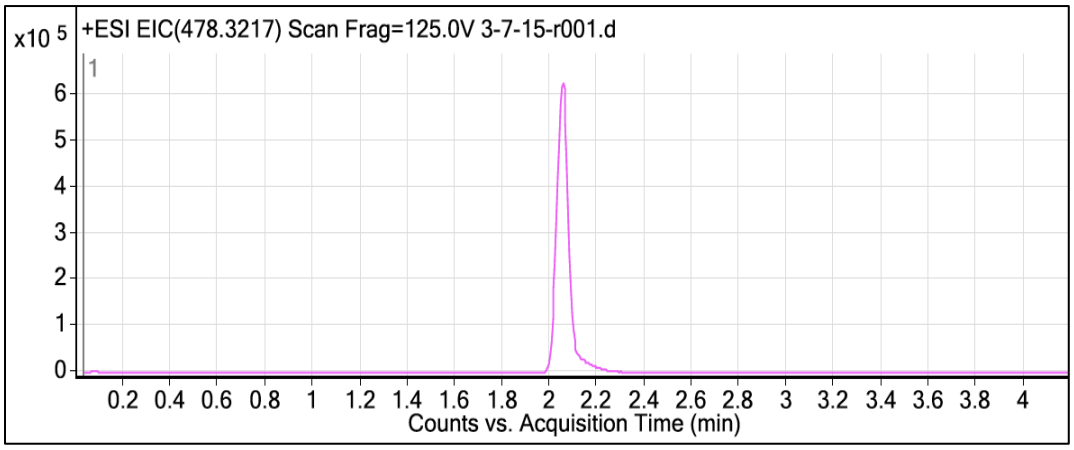

Starting material = Victoria Blue BO.

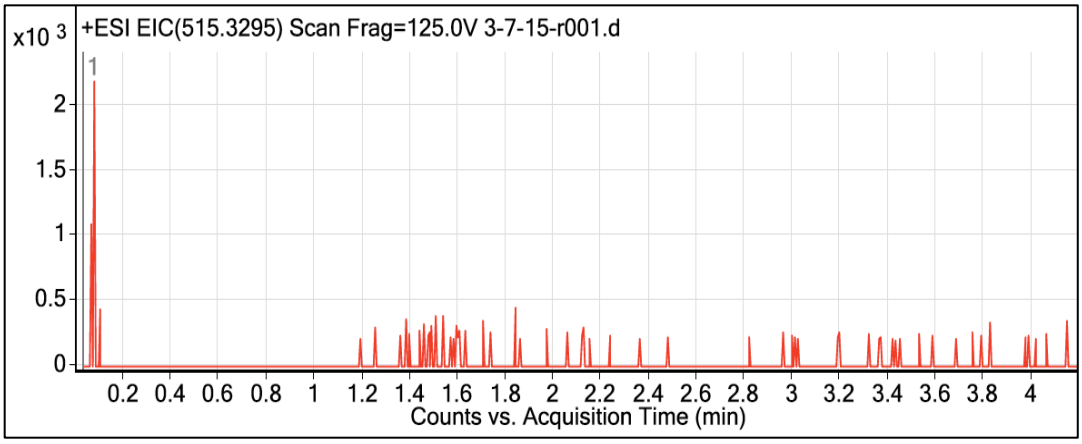

Expected product not present.

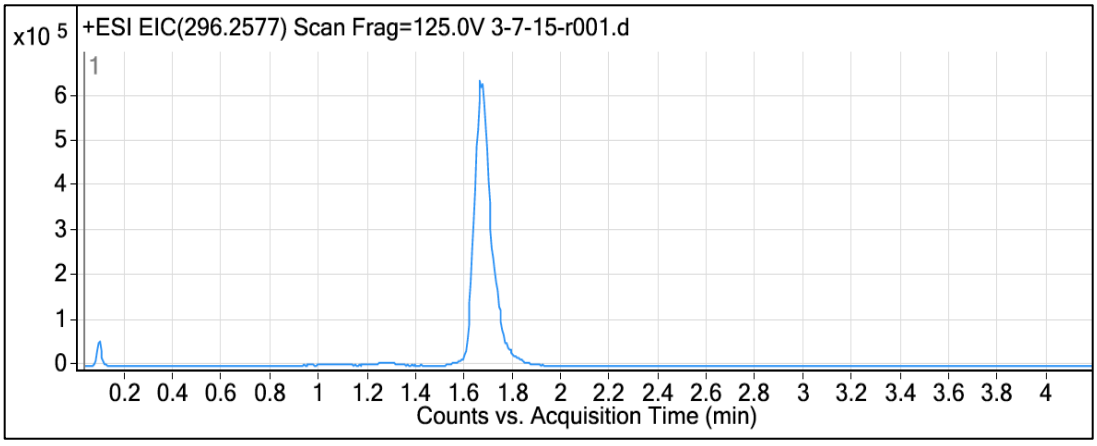

Unknown component 1.

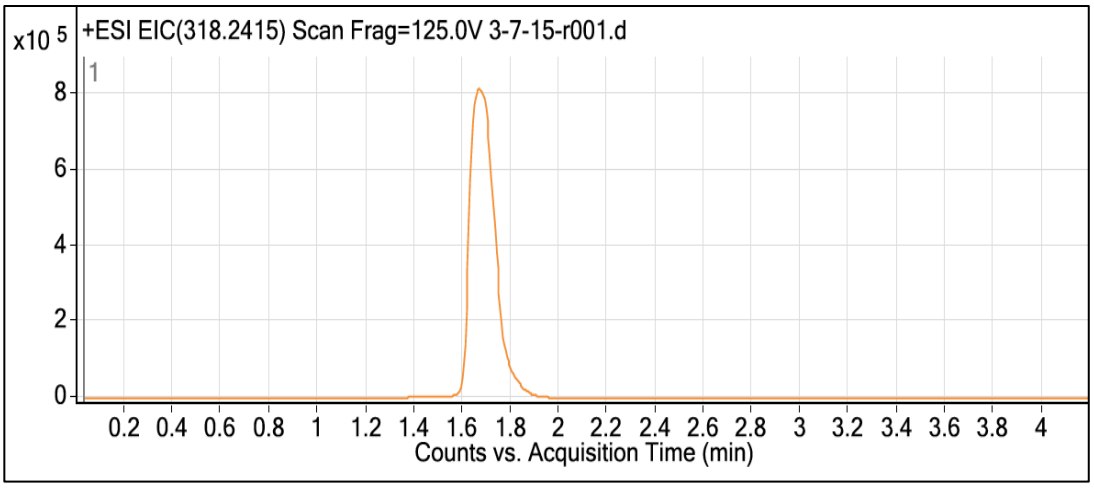

Unknown component 2. Rounded peak indicates detector saturation.

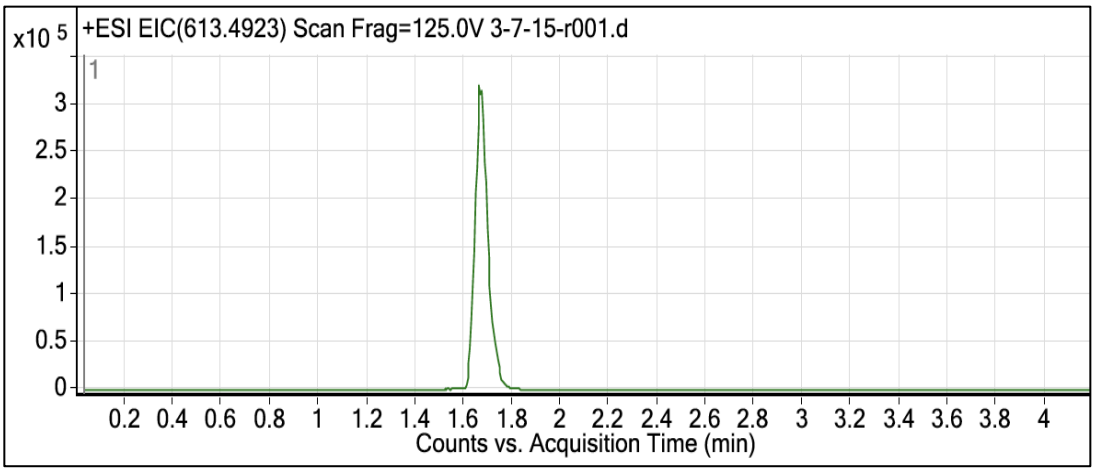

Unknown component 3.

$(VB)_2(CH_2)_2$ Synthesis run 3 (ACN) M&L prep TLC band A – Overload sample

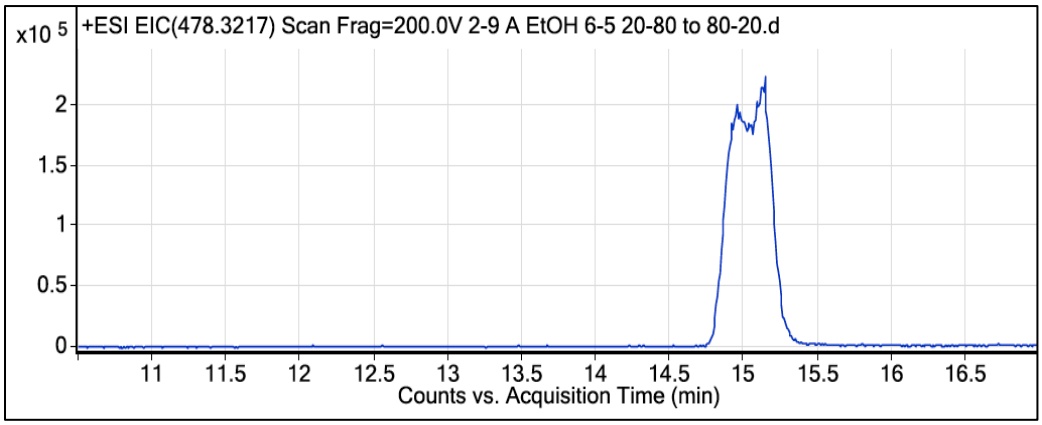

Starting material = Victoria Blue BO.

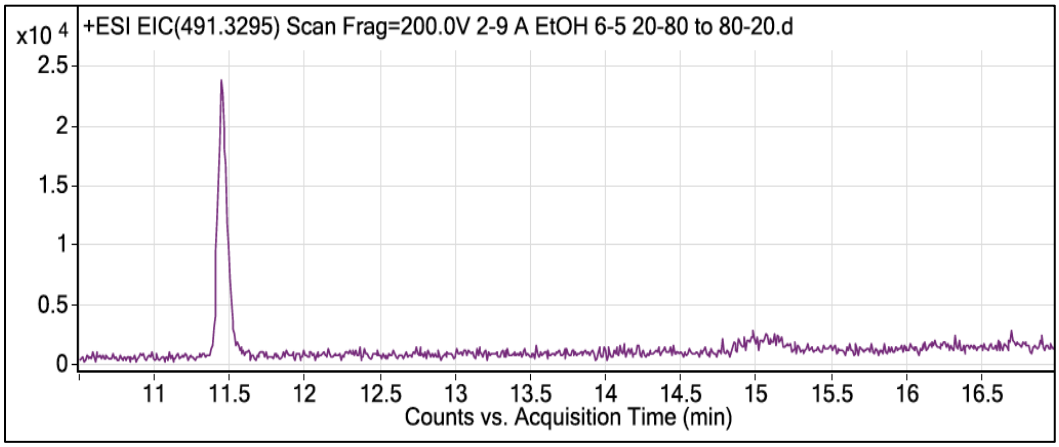

Expected product.

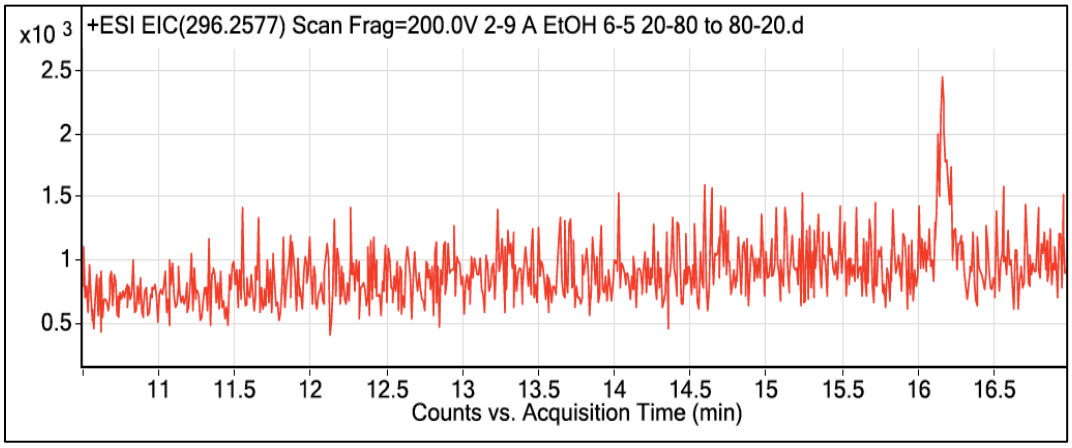

Unknown component 1 not present.

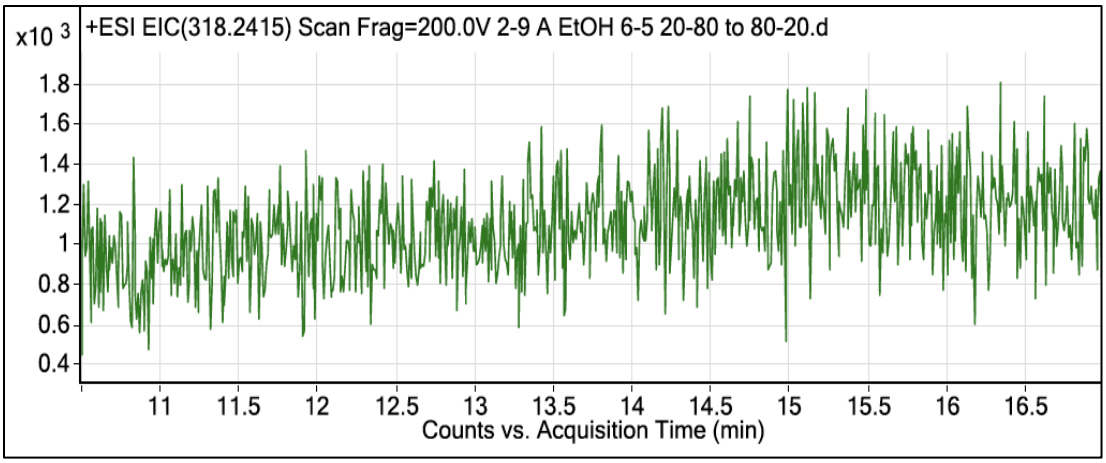

Unknown component 2 not present.

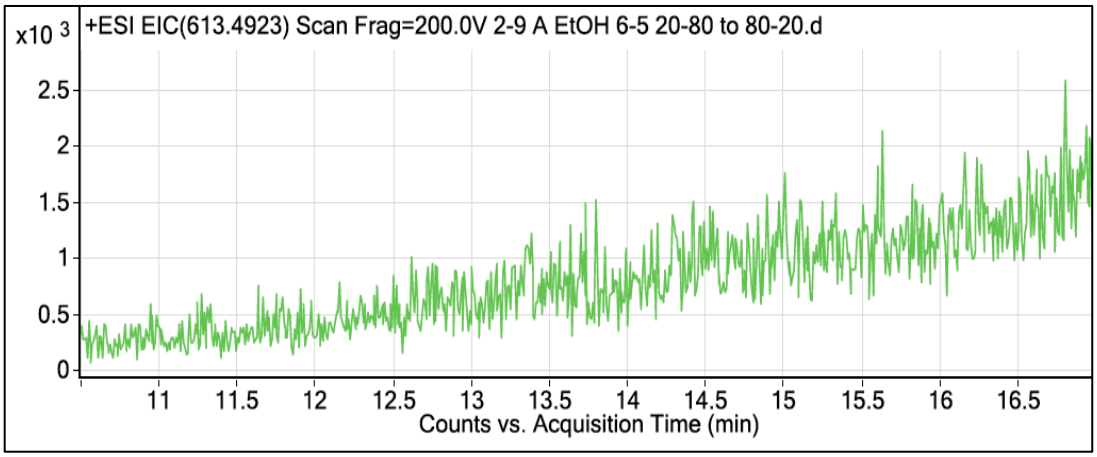

Unknown component 3 not present.

$(VB)_2(CH_2)_2$ Synthesis run 3 (ACN) M&L prep TLC band B – Overload sample

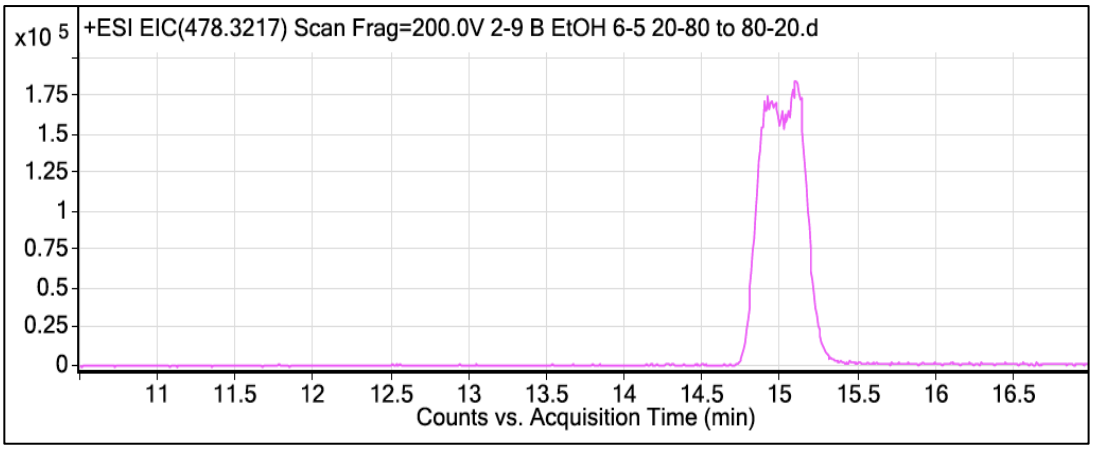

Starting material = Victoria Blue BO.

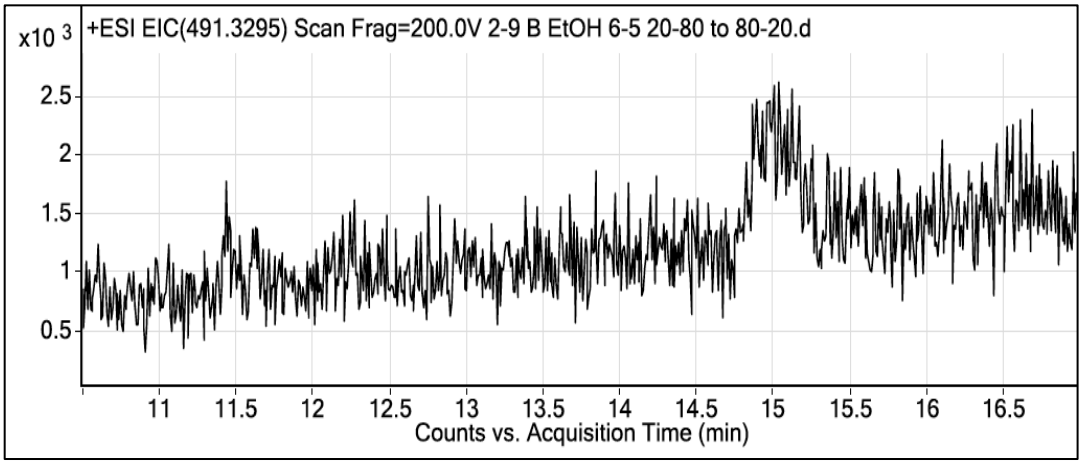

Expected product not present.

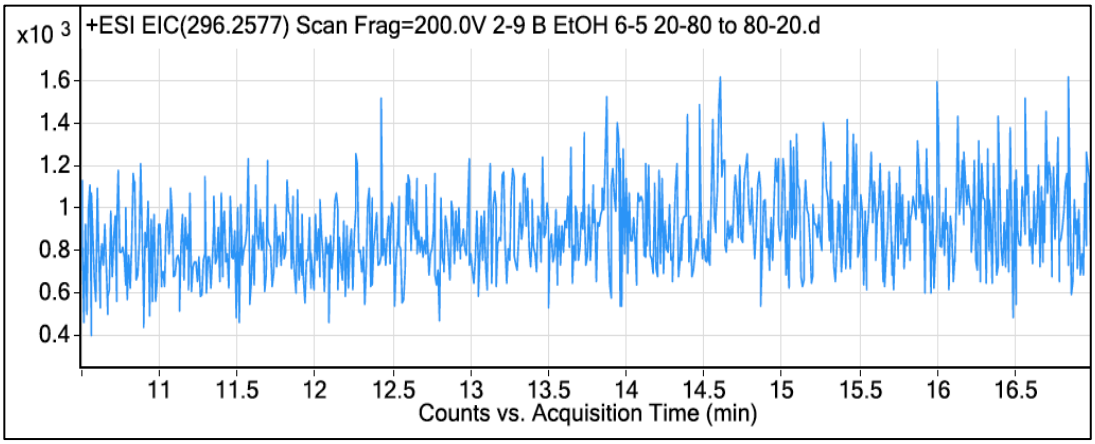

Unknown component 1 not present.

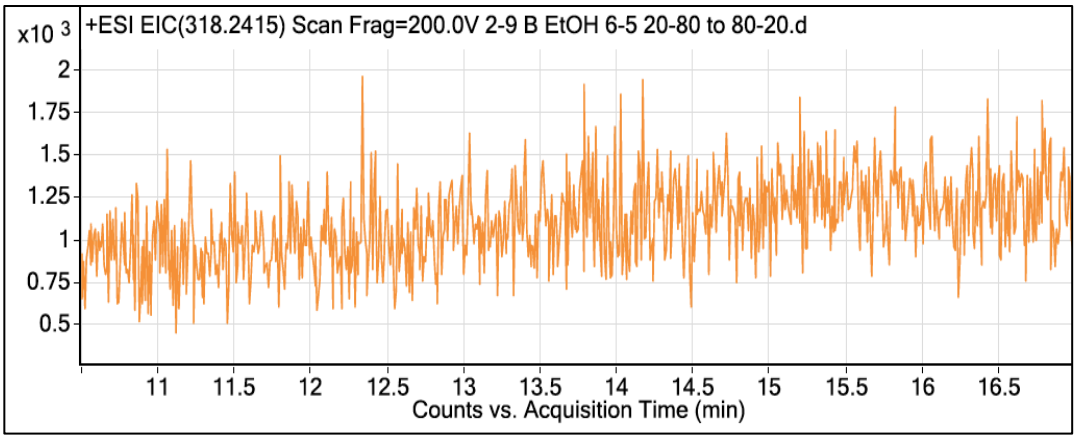

Unknown component 2 not present.

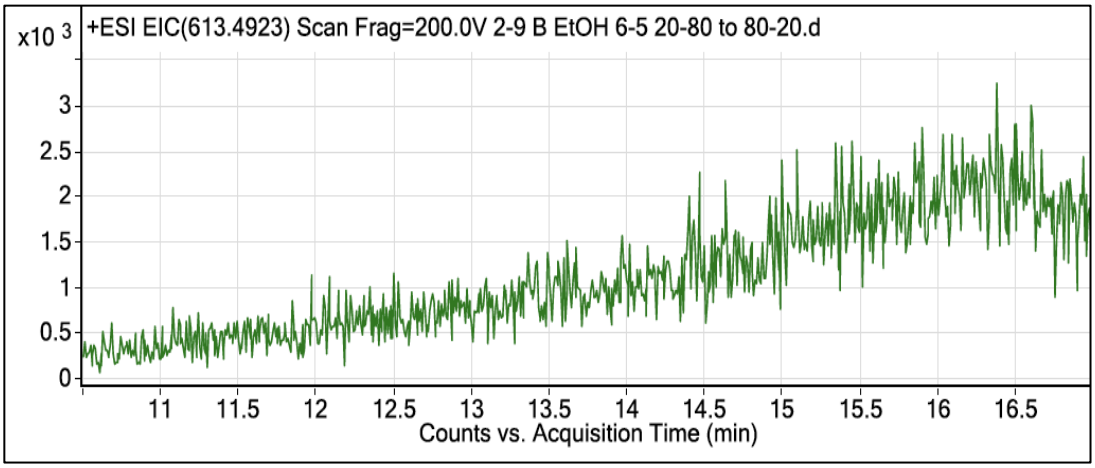

Unknown component 3 not present.

$(VB)_2(CH_2)_2$ Synthesis run 3 (ACN) M&L prep TLC band C – Overload sample

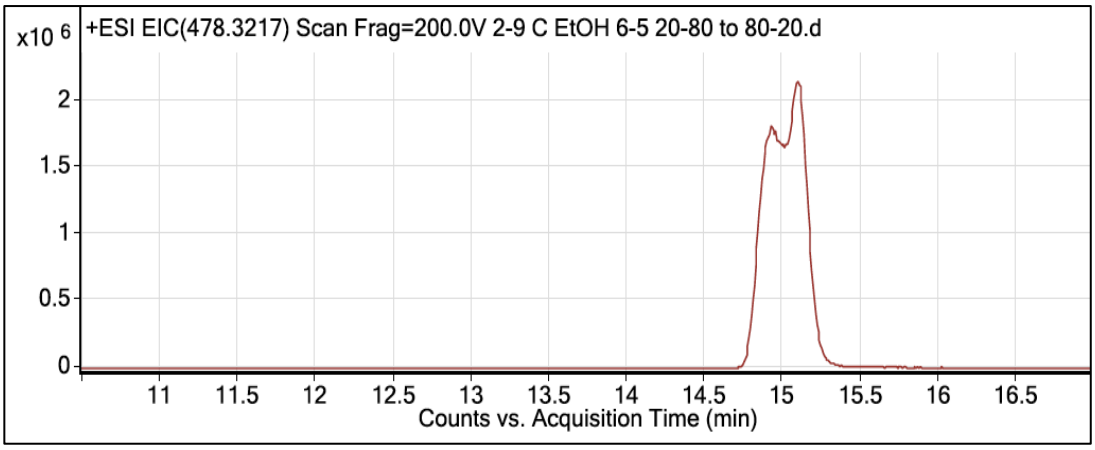

Starting material = Victoria Blue BO.

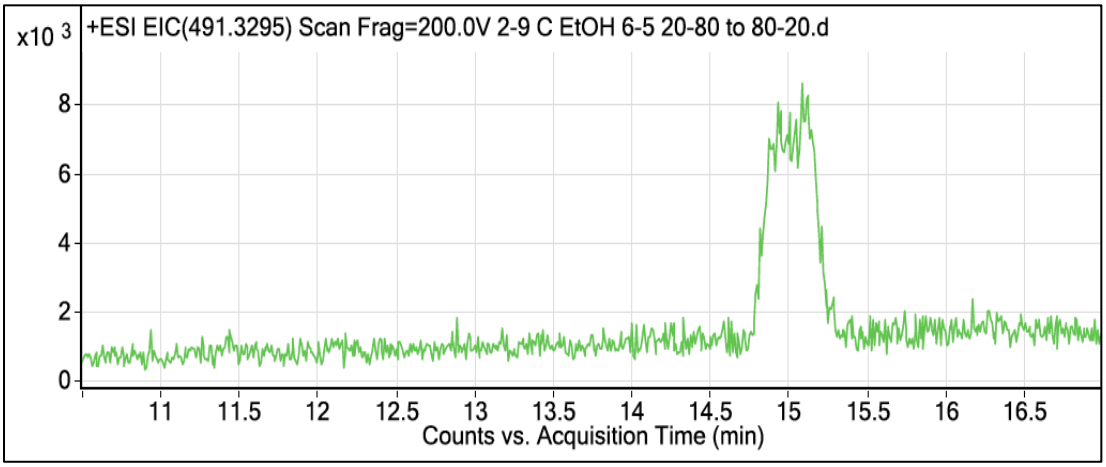

Some expected product present.

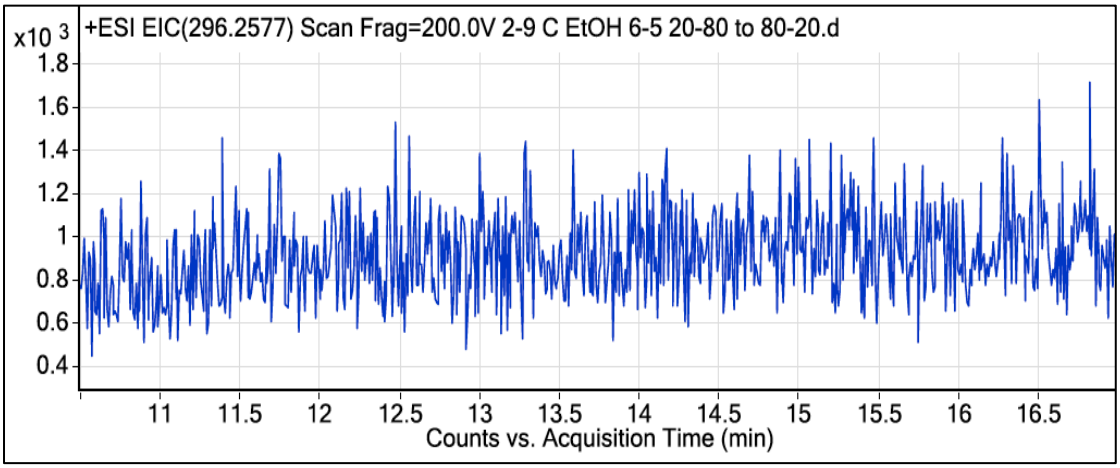

Unknown component 1 not present.

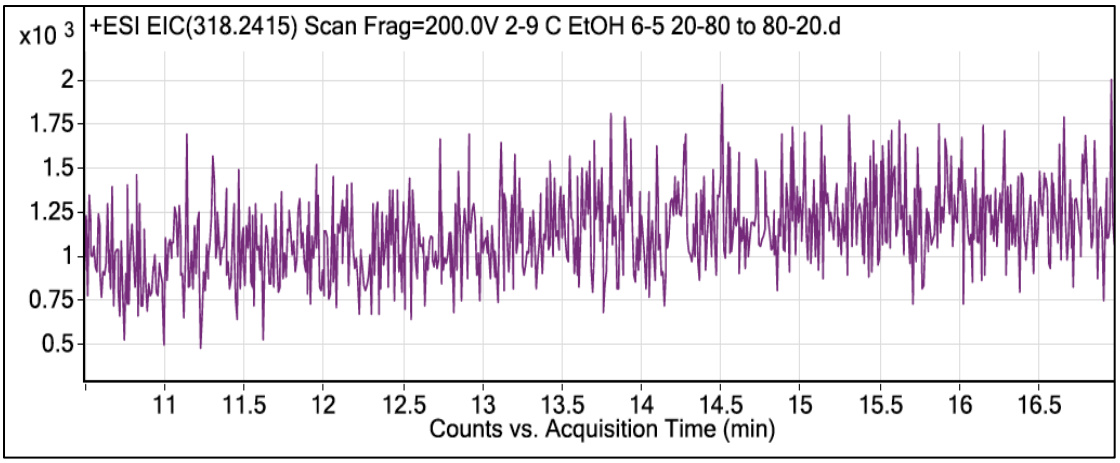

Unknown component 2 not present.

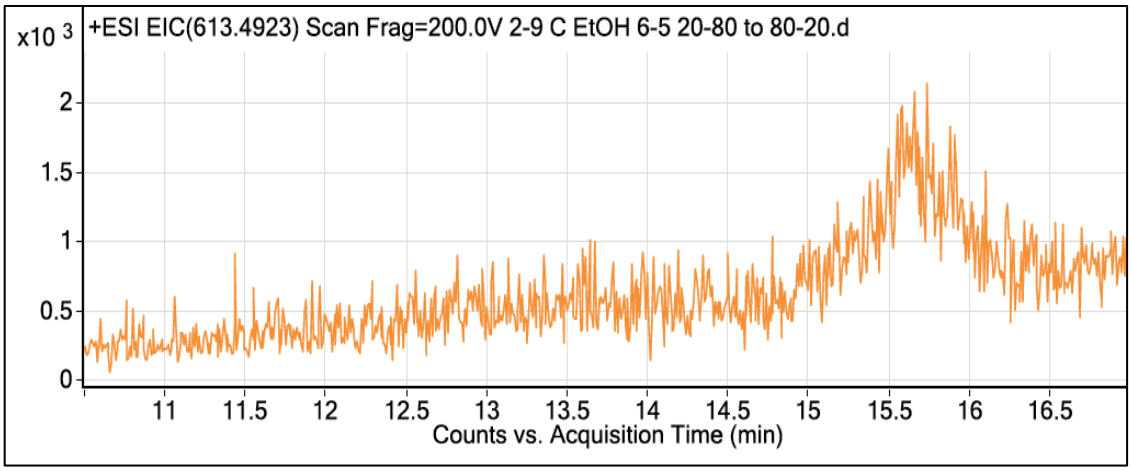

Unknown component 3 not present.

[1] Frizzell, R. A.; Rechkemmer, G.; Shoemaker, R. L., Altered Regulation of Airway Epithelial Cell Chloride Channels in Cystic Fibrosis. *Science* **1986,** *233* (4763), 558-560.
[2] De Boeck, K.; Wilschanski, M.; Castellani, C.; Taylor, C.; Cuppens, H.; Dodge, J.; Sinaasappel, M., Cystic fibrosis: terminology and diagnostic algorithms. *Thorax* **2006,** *61* (7), 627-635.
[3] Laguna, T. A. e. a., Comparison of Quantitative Sweat Chloride Methods After Positive Newborn Screen for Cystic Fibrosis. *Pediatric Pulmonology* **2012,** *47*, 736-742.
[4] Jentsch, T. J.; Stein, V.; Weinreich, F.; Zdebik, A. A., Molecular Structure and Physiological Function of Chloride Channels. *Physiological Reviews* **2002,** *82* (2), 503-568.
[5] Premo™ Halide Sensor. Invitrogen, Ed. Molecular Probes, Inc.: Eugene, Oregon, 2011.
[6] Premo™ Halide Sensor. http://products.invitrogen.com/ivgn/product/P10229?ICID=search-product (accessed July).
[7] Bakker, E.; Pretsch, E., Modern Potentiometry. *Angewandte Chemie International Edition* **2007,** *46* (30), 5660-5668.
[8] Verma, M., What is Capillary Ion Chromatography? T. F. S., Ed. 2013.
[9] Yokoi, K., Colorimetric Determination of Chloride in Biological Samples by Using Mercuric Nitrate and Diphenylcarbazone. *Biological Trace Element Research* **2002,** *85*, 88-94.
[10] Chloride in drinking-water: Background document for development of WHO Guidelines for Drinking-water Quality. World Health Organization: Geneva, Switzerland, 2003.
[11] Chloride Method 8113: Mercuric Thiocyanate Method. 7 ed.; Company, H., Ed. 2012.
[12] Toxological Profile for Iodine: 7. Analytical Methods. Registry, A. f. T. S. a. D., Ed. 2004.
[13] Sodium in drinking-water: Background document for development of WHO Guidelines for Drinking-water Quality. World Health Organization: Geneva, Switzerland, 2003.
[14] Hallenbeck, W. H.; Brenniman, G. R.; Anderson, R. J., High sodium in drinking water and its effect on blood pressure. *American Journal of Epidemiology* **1981,** *114* (6), 817-26.
[15] Cadmium in drinking-water: Background document for development of WHO Guidelines for Drinking-water Quality. World Health Organization: Geneva, Switzerland, 2011.
[16] Morikawa, Y.; Nakagawa, H.; Tabata, M.; Nishijo, M.; Senma, M.; Kitagawa, Y.; Kawano, S.; Teranishi, H.; Kido, T., Study of an outbreak of itai-itai disease. *Nihon Eiseigaku Zasshi* **1992,** *46* (6), 1057-62.
[17] Flury, M.; Papritz, A., Bromide in the Natural Environment: Occurrence and Toxicity. *Journal of Environmental Quality* **1993,** *22* (4), 747-758.
[18] Bonacquisti, T. P., A drinking water utility's perspective on bromide, bromate, and ozonation. *Toxicology* **2006,** *221* (2–3), 145-148.
[19] Fawell, J. e. a., Fluoride in Drinking-water. Organization, W. H., Ed. IWA Publishing, Alliance House: London, UK, 2006.
[20] von Hippel, F. N., The radiological and psychological consequences of the Fukushima Daiichi accident. *Bulletin of the Atomic Scientists* **2011,** *67* (5), 27-36.
[21] Unno, N.; Minakami, H.; Kubo, T.; Fujimori, K.; Ishiwata, I.; Terada, H.; Saito, S.; Yamaguchi, I.; Kunugita, N.; Nakai, A.; Yoshimura, Y., Effect of the Fukushima nuclear power plant accident on radioiodine (131I) content in human breast milk. *Journal of Obstetrics & Gynaecology Research* **2012,** *38* (5), 772-779.
[22] Hughes, M. F., Arsenic toxicity and potential mechanisms of action. *Toxicology Letters* **2002,** *133* (1), 1-16.
[23] Rahman, M. M.; Chowdhury, U. K.; Mukherjee, S. C.; Mondal, B. K.; Paul, K.; Lodh, D.; Biswas, B. K.; Chanda, C. R.; Basu, G. K.; Saha, K. C.; Roy, S.; Das, R.; Palit, S. K.; Quamruzzaman, Q.; Chakraborti, D., Chronic arsenic toxicity in Bangladesh and West Bengal, India--a review and commentary. *Journal Of Toxicology. Clinical Toxicology* **2001,** *39* (7), 683-700.
[24] Naumann, C. Expanding Cavitand Chemistry. University of British Columbia, British Columbia, Canada, 2002.
[25] Biavardi, E.; Tudisco, C.; Maffei, F.; Motta, A.; Massera, C.; Condorelli, G. G.; Dalcanale, E., Exclusive recognition of sarcosine in water and urine by a cavitand-functionalized silicon surface. *Proceedings of the National Academy of Sciences* **2012**.
[26] Ludwig, R.; Dzung, N. T. K., Calixarene-Based Molecules for Cation Recognition. *Sensors* **2002,** *2* (10), 397-416.
[27] Boerrigter, H.; Lugtenberg, R. J. W.; Egberink, R. J. M.; Verboom, W.; Reinhoudt, D. N.; Spek, A. L., Resorcinarene Cavitands as Building Blocks for Cation Receptors. *Gazzetta Chimica Italiana* **1997,** *127*, 709-716.
[28] Shortreed, M.; Bakker, E.; Kopelman, R., Miniature Sodium-Selective Ion-Exchange Optode with Fluorescent pH Chromoionophores and Tunable Dynamic Range. *Analytical Chemistry* **1996,** *68* (15), 2656-2662.

[29] Yamamoto, H.; Ueda, K.; Sandanayaka, K.; Shinkai, S., Molecular design of chromogenic calix[4]crowns which show very high Na^+ selectivity. *Chemistry Letters* **1995**, 497-498.
[30] Duke, R. M.; Veale, E. B.; Pfeffer, F. M.; Kruger, P. E.; Gunnlaugsson, T., Colorimetric and fluorescent anion sensors: an overview of recent developments in the use of 1,8-naphthalimide-based chemosensors. *Chem Soc Rev* **2010,** *39* (10), 3936-53.
[31] Quinlan, E.; Matthews, S. E.; Gunnlaugsson, T., Colorimetric Recognition of Anions Using Preorganized Tetra-Amidourea Derived Calix[4]arene Sensors. *Journal of Organic Chemistry* **2007**.
[32] Suksai, C.; Tuntulani, T., Chromogenic anion sensors. *Chemical Society Reviews* **2003,** *32* (4), 192-202.
[33] Cametti, M.; Rissanen, K., Highlights on contemporary recognition and sensing of fluoride anion in solution and in the solid state. Ibid.**2013,** *42* (5), 2016-2038.
[34] Kato, R.; Nishizawa, S.; Hayashita, T.; Teramae, N., A thiourea-based chromoionophore for selective binding and sensing of acetate. *Tetrahedron Letters* **2001,** *42* (30), 5053-5056.
[35] Hunger, K.; Mischke, P.; Rieper, W.; Raue, R.; Kunde, K.; Engel, A., Azo Dyes. In *Ullmann's Encyclopedia of Industrial Chemistry*, Wiley-VCH Verlag GmbH & Co. KGaA: 2000.
[36] Sancenón, F.; Martínez‐Máñez, R.; Soto, J., A Selective Chromogenic Reagent for Nitrate. *Angewandte Chemie International Edition* **2002,** *41* (8).
[37] Robison, H. M. The First Effective Method of Analysis for the Development of Ionochromic Azo Dyes for Aqueous Halide Detection. The Ohio State University, Columbus, Ohio, 2012.
[38] Lyon, H. O., Dye purity and dye standardization for biological staining. *Biotech Histochem* **2002,** *77* (2), 57-80.
[39] Marshall, P. N., Thin-layer chromatography of Sudan dyes. *Journal of Chromatography* **1977,** *136*, 353-357.
[40] Gessner, T.; Mayer, U., Triarylmethane and Diarylmethane Dyes. In *Ullmann's Encyclopedia of Industrial Chemistry*, Wiley-VCH Verlag GmbH & Co. KGaA: 2000.
[41] Kandela, I. K.; Bartlett, J. A.; Indig, G. L., Effect of molecular structure on the selective phototoxicity of triarylmethane dyes towards tumor cells. In *Photochemical & Photobiological Sciences*, 2002; Vol. 1, pp 309-314.
[42] Lueck, H. B.; McHale, J. L.; Edwards, W. D., Symmetry-breaking Solvent Effects on the Electronic Structure and Spectra of a Series of Triphenylmethane Dyes. *Journal of the American Chemical Society* **1992,** *114* (7), 2342-2348.
[43] Gil, J.; Song, X. Water-triggered coloring or color changing indicator. 2012-10-24, 2012.
[44] Beifuss, U., et al., Generation of cationic 2-azabutadienes from *N,S*-acetals and their use for the regio- and diastereoselective synthesis of 1,2,3,4-tetrahydroquinolines by intermolecular [$4\pi^+ + 2\pi$] cycloadditions. *ARKIVOC* **2005,** *2005* (5), 147-173.
[45] Spencer, T. A.; Onofrey, T. J.; Cann, R. O.; Russel, J. S.; Lee, L. E.; Blanchard, D. E.; Castro, A.; Gu, P.; Jiang, G.; Shechter, I., Zwitterionic Sulfobetaine Inhibitors of Squalene Synthase. *The Journal of Organic Chemistry* **1999,** *64* (3), 807-818.
[46] Marshall, P. N.; Lewis, S. M., A rapid thin-layer chromatographic system for Romanowsky blood stains. *Stain Technol* **1974,** *49* (4), 235-240.
[47] Marshall, P. N., Thin-layer chromatography of some cationic dyes commonly used in histology. *Journal of Chromatography* **1976,** *129*, 277-285.
[48] Lawrence, S. A., *Amines: Synthesis, Properties and Applications*. Cambridge University Press: Cambridge, UK, 2004.
[49] Palladium-Catalysed Coupling Chemistry. Thermo Fisher Scientific, Inc.: 2010.
[50] Wolfe, J. P.; Wagaw, S.; Buchwald, S. L., An Improved Catalyst System for Aromatic Carbon−Nitrogen Bond Formation: The Possible Involvement of Bis(Phosphine) Palladium Complexes as Key Intermediates. *Journal of the American Chemical Society* **1996,** *118* (30), 7215-7216.
[51] Wikimedia Commons.
[52] Ito, A.; Sakamaki, D.; Ichikawa, Y.; Tanaka, K., Spin-Delocalization in Charged States of para-Phenylene-Linked Dendritic Oligoarylamines†. *Chemistry of Materials* **2010,** *23* (3), 841-850.